Diese Dissertation haben begutachtet:

Prof. Christoph Herwig   Prof. Peter Neubauer   Prof. Gerald Striedner

TU
WIEN
TECHNISCHE
UNIVERSITÄT
WIEN
Vienna University of Technology

Dissertation

A scale-down approach to assess scale-up induced process variability in mammalian cell culture

ausgeführt zum Zwecke der Erlangung des akademischen Grades eines Doktors der technischen Wissenschaften unter der Leitung von

Univ. Prof. Dr. Christoph Herwig
Institut 166/4
Institut für Verfahrenstechnik, Umwelttechnik und technische Biowissenschaften

eingereicht an der Technischen Universität Wien
Fakultät für Technische Chemie

von

Dipl.-Ing. Matthias Brunner
Matrikelnummer: 01429686
Auchtertweg 1-13, 88400 Biberach

_01.05.2017_

Biberach, am   Unterschrift

Acknowledgements

At first I would like to thank Christoph Herwig for giving me the opportunity to carry out my PhD thesis in his department of Biochemical Engineering at the Vienna University of Technology. I further greatly appreciate his scientific advice and input to my research. His guidance encouraged me to pursue my goals and helped me developing my scientific mindset.

I also want to thank Prof. Peter Neubauer and Prof. Gerald Striedner for their time and effort in reviewing this thesis.

Furthermore, I would like to thank all the Post-Docs involved in my thesis as Lukas Neutsch, Tobias Klein and Jens Fricke who were always supportive, constructive and created a positive atmosphere. Their advice and opinion was always helpful along the three years of my thesis. A special thanks to Oliver Spadiut for his help and support.

Moreover, I would like to thank Sandoz GmbH in particularly Dirk Behrens and Christoph Posch for their support. I enjoyed the discussion and I am thankful for their scientific contributions as well as for the pleasant atmosphere during our meetings.

I further would like to thank all my students for their hard work and dedication to their topics, especially Julia Moser, Nadja Seidl, Philipp Braun and Philipp Doppler.

A special thanks to all my colleagues and friends at the Technical University that made me enjoy my time in Vienna particularly Manuela Frank, Britta Eggenreich, Thomas Gundinger, Lukas Veiter, David Wurm, Daniela Ehgartner, Vanessa Karabetian, Paul Ruschitzka, Viktor Konakovsky, Civan Yagtu, Julian Quehlenberger, Vignesh Rajamanickam and Kulwant Kandra.

At last I want to thank my family and friends in Germany for their support and frequent visits.

Abstract

A great share of biopharamceutical products is nowadays derived from mammalian cell cultivations. However, the scale-up of cell culture processes is a challenging task, often resulting in variable process performances across the scales. Due to the nature of bioreactor scale-up it is impossible to maintain all operational conditions equal between small-scale and large-scale cultivations. Variations in operational parameters can lead to a physiochemical variability with direct influence on cell specific physiological conditions, finally altering product quality and process performance. The goal of this thesis was to evaluate the impact of large-scale inhomogeneities, that arise during process scale-up, on cell physiology and process performance using a scale-down approach. Hereby physiological effects of large-scale inhomogeneities were uncovered through application and combination of a decoupled control strategy for process parameters (pH, pO_2 and pCO_2) with multivariate data analysis as well as metabolic flux analysis and the establishment of a two-compartment bioreactor system. Through this methodology novel process parameter interaction effects as well as intracellular metabolic regulations were revealed. Furthermore, the development and application of the two-compartment bioreactor system led to an improved understanding of the impact of temporary pH gradients on cell physiology and process performance. The gathered results demonstrate that the used scale-down approach in combination with appropriate investigative methods is capable of revealing novel effects that might occur during large-scale mammalian fermentation processes. The transferability of these obtained results back to the large-scale is however challenging due to the lack of knowledge of the actual large-scale conditions.

Zusammenfassung

Ein grosser Anteil an biopharmazeutschen Produkten wird heutzutage von Säugetierzellkulturen hergestellt Der Scale-up von Zellkulturprozessen ist jedoch eine komplexe Aufgabe, die meist in unterschiedlichen Prozessverhalten in den verschiedenen Scales endet, da es unmöglich ist während dem scale-up alle Operationsparameter konstant zu halten. Variationen in den Operationsparametern können letztendlich zu einer physiochemischen Variabilität führen mit direktem Einfluss auf die zellphysiologischen Eigenschaften und damit auf die Produktqualität und den Prozess. Das Ziel dieser Arbeit war es, den Einfluss von Large-Scale-Inhomogenitäten auf die Zellphysiologie und das Prozessverhalten mit Hilfe eines Scale-Down-Ansatzes zu evaluieren. Hierbei wurden physiologische Effekte von Inhomogenitäten, mit Hilfe einer entkoppelten Kontrollstrategie für die Prozessparameter pH, pO_2 und pCO_2 und in Kombination mit Multivariater Datenanalyse und Metabolischer Flussanalyse sowie der Etablierung eines Zwei-Kompartiment-Bioreaktorsystems, aufgedeckt. Durch diese Methodik konnten neue Interaktionseffekt von Prozessparametern und intrazelluläre Regulationsmechanismen aufgezeigt werden. Des Weiteren führte die Entwicklung und Anwendung des Zwei-Kompartiment-Bioreaktorsystems zu einem vertieften Verständnis von Effekten temporärer pH-Gradienten auf die Zellphysiologie und den Prozess. Die Resultate dieser Arbeiten zeigen, dass der Scale-Down-Ansatz in Kombination mit den richtigen Experimental- und Analysemethoden dazu in der Lage ist neue Effekte, die in Large-Scale-Fermentationsprozessen auftreten aufzudecken. Die Transferierbarkeit der Ergebnisse zurück in die Großfermenter ist allerdings herausfordernd, da die tatsächlichen lokalen Begebenheiten in Large-Scale-Bioreaktoren nicht bekannt sind.

Table of Contents

Introduction and Problem Statement

Mammalian cell culture in the biopharmaceutical industry

The importance of mammalian cell culture for the biopharmaceutical industry can be derived from the latest biopharmaceutical benchmark by Walsh (2014). He stated that from 2012 to 2014, around 60% of the total number of biopharmaceutical product approvals derived from mammalian cells (Walsh 2014). In contrast to other expression systems mammalian cells are capable of human like posttranslational modifications, which are essential for drug safety and efficacy. Within mammalian derived products, chinese hamster ovary (CHO) cells are the predominant expression system (Zhou and Kantardjieff 2014) due to several factors (Beck et al. 2008; Jayapal 2007):

- CHO cells can be easily transfected, clone selection and gene amplification methods are well established

- Relatively stable clones can be achieved with high extracellular protein expression rates

- CHO cells are able to grow in suspension which makes them easy to cultivate in large-scale

- Several human viruses do not replicate in CHO cells

- Posttranslational glycosylation is more similar to humans in contrast to other cell lines (e.g. murine cells)

- Most importantly large-scale upstream and downstream processes, as well as regulatory approval processes are already well established

The most common biopharmaceutical product derived today from mammalian cells are monoclonal antibodies (Walsh 2014).

A typical production process for monoclonal antibodies

The genetic information for the monoclonal antibody itself is usually obtained from hybridoma technology, phage display or transgenic animals (Nelson et al. 2010) and after potential further engineering (e.g. humanization), transfected into a host cell line. After primary screening, single cell clones can be obtained (e.g. by limited dilution) which undergo further screening for stability, cell growth and productivity (Lai et al. 2013). The final clone will then be used in process development and scale-up studies until final production (Wurm 2004). The industrial manufacturing process for monoclonal antibody production in chinese hamster ovary cells is usually a fed-batch process (Abu-Absi et al. 2014). Subsequently to large-scale production the supernatant is usually harvested using centrifugation and depth filtration. The first purification step is a protein A chromatography often followed by a viral inactivation step. Afterwards ion exchange chromatography (IEC) is mostly performed for impurity removal and further polishing. Additional process steps often include viral filtration and diafiltration into final buffers for storage until final filling into vials (Vazquez-Rey and Lang 2011).

Large-scale monoclonal antibody production is a very complex process that involves several complicated procedures and needs clever linkage of all process steps. This thesis will only focus on the upstream process and more specifically on the challenges that might occur during the scale-up of the upstream process.
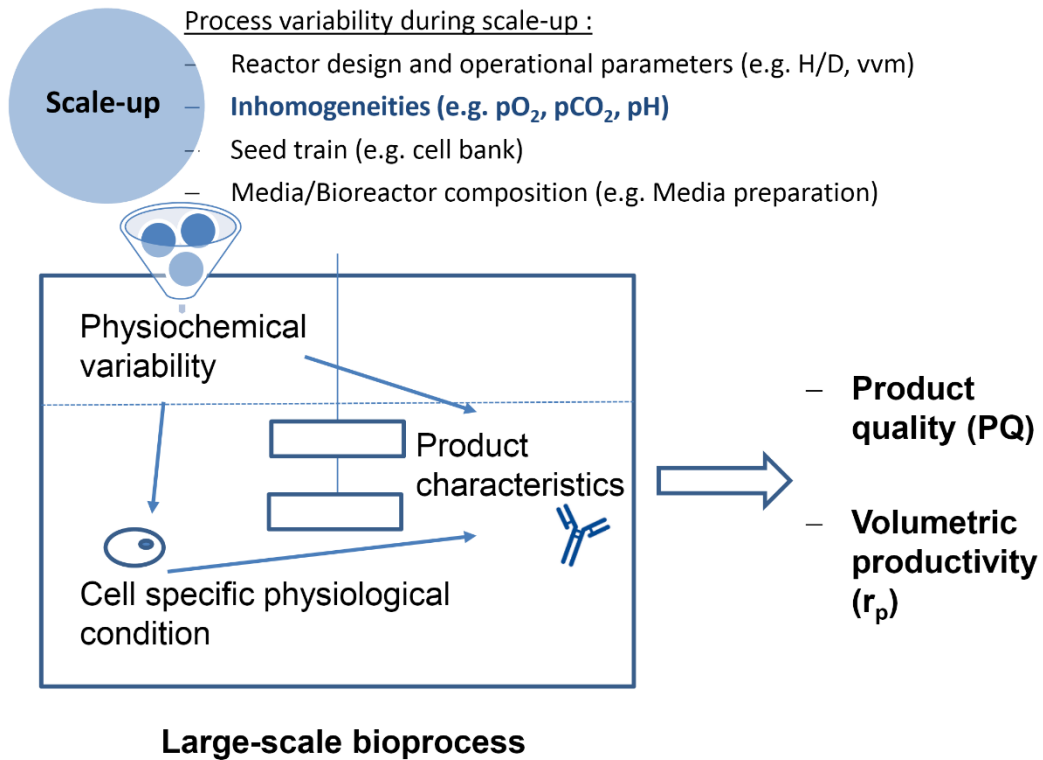
Scale-up induced process variability in mammalian cell culture

The transition between the early process development and the late stage process development/manufacturing stage of a biopharmaceutical product is usually accompanied by a dramatic increase in bioreactor scale (Figure 1).
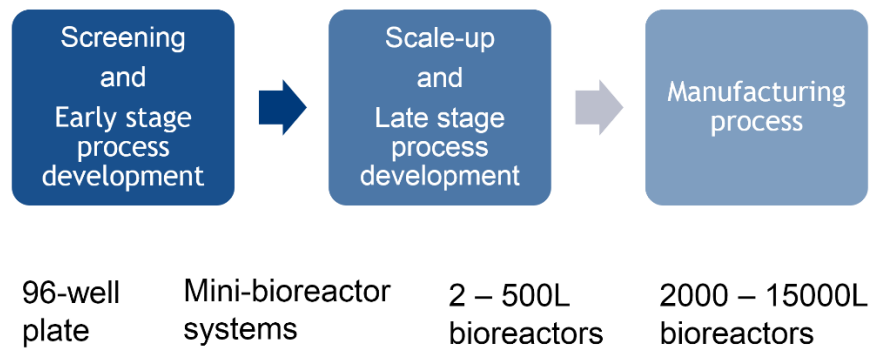
Figure 1. Scale-up from process development to manufacturing process. Upstream cultivation systems increase strongly in scale from early stage process development to the final manufacturing process.

The scale-up of cell culture processes is challenging and deviations between the small-scale and large-scale performances are frequently observed (Xing et al. 2009). Variations in e.g. operational parameters, media composition or seed train procedures can lead to a physiochemical or biological variability with direct influence on cell specific physiological conditions and product characteristics (Figure 2). Thus, the two key parameters product quality (PQ) and volumetric productivity (r_P) of a process can be significantly altered during process scale-up.

Figure 2. Scale-up induced process variability. Variability occurs due to several factors influencing the cell specific physiological conditions as well as product characteristics and final process performance.

During biopharmaceutical process development, a process design space is defined based on the product design space and characterization studies (e.g. Design of Experiments fermentation runs) that are usually performed in small-scale fermentation systems. However, these studies imply the assumption that the small-scale systems are capable of accurately modelling the large-scale reactor. Nowadays, small-scale state of the art bioreactor systems are powerful tools in cell screening but are commonly performed using similar control strategies (e.g. pH, pO_2 set-points) than in production-scale. Therefore, these systems do not consider large-scale phenomena as inhomogeneities (Neubauer and Junne, 2010).

The goal of this thesis was to evaluate the impact of large-scale inhomogeneities, that arise during process scale-up, on cell physiology and process performance using a scale-down approach.

Bioreactor scale-up and subsequent large-scale inhomogeneities

Typical scale-up criteria in mammalian cell culture are constant specific power input (*P/V*) or constant volumetric mass transfer coefficient (*kla*) (Garcia-Ochoa and Gomez 2009; Nienow 2006; Xing et al. 2009). However, keeping one of those parameters constant, usually results in an increased mixing time in large-scale bioreactors. This subsequently results in substrate or pH gradients after addition of these components to the bioreactor. Application of constant mixing time is not an appropriate scale-up parameter because this results in impractical high power inputs (Lara et al. 2006). Constant impeller tip speed or constant Reynolds number are two scale-up criteria that would lead to even higher mixing times in large-scale, when compared to the *P/V* or *kla*-criteria and are therefore not commonly used (Lara et al. 2006).

Elevated pCO$_2$ values can be often detected in large-scale processes. This can be mostly attributed to a decreased volumetric flowrate (*vvm*) in large-scale when compared to the small-scale systems (Nienow 2006). Decreased *vvm* values are usually applied to maintain a certain superficial gas velocity (*Vs*) upon scale-up. This is crucial since elevated superficial gas velocities would contribute to foam formation (Pilon and Viskanta 2004) finally resulting in cell loss and the need of chemical antifoam addition (Delvigne et al. 2009). Moreover, the superficial gas velocity is linked to the volumetric mass transfer coefficient (*kla*) via Equation (1) and is connected to *vvm* via Equation (2).

$$kla = a \times (\frac{P}{V})^b \times (Vs)^c \quad [s^{-1}] \qquad (1)$$

with *a*, *b* and *c* as empirical constants.

$$Vs = \left(\frac{vvm}{60}\right) \times \left(\frac{V_l}{A}\right) \quad [\frac{m}{s}] \qquad (2)$$

with V_l being the volume of the culture broth and *A* being the cross-sectional area of the bioreactor.

It has to be mentioned that the pCO_2 in large-scale is further dependent from the local bioreactor conditions since hydrostatic effects and the limited capability of bubbles to take up CO_2 have to be considered as well (Lara et al. 2006; Sieblist et al. 2011a). This can furthermore result in local pCO_2 and subsequently pH gradients.

Oxygen mass transfer is a key parameter during aerobic fermentation processes to supply the cells with enough oxygen. The oxygen transfer rate (OTR) can be influenced by the volumetric mass transfer coefficient according to Equation (3).

$$OTR = kla \times (c^* - c) \qquad (3)$$

with c^* being the O_2 concentration at the phase boundary and c being the O_2 concentration in the liquid.

However, *kla* is dependent on the local power dissipation density and therefore varies inside of the bioreactor (Garcia-Ochoa and Gomez 2009; Sieblist et al. 2011b). O_2 is usually added to the bottom of the bioreactor leading to different oxygen concentrations in the gas phase across the bioreactor (Hristov et al. 2001) further contributing to variable OTR values inside of the system. Due to the stated phenomena dissolved oxygen gradients are most likely to occur in large-scale processes.

The described effects demonstrate that inhomogeneities in critical process parameters as pO_2, pH and pCO_2 do occur in large-scale production processes. However, in contrast to biological effects from different seed train procedures or media preparation influences, which could be both detected during small-scale satellite runs parallel to the large-scale studies, effects from process parameter inhomogeneities (e.g. in pH, pO_2, pCO_2) cannot be detected in the usually used scale-down model bioreactors.
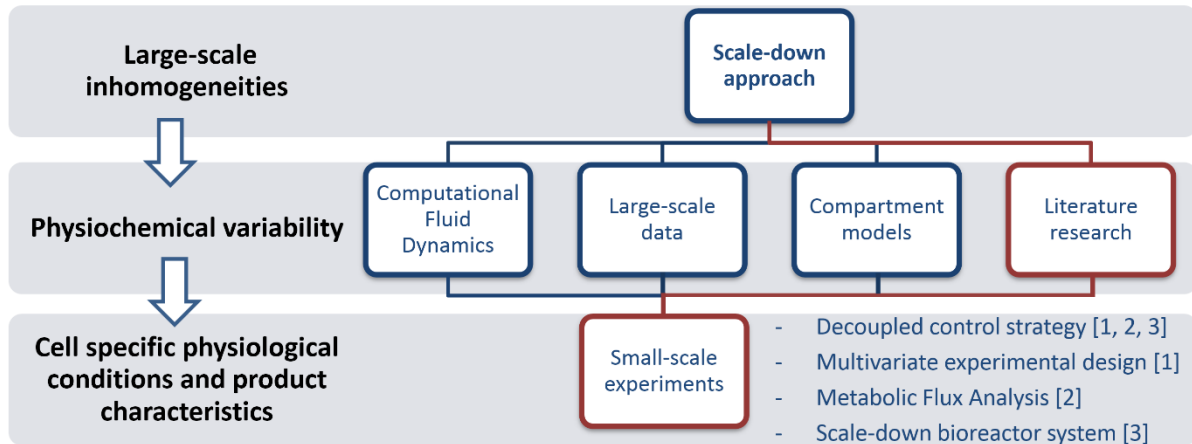
A scale-down approach to assess large-scale inhomogeneities

In this thesis, a scale-down approach was used to assess the impact of large-scale inhomogeneities on the cell physiology and product attributes. A scale-down approach is usually characterized by several steps.

(i) In a first step the physiochemical variability inside of the large-scale bioreactor has to be identified. Actual large-scale bioprocess data of process parameter inhomogeneities are usually not available because they would need the application of multiposition sensors or in flow follower, which are still under development and far away from industrial application (Bockisch et al. 2014; Zimmermann et al. 2013). Mathematical models as compartment models or Computational Fluid Dynamics (CFD) models can be strong tools to predict the hydrodynamics and mass transfer characteristics of a bioreactor but are very complicated and include many challenges as bubble coalescence/break-up prediction and local gas-phase composition dynamics (Garcia-Ochoa and Gomez 2009; Hristov et al. 2001; Noorman 2011). Due to the lack of inhomogeneity-data from the industrial scale as well as the absence of CFD data in this thesis, the physiochemical conditions used in the scale-down studies were finally derived from an extensive literature research.

(ii) The second step is simulating the large-scale conditions in a small-scale setup. Through this methodology the effects of large-scale inhomogeneities on cell specific physiological responses as well as product quality attributes can be investigated. Hereby the exact simulation of temporary large-scale inhomogeneities experienced by cells travelling through the bioreactor, is a challenging task which usually requires multi-compartment bioreactor systems (Neubauer and Junne 2010). However, general metabolic responses of the cells to changing environments can be further derived from pulse experiments or steady-state cultures at different process parameter set-points.

The first two steps of the scale-down approach were performed within this thesis and build the background for the published manuscripts (Figure 3).

Figure 3. The first two steps of a scale-down approach to assess large-scale inhomogeneities. The specific scale-down approach used in this thesis is highlighted in red. Essential methods used in the small-scale experiments are shown in conjunction with their related manuscript. Numbers in square brackets refer to the manuscripts included in this thesis.

(iii) After the scale-down experiments, the obtained knowledge and results should be ideally transferred back to the industrial scale. Finally leading to an improvement of the large-scale process. The third step will be discussed in more detail in the conclusion and outlook chapter of this thesis.

Goal of the thesis and scientific contribution to the field

The goal of this thesis was to evaluate the impact of large-scale inhomogeneities that arise during process scale-up on cell physiology and process performance using a scale-down approach. The thesis includes three peer reviewed manuscripts. The individual novelty aspects, achievements as well as author contributions to the manuscripts are shown in Table 1.

Table 1. Achievements, novelty aspects and author contributions of Matthias Brunner (MBR).

	Manuscript Title	Novelty	Achievements	Author contributions of MBR
Manuscript No. 1	Investigation of the interactions of critical scale-up parameters (pH, pO_2 and pCO_2) on CHO batch performance and critical quality attributes.	Interactions of scale-up critical process parameters on cell physiology and product quality	- A specific control strategy allows the analysis of interactions as well as decoupled effects of pH, pO_2 and pCO_2 - Interactions of pH and pCO_2 on cell physiology and product quality have to be considered during process scale-up - pH and pCO_2 revealed strongest effects on process performance	MBR partially designed the experiments, conducted the experiments, performed the data analysis and drafted the manuscript
Manuscript No. 2	Elevated pCO_2 affects lactate metabolic shift in CHO cell culture processes.	Elevated pCO_2/bicarbonate can affect the lactate metabolic shift in CHO cell culture processes	- pCO_2 or bicarbonate concentrations respectively affect the lactate metabolism during CHO cell culture processes - The onset of the lactate metabolic shift could be correlated to an intracellular redox balance via metabolic flux analysis	MBR designed the experiments, performed the data analysis and drafted the manuscript
Manuscript No. 3	The impact of pH inhomogeneities on CHO cell physiology and fed-batch process performance – two-compartment scale-down modelling and intracellular pH excursion	Short-term exposure of cells to increased pH values affects their intracellular pH and overall process performance	- A two-compartment scale-down model of a $10m^3$ STR was successfully set-up - Short term intracellular pH changes due to extracellular pH variations were detected - Simulation of elevated pH inhomogeneities during fed-batch processes, using the scale-down system, reveled significant effects on overall process performance	MBR designed the experiments, performed the data analysis and drafted the manuscript

References Introduction

Abu-Absi S, Xu S, Graham H, Dalal N, Boyer M, Dave K. 2014. Cell culture process operations for recombinant protein production. Adv. Biochem. Eng. Biotechnol. 139:35-68.

Beck A, Wagner-Rousset E, Bussat MC, Lokteff M, Klinguer-Hamour C, Haeuw JF, Goetsch L, Wurch T, Van Dorsselaer A, Corvaia N. 2008. Trends in glycosylation, glycoanalysis and glycoengineering of therapeutic antibodies and Fc-fusion proteins. Curr Pharm Biotechnol 9(6):482-501.

Bockisch A, Biering J, Päßler S, Vonau W, Junne S, Neubauer P. 2014. In Situ Investigation of the Liquid Phase in Industrial Yeast Fermentations with Mobile Multiparameter Sensors. Chem. Ing. Tech. 86(9):1582-1582.

Delvigne F, Lecomte J-p, Flickinger MC. 2009. Foam Formation and Control in Bioreactors. Encyclopedia of Industrial Biotechnology: John Wiley & Sons, Inc.

Garcia-Ochoa F, Gomez E. 2009. Bioreactor scale-up and oxygen transfer rate in microbial processes: an overview. Biotechnol Adv 27(2):153-76.

Hristov H, Mann R, Lossev V, Vlaev SD, Seichter P. 2001. A 3-D Analysis of Gas-Liquid Mixing, Mass Transfer and Bioreaction in a Stirred Bio-Reactor. Food and Bioproducts Processing 79(4):232-241.

Jayapal KW, KF; Hu, WS; Yap, MG. 2007. Recombinant protein therapeutics from CHO cells- 20 years and counting. Chemical Engineering Progress 103:40 -47.

Lai T, Yang Y, Ng SK. 2013. Advances in Mammalian Cell Line Development Technologies for Recombinant Protein Production. Pharmaceuticals 6(5):579-603.

Lara AR, Galindo E, Ramirez OT, Palomares LA. 2006. Living with heterogeneities in bioreactors: understanding the effects of environmental gradients on cells. Mol. Biotechnol. 34(3):355-81.

Nelson AL, Dhimolea E, Reichert JM. 2010. Development trends for human monoclonal antibody therapeutics. Nat Rev Drug Discov 9(10):767-774.

Neubauer P, Junne S. 2010. Scale-down simulators for metabolic analysis of large-scale bioprocesses. Curr. Opin. Biotechnol. 21(1):114-21.

Nienow AW. 2006. Reactor engineering in large scale animal cell culture. Cytotechnology 50(1-3):9-33.

Noorman H. 2011. An industrial perspective on bioreactor scale-down: what we can learn from combined large-scale bioprocess and model fluid studies. Biotechnol. J. 6(8):934-43.

Pilon L, Viskanta R. 2004. Minimum superficial gas velocity for onset of foaming. Chemical Engineering and Processing: Process Intensification 43(2):149-160.

Sieblist C, Hageholz O, Aehle M, Jenzsch M, Pohlscheidt M, Lubbert A. 2011a. Insights into large-scale cell-culture reactors: II. Gas-phase mixing and CO(2) stripping. Biotechnol J 6(12):1547-56.

Sieblist C, Jenzsch M, Pohlscheidt M, Lubbert A. 2011b. Insights into large-scale cell-culture reactors: I. Liquid mixing and oxygen supply. Biotechnol J 6(12):1532-46.

Vazquez-Rey M, Lang DA. 2011. Aggregates in monoclonal antibody manufacturing processes. Biotechnol Bioeng 108(7):1494-508.

Walsh G. 2014. Biopharmaceutical benchmarks 2014. Nat. Biotech. 32(10):992-1000.

Wurm FM. 2004. Production of recombinant protein therapeutics in cultivated mammalian cells. Nat Biotech 22(11):1393-1398.

Xing Z, Kenty BM, Li ZJ, Lee SS. 2009. Scale-up analysis for a CHO cell culture process in large-scale bioreactors. Biotechnol. Bioeng. 103(4):733-46.

Zhou W, Kantardjieff A. 2014. Mammalian Cell Cultures for Biologics Manufacturing. Advances in Biochemical Engineering/Biotechnology 139.

Zimmermann R, Fiabane L, Gasteuil Y, Volk R, Pinton J-F. 2013. Characterizing flows with an instrumented particle measuring Lagrangian accelerations. New J. Phys. 15(1).

Manuscripts

Manuscript 1: Investigation of the interactions of critical scale-up parameters (pH, pO$_2$ and pCO$_2$) on CHO batch performance and critical quality attributes

Authors: Matthias Brunner, Jens Fricke, Paul Kroll and Christoph Herwig

Published online: 17. October.2016 in Bioprocess and Biosystems Engineering

CrossMark

RESEARCH PAPER

Investigation of the interactions of critical scale-up parameters (pH, pO_2 and pCO_2) on CHO batch performance and critical quality attributes

Matthias Brunner[1,2] · Jens Fricke[1,2] · Paul Kroll[1,2] · Christoph Herwig[1,2,]

Abstract Understanding process parameter interactions and their effects on mammalian cell cultivations is an essential requirement for robust process scale-up. Furthermore, knowledge of the relationship between the process parameters and the product critical quality attributes (CQAs) is necessary to satisfy quality by design guidelines. So far, mainly the effect of single parameters on CQAs was investigated. Here, we present a comprehensive study to investigate the interactions of scale-up relevant parameters as pH, pO_2 and pCO_2 on CHO cell physiology, process performance and CQAs, which was based on design of experiments and extended product quality analytics. The study used a novel control strategy in which process parameters were decoupled from each other, and thus allowed their individual control at defined set points. Besides having identified the impact of single parameters on process performance and product quality, further significant interaction effects of process parameters on specific cell growth, specific productivity and amino acid metabolism could be derived using this method. Concerning single parameter effects, several monoclonal antibody (mAb) charge variants were affected by process pCO_2 and pH. N-glycosylation analysis showed positive correlations between mAb sialylation and high pH values as well as a relationship between high mannose variants and process pH. This study additionally revealed several interaction effects as process pH and pCO_2 interactions on mAb charge variants and N-glycosylation pattern. Hence, through our process control strategy and multivariate investigation, novel significant process parameter interactions and single effects were identified which have to be taken into account especially for process scale-up.

Introduction

Monoclonal antibodies (mAbs) have become the main products of biopharmaceutical industries throughout the past decades. Despite their typically low growth rate, unstable productivity and high process costs, mammalian cells benefit from their ability to perform human-like posttranslational modifications and thus represent the main expression system for mAb production [1–3]. Chinese hamster ovary (CHO) cells are the most commonly used cell systems for mammalian processes. Since GMP certificated processes are readily available and high throughput cell screening and fed-batch processing are established and well understood CHO cells will remain the main expression system in the near future [3–5]. Advanced understanding of CHO cell metabolism and interaction with process parameters is of high importance for process optimization, scale-up; and moreover, is a major requirement of quality by design (QbD) guidelines as claimed by the Federal Drug Association (FDA) [6]. Furthermore,

✉ Christoph Herwig
christoph.herwig@tuwien.ac.at

1 Research Division Biochemical Engineering, Vienna University of Technology, Gumpendorferstrasse 1a 166/4, Vienna 1060, Austria

2 CD Laboratory on Mechanistic and Physiological Methods for Improved Bioprocesses, Vienna University of Technology, Gumpendorferstrasse 1a/166, 1060 Vienna, Austria

⚫ Springer

13

modeling approaches as hybrid models may benefit from the knowledge of process parameter interactions and single effects to improve model fit and model quality [7]. Understanding of process parameter interactions is especially useful during process scale-up, where unwanted variations of pH, dissolved oxygen tension (pO_2) and carbon dioxide tension (pCO_2) are most likely to occur [8–10]. Manufacturing processes aim towards high product titers and space–time-yields but, moreover, good and consistent final product quality is of upmost importance. Monoclonal antibodies are very complex molecules and can be modified during up- and downstream process thus leading to heterogeneous final products [11]. Product heterogeneity may lead to various changes in physiochemical, biological and immunogenic properties compared to the desired homogeneous antibody drug. In more detail, protein heterogeneity may lead to different protein binding, stability, immune responses and pharmacokinetics [12]. Therefore, control of product heterogeneity within predefined analytical specifications is of high importance for cGMP manufacturing.

Process parameters such as temperature, pH, pO_2 and pCO_2 can have enormous effects on CHO cell process performance and critical quality attributes as described widely in the literature [13–17]. Link et al. [15] discovered that changing dissolved oxygen concentration can have an effect on specific productivity of CHO-K1 cells. Additionally, a study conducted by Trummer et al. [13] showed significant influences of culture temperature and culture pH on cell metabolism, growth and product quality in a CHO batch fermentation producing EPO-Fc. However, influences of different carbon dioxide tensions are most often neglected although it has been shown in other studies that pCO_2 can have significant effects on specific cell growth, productivity and product quality [18–20]. Studies about interaction effects of parameters are less prominent in the literature, however, Zanghi et al. [19] showed that at elevated pH or pCO_2 in a CHO culture, osmolality and bicarbonate concentration significantly influence product polysialylation.

In contrast to the current state of the art, the goal of our study was to derive interaction effects of critical scale-up parameters on cell physiology as well as on process performance and critical product quality attributes. Therefore, our approach consisted of a central composite face-centered design of experiments and various in-process analytics as well as product quality analytics for charge, size and glycan heterogeneity. This investigation was only possible through usage of a novel control strategy via decoupling of pO_2, pH and pCO_2 process control and thus investigating the individual effects and interactions of these critical scale-up parameters in one systematic approach. The novelty of this work is therefore the elucidation of interaction effects of scale dependent process parameters on a large number of responses including amino acids and product quality attributes.

Materials and methods

Design of experiment and data evaluation

Experiments were carried out according to a central composite face-centered design with the factors pH ranging from 6.8 to 7.2, pO_2 from 10 to 40 % and pCO_2 from 5 (37 mmHg) to 20 % (150 mmHg) (Table 1). Boundaries were set for pCO_2 in between physiological values and levels that might occur during large-scale fermentation processes [9], whereas pH was mostly set in between boundaries of physiological ranges to allow constant fermentation conditions. However, pH variations to 6.8 may also occur during large-scale fermentation due to CO_2 gradients [21]. The dissolved oxygen tension concentration upper limit was set to 40 % according to common industrial settings. Since in large-scale fermentations at high cell densities pO_2 gradients are likely to occur [9], the lower limit for pO_2 was set to 10 %. In total, the experimental design space consisted of 19 batch fermentations, whereas five fermentation runs were carried out at the center point settings of the DoE. Due to problems with one of the pH-probes, one fermentation run at pH 7.2, pO_2 40 % and pCO_2 20 % finally had to be excluded from data evaluation. Since all other 14 set points of the experimental design space were carried out successfully, this one missing run was found not to compromise the quality of the experimental design to any significant extent. Furthermore, two fermentation runs (pH 7; pCO_2 20 %; pO_2 25 % and pH 7; pCO_2 12.5 %; pO_2 10 %) revealed unusually high mAb aggregation rates and thus their mAb quality data were excluded from data evaluation.

Experimental planning and data evaluation was carried out by the help of the software MODDE® (Umetrics, Sweden). For each selected response MODDE® generates a PLS Model and the final parameters after model optimization are illustrated in this report. Key parameters of the models are the coefficient of determination R^2, goodness of prediction Q^2, model validity MV and reproducibility RP. Ideally, R^2, Q^2, MV and RP should be close to 1 and above 0.5, or 0.25 concerning MV, for a significant model. Furthermore, tables with normalized coefficients derived out of PLS models are shown in this work. Since errors for specific growth and metabolite production/consumption rates are generally high in mammalian processes [22], confidence intervals were set to 0.90 for all calculated growth, consumption and production rates. For all other responses, confidence levels were set to 0.95. The

Table 1 Specific process parameter conditions of the experimental design space

Exp. No.	1	2	3	4	5	6	7	8	9	10
pH	6.8	7.2	6.8	7.2	6.8	7.2	6.8	7.2	7	7
pCO_2	5	5	20	20	5	5	20	20	12.5	12.5
pO_2	10	10	10	10	40	40	40	40	25	25

Exp. No.	11	12	13	14	15	16	17	18	19	
pH	7	7.2	6.8	7	7	7	7	7	7	
pCO_2	12.5	12.5	12.5	5	20	12.5	12.5	12.5	12.5	
pO_2	25	25	25	25	25	10	40	25	25	

Experiment number 8 had to be excluded from data evaluation due to a defect pH probe

responses analyzed were maximum and average specific growth rate (μ_{max}, $\mu_{average}$), specific lactate and ammonia production (q_{lac}, q_{amm}), specific glucose and glutamine consumption (q_{gluc}, q_{gln}), further specific amino acid consumption and production rates (q_{Ala}, q_{Arg}, q_{Asn}, q_{Asp}, q_{Cys}, q_{Glu}, q_{Gly}, q_{His}, q_{Ile}, q_{Leu}, q_{Lys}, q_{Meth}, q_{Phe}, q_{Pro}, q_{Ser}, q_{Thr}, q_{Tyr}, q_{Try}, q_{Val}) and specific productivity (q_p). Moreover, critical product quality attributes were analyzed as charge, size and glycan variants.

Cell line, seed train and batch fermentations

An industrial CHO cell line producing a mAb was cultivated in chemically defined media. Precultures for batch fermentation processes were cultivated in shake flasks and incubated at 10 % pCO_2 and 37 °C temperature. Exponentially growing cells were transferred into 3 L glass bioreactors resulting in an inoculation density of 3×10^5 cells/mL. All batch cultivations were carried out at 37 °C.

Using a novel control strategy, pO_2, pCO_2 and pH set points were set and kept constant throughout the fermentation process according to the DoE. Usually, pH control in cell culture is performed using pCO_2 as acid; this had to be changed to decouple pH and pCO_2 control. pH regulation was therefore realized by the addition of 0.5 M HCL and 0.5 M NaOH, respectively. Dissolved oxygen tension and carbon dioxide tension were regulated independently through gas mixing while keeping stirrer speed and gas volumetric flow rate constant. pCO_2 measurement and control was done by use of an off-gas sensor (BlueInOne, Bluesens, Germany) and based on calculations from Frahm et al. [23]. pH and pO_2 were measured by in-line probes (EasyFerm, Hamilton, United States and VisiFerm, Hamilton, United States).

In-process control, mAb and amino acid determination

Cultivation samples were taken every 12 h and cell counting/viability determination was performed using the automatic picture analyzer Cedex HiRes Analyzer (Roche,

Germany). Osmolality of supernatant was determined via freeze point depression (Mikro-Osmometer TypOM806, Löser, Germany). Analysis of metabolites glucose, glutamine, glutamate, lactate and ammonium were performed using Cedex Bio HT Analyzer (Roche, Germany). Antibody titer determination was carried out by HPLC (Ultimate 3000, Dionex, United States) with a Protein A sensor cartridge (Applied Biosystems, The Netherlands). Amino acid concentrations were determined by HPLC measurement (Ultimate 3000, Dionex, United States; ZORBAX Eclipse Plus C18 column, Agilent Technologies, United States) and prior sample-derivatization with ortho-phthalaldehyde (OPA) and 9-fluorenylmethyloxycarbonyl (FMOC).

Product quality analytics

Harvest samples for product quality analytics were taken only once at the end of batch processes as soon as viability dropped below 75 % and supernatants were stored at −80 °C.

Cation exchange chromatography

Determination of charge variants was performed using a ProPac WCX-10 (4 × 250 mm) analytical column (Dionex, United States) connected to HPLC system (Agilent Technologies 1100/1200 Series, United States) with UV detection at 220 nm.

Size exclusion chromatography

Size exclusion chromatography was performed using a TSKgel G3000SWXL column (Tosoh, Japan) connected to a HPLC system (Agilent Technologies 1100/1200 Series, United States) with UV detection at 210 nm.

N-glycan determination

Quantitative determination of N-glycans was performed after digest with N-glycosidase F (PNGase F, Roche, Germany). After separation from the protein using ultra

centrifugal filters, released *N*-glycans were labeled with 2-aminobenzamide (2-AB) at 37 °C overnight. Afterwards 2-AB labeled glycans were profiled by normal phase chromatography using a ACQUITY UPLC BEH column (Waters, United States) connected to an HPLC system (Agilent 1200 series, United States) with FLD detection.

Calculation of specific rates and degree of glycosylation

Calculation of the specific growth rate μ was performed using the integral of viable cell density as described by Klein et al. [24] and shown in Eq. (1):

$$\mu = \frac{d(VCD)}{d(IVCD)}, \tag{1}$$

with VCD being the viable cell density and IVCD the integral of viable cell density.

Calculation of the specific production or consumption rates was performed as shown in Eq. (2), with c_i being the concentration of either a specific metabolite or product *i*:

$$q_i = \frac{d(c_i)}{d(IVCD)}. \tag{2}$$

Calculation of the specific growth and production or consumption rates were performed for each time point and average rates were calculated for the relevant process phase using values between inoculation and peak VCD. The maximum specific growth rate, however, was calculated only for time points within the exponential growth phase of the processes. All cell specific metabolic rates were assigned positive for production and negative for consumption.

The degree of galactosylation (GI) was calculated as shown in Eq. (3) and described earlier by Ivarsson et al. [17]:

$$GI = \frac{3 \times G3 + 2 \times G2 + G1}{(G0 + G1 + G2 + G3) \times 3}. \tag{3}$$

The degrees of sialylation (SI) and afucosylation (aFI) were calculated in the same manner.

Results and discussion

Experiments were carried out according to our experimental design as specified in the "Materials and methods" section. The specific data points for the PLS models are summarized in the supplementary file. Concerning the evaluation of the data, additionally to our controlled process parameters, the influences of important uncontrolled parameters on the responses of the design of experiments were considered. Especially effects that might occur due to different osmolalities, average cell viabilities and overall process time.

Although only minor variations in osmolality occurred during cell growth (mostly between 290 and 330 mOsm/kg), the influence of variations in osmolality was investigated in separate experiments and no significant differences in cell specific growth, productivity or metabolite production/consumption could be derived for this cell line (data not shown).

The overall batch process time and mean cell viabilities in this study correlate strongly with process pH but not with pO_2 and pCO_2 (Fig. 1). Therefore, effects on product quality data attributed to process pH might furthermore derive from different process times or mean cell viabilities. Effects of pCO_2 and pO_2 were found to be independent from process time. The authors would like to state that due to the complexity of mammalian cell culture processes, only a certain portion of the data variability can be explained by the presented models. Therefore, the goodness of fit R^2, a measure how good the model fits the observed data, and the goodness of prediction Q^2, an estimate of the predictive ability of the model, deviate from the ideal value of 1. However, R^2 and Q^2 values are presented in the corresponding data tables and only significant models with values above 0.5 are discussed.

Effects on cell growth and viability

Cell growth and cell viability are essential parameters that have to be monitored closely during mammalian fermentation processes. This is usually done by automated offline cell counting and live/dead cell staining. Through determination of viable and total cell densities (VCD and TCD) specific cell growth and cell viabilities were evaluated.

Comparing the maximum viable cell density (VCD) of all batch processes, it can be derived that processes at pH 7.0 reached the highest maximum viable cell densities (Fig. 1a). All processes declined in viabilities to values lower than 75 % shortly after limitation of the main C-source. Therefore, differences in maximum VCD derived not only from different growth behavior but furthermore from nutrient availability. Cell viabilities stayed at high values and decreased dramatically as soon as glucose became limiting. Furthermore, slight decreases in cell viabilities could be detected for processes at pH 7.0 and 6.8, most probably due to glutamine limitation before final glucose depletion (Figs. 1b, 2a/b).

Regarding specific cell growth during exponential growth (μ_{max}) and total growth phase ($\mu_{average}$) significant influences of pH, pO_2 and pCO_2 as well as a significant interaction of pH and pCO_2 could be detected (Table 2). μ_{max} and $\mu_{average}$ were strongly affected by process conditions, whereby the lowest growth rates were reduced to
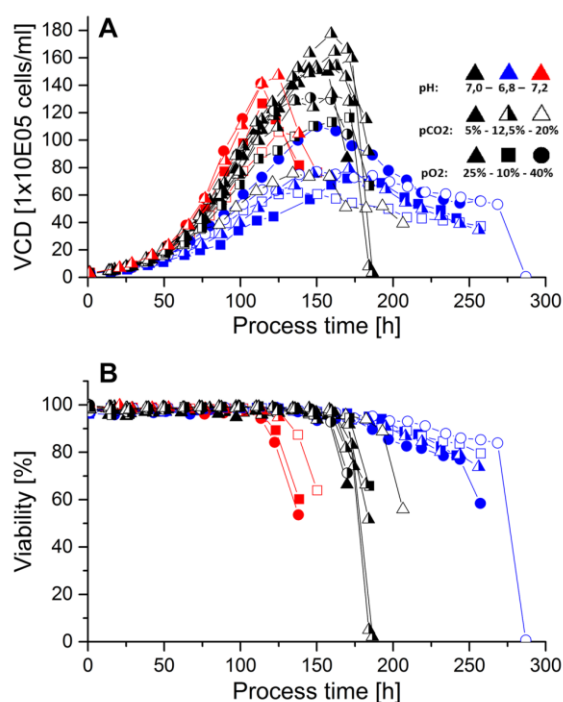
Fig. 1 Viable cell density (**a**) and cell viability (**b**) over process time for all batch fermentations. (*Black symbols* represent processes at pH 7.0, *blue symbols* at pH 6.8, *red symbols* at pH 7.2; *closed symbols* represent processes at pCO_2 5 %, *half-closed* at 12.5 % and *open symbols* at 20 %; *triangles* represent processes at pO_2 25 %, *squares* at 10 %, *circles* at 40 %). High pH values led to high viable cell densities but concurrently to shorter process time due to faster depletion of the main c-source. Cell viabilities stayed at high values as long as glutamine was available

around 35 and 45 %, respectively, when compared to the maximum values obtained in this DoE.

Table 2 shows that pH affected specific cell growth the most and higher pH values led to higher cell growth. Increased pCO_2 had a negative impact on cell growth, whereas increased pO_2 seemed to stimulate specific cell growth between the borders of our experimental design. These general results confirm other publications as Link et al. [15], Yoon et al. [25], Trummer et al. [13] and Dezengotita et al. [18]. Remarkably, through the independent control of process parameters our study derived additional significant interaction effects of pH and pCO_2 on specific growth.

Effects on cell metabolism and productivity

CHO cell metabolism strongly depends on the main carbon and energy sources, glucose and glutamine. Furthermore, by-product accumulation can be of high interest since lactate and ammonia concentrations can affect cell

physiology at elevated levels [26]. Moreover, specific productivity of cells is clearly of high importance, because final product titer levels are directly correlated with this entity. Additionally, amino acids are one of the most important cell culture media components, influencing cell growth and productivity [27].

In Table 2 the result for the DoE evaluation regarding the average specific glucose uptake rate q_{gluc} is shown. q_{gluc} was significantly influenced by process pH whereby lowest rates were reduced to around 60 % when compared to the maximum consumption rates obtained in this DoE. No significant pO_2, pCO_2 or quadratic/interaction terms could be determined. These results can be confirmed by other studies [13, 25, 26].

The mean specific glutamine uptake rate was not significantly influenced by pH or pCO_2 or pO_2 (data not shown). Concerning pH this is in accordance to the results from Yoon et al. [25] but contrary to Trummer et al. [13] who observed higher specific consumption rates at higher pH values. Processes at high pH values depleted earlier of glutamine than processes at low pH (Fig. 2). Since no effects on specific glutamine uptake rates could be determined, this effect is most probably due to higher viable cell densities and thus higher total glutamine consumptions at high pH values.

The average specific lactate production rate q_{lac} was significantly affected by process conditions (Table 1), whereby lowest rates were reduced to around 80 % when compared to the maximum production rates obtained in this study. Comparing the specific lactate production q_{lac} during the growth phase, data clearly shows a direct link between pH and lactate production. Runs at highest pH values produced significantly more lactate than cells at lower pH. This effect is well reported in literature [13]. Furthermore, the yield of glucose to lactate was affected by culture pH, higher pH values leading to higher yields. Dependencies of q_{lac} from pO_2 or pCO_2 could not be found.

No significant effects of either pH, pCO_2 or pO_2 on specific ammonia production could be observed (data not shown). This is in agreement with the results from Yoon et al. [25] but contrary to Trummer et al. [13], who found a dependency of specific ammonia production from culture pH. The contrary findings on specific ammonia production and glutamine consumption in the stated literature may indicate that effects on ammonia and glutamine metabolism are more cell line specific than effects on glucose and lactate metabolism.

Due to higher specific glucose consumption rates and higher cell growth, processes became glucose-limited earliest at pH 7.2 (Fig. 2a). Ammonia profiles varied between phases of ammonia production and consumption throughout most processes at 7.0 (Fig. 2c). All fermentation runs at
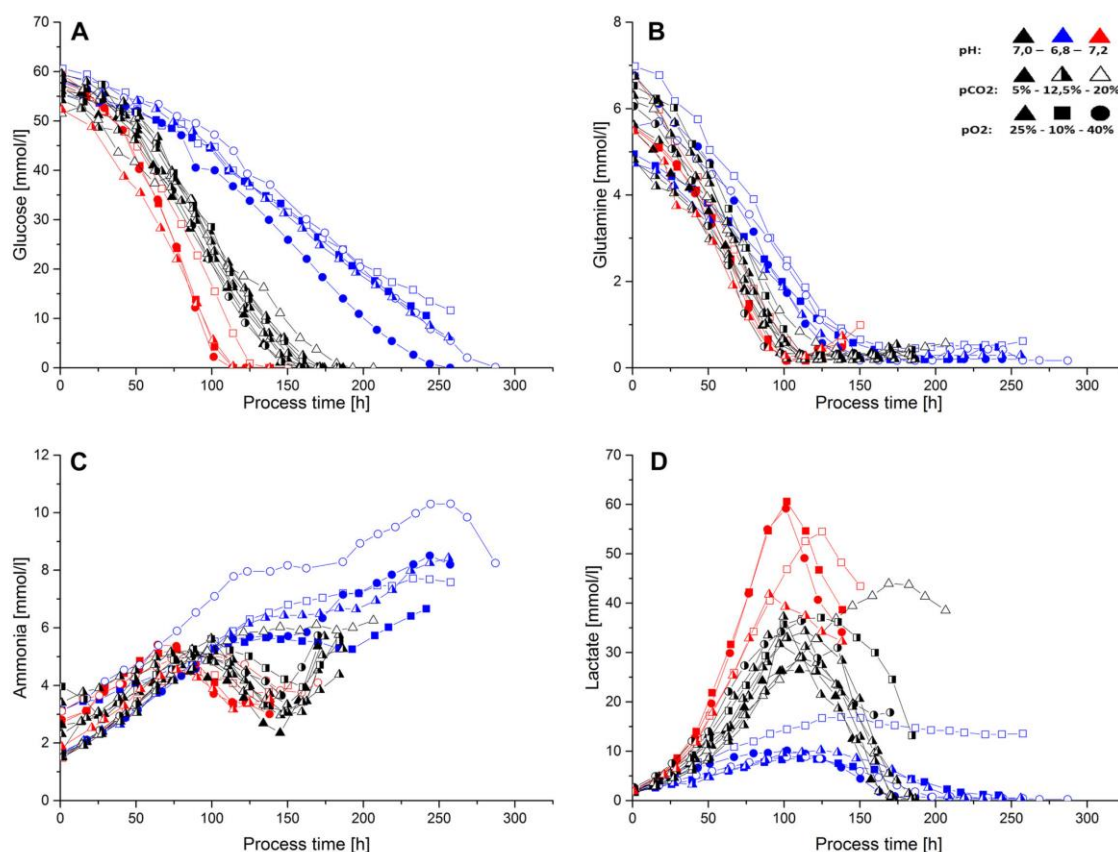
Fig. 2 Metabolite profiles for all conducted batch processes. (*Black symbols* represent processes at pH 7.0, *blue symbols* at pH 6.8, *red symbols* at pH 7.2; *closed symbols* represent processes at $p\mathrm{CO_2}$ 5 %, *half-closed* at 12.5 % and *open symbols* at 20 %; *triangles* represent processes at $p\mathrm{O_2}$ 25 %, *squares* at 10 %, *circles* at 40 %). **a** Glucose became limiting in almost all fermentations before reaching the harvest criteria of 75 % viability. **b** Glutamine profiles showed glutamine limitations after 100–150 h of process time for all batches. **c** Ammonia concentrations showed process phases of production and consumption for almost all runs at pH values of 6.8 and 7.0, whereas only production and steady-state values were derived from fermentation runs at pH 6.8. **d** Lactate was produced and consumed during all processes

Table 2 Coefficient table and summary of fit of the models obtained for specific growth rates, specific glucose consumption, specific lactate and IgG production rates

	pH	$p\mathrm{O_2}$	$p\mathrm{CO_2}$	$\mathrm{pH^2}$	$p\mathrm{O_2^2}$	$p\mathrm{CO_2^2}$	$\mathrm{pH} \times p\mathrm{CO_2}$	R^2	Q^2	MV	RP
μ_average	0.83	0.28	−0.18	–	–	–	−0.18	0.88	0.70	0.93	0.79
μ_max	0.67	0.32	−0.18	−0.19	−0.21	−0.22	−0.23	0.95	0.82	0.87	0.90
q_glucose	−0.85	–	–	−0.26	–	–	–	0.82	0.78	0.65	0.89
q_lactate	0.93	–	–	–	–	–	–	0.87	0.85	0.98	0.65
q_p	0.58	0.34	*−0.14*	–	–	−0.31	−0.28	0.76	0.55	0.63	0.81

The coefficients according to the individual factors of the DoE are normalized. Coefficients that are shown in italic are not considered as significant regarding the applied significance level

pH 6.8 showed no significant ammonia consumption over process time and thus resulted in general higher final ammonia concentrations. Similar to Li et al. [28] low levels of lactate during the lactate consumption phase, present at most processes at pH 7.0 and 6.8, led to the consumption of alanine (data not shown) and subsequently to an increase in final ammonia levels.

Additionally to glutamine, 19 other amino acids were analyzed by HPLC. Specific consumption or production rates were calculated during the growth phase and

significant models could be derived for nine amino acids (Table 3). Hereby, higher pH values led to a higher consumption of several amino acids (Ser, Asp, Val, Ile, Arg and His). Similar effects were reported from Trummer et al. [13]. Furthermore, significant effects of pO_2 and pCO_2 on various amino acid consumption rates could be derived indicating higher consumption rates at process conditions that were favorable for cell growth (μ_{max}, $\mu_{average}$). To our knowledge, no effects of pO_2 or pCO_2 on specific amino acid consumption or production rates in CHO cells have been shown before in the literature. Seven out of nine specific amino acid consumption or production rates were significantly affected by process parameter interactions; this demonstrates that interaction effects of process parameters on cell physiology have to be considered.

Amino acids could be divided into three groups. The first group consisted of amino acids that were only consumed throughout the batch processes (Arg, Val, Phe, Iso, Leu, Pro, Asn, Ser, His, Tyr, Lys, Trp and Met), the second contains amino acids that were only produced over process time (Gly, Cys, Glu) and the last one consists of aspartate and alanine, which were produced and/or consumed during the batch processes (data not shown). In contrast to Trummer et al. [13], aspartate was only produced at lower pH values. Processes were not limited in any amino acid before process harvest except of glutamine for processes at pH 7.0 and 6.8 (Fig. 2b). Similar to effects reported from Zagari et al. [29] and Wahrheit et al. [30] cells reacted to glutamine limitation via uptake of alternative carbon sources as lactate and aspartate, except processes at pH 7.0, pCO_2 20 %, pO_2 25 % and pH 6.8, pCO_2 20 % and pO_2 10 % which showed no lactate consumption or very low consumption after glutamine limitation (Fig. 2d).

The average specific IgG production rate q_P was significantly affected by process conditions, whereby lowest rates were reduced to around 30 % when compared to the maximum production rates obtained in this study.
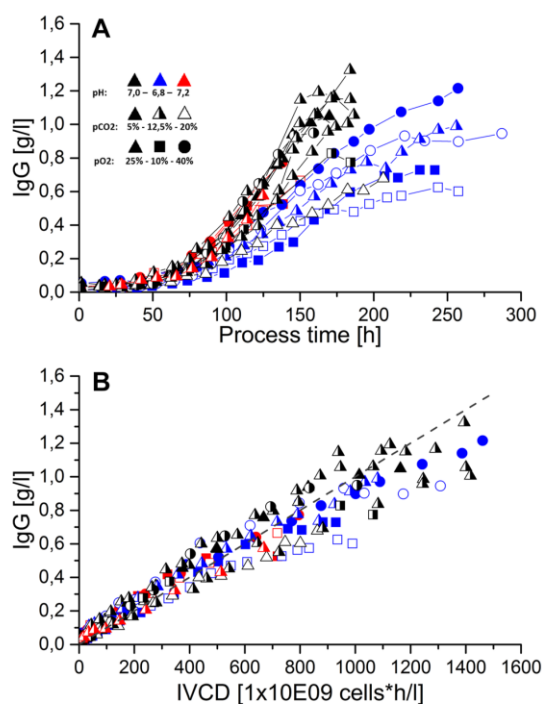
The model data out of Table 2 indicates that pH strongly affected specific productivity in a way that high pH set points led to high q_p values. Furthermore, quadratic effects of pCO_2, linear effects of pO_2 and an interaction term of pCO_2 and pH were identified. Positive effects of pO_2 on q_p are also reported in Link et al. [15], whereas Trummer et al. [13] found no connections between pO_2 and q_p. Concerning pCO_2 Gray et al. [20] showed optimum levels around 76 mmHg, which is in agreement with our findings. No effects of culture pH on q_p could be shown in studies from Trummer et al. [13] and Yoon et al. [25]. However, other authors reported similar results, whereby q_p increased with increasing pH between pH 6.8 and 7.2 [31]. Contradictions between the stated findings might derive from the different cell lines used in these studies. Additionally, pH and pCO_2 interaction effects similar to those already observed for $\mu_{average}$ and μ_{max} could be detected for q_p. To our knowledge, no interaction effects of pH and pCO_2 on cell specific productivity have been reported so far in the literature. The derived model showed similar coefficients to that one obtained for μ_{max} and $\mu_{average}$. This indicates that fermentation conditions that induce high specific growth rates also induce high specific production rates for this cell line.

Overall process titer of batch processes was mostly dependent from the integral viable cell density similar to Trummer et al. [13]. Therefore, highest final product concentrations could be derived at pH 7.0 and 6.8, whereas space–time-yields were higher for processes at pH 7.0 (Fig. 3).

Effects on critical quality attributes (CQAs)

Size exclusion chromatography (SEC) for determination of antibody size heterogeneity

During manufacturing and storage antibody size variants (e.g., aggregates and fragments) occur. Since size variants can influence immunogenicity, potency and

Table 3 Coefficient table and summary of fit of the models obtained for specific amino acid production and consumption rates

	pH	pO_2	pCO_2	pH^2	pCO_2^2	pH × pCO_2	pH × pO_2	R^2	Q^2	MV	RP
q_{Asp}	−0.58	−0.2	−0.25	–	0.67	–	–	0.96	0.82	0.91	0.91
q_{Glu}	–	–	−0.76	–	0.39	–	–	0.76	0.69	0.90	0.66
q_{Ser}	−0.45	–	−0.47	*−0.31*	*−0.22*	0.26	–	0.82	0.58	0.90	0.67
q_{His}	−0.36	−0.37	*−0.13*	*−0.29*	–	0.37	–	0.75	0.52	0.75	0.71
q_{Arg}	−0.67	−0.59	*−0.2*	–	−0.2	–	0.24	0.93	0.72	0.79	0.90
q_{Gly}	*−0.20*	−0.58	0.37	–	–	–	0.42	0.81	0.63	0.52	0.89
q_{Cys}	−0.31	−0.57	–	–	–	–	0.49	0.78	0.70	0.77	0.78
q_{Val}	−0.58	–	*0.12*	–	−0.49	0.32	–	0.94	0.61	0.57	0.95
q_{Ile}	−0.44	–	*0.20*	–	−0.31	0.47	–	0.77	0.51	0.33	0.92

q_{Gly} and q_{Cys} refer to specific amino acid production and all other amino acids to consumption rates. The coefficients according to the individual factors of the DoE are normalized. Coefficients that are shown in italic are not considered as significant regarding the applied significance level

Fig. 3 IgG concentration over process time (**a**) and integral viable cell density (**b**) for all batch fermentations. (*Black symbols* represent processes at pH 7.0, *blue symbols* at pH 6.8, *red symbols* at pH 7.2; *closed symbols* represent processes at pCO_2 5 %, *half-closed* at 12.5 % and *open symbols* at 20 %; *triangles* represent processes at pO_2 25 %, *squares* at 10 %, *circles* at 40 %). Highest process titers were obtained for fermentation runs conducted at pH 7.0 and 6.8, mainly due to the highest IVCD values at these process conditions

pharmacokinetics their levels are monitored during lot release, stability and characterization [32].

Data out of SEC analysis show minor variations with overall purity levels between 96 and 98 % relative Area (data not shown). PLS models for sum of aggregates and sum of fragments were conducted. No dependencies of pCO_2, pO_2 or pH on antibody aggregation or fragmentation were obtained from the gathered model data. Jing et al. [33] observed a significant increase in protein aggregation when changing dissolved oxygen from 50 to 15 % air saturation. Concerning pH, values far away from the isoelectric point of the desired antibody showed better protein solubility [34, 35, 36]. In contrast to Gomes and Hiller [37], we could not detect any changes in protein aggregation when varying culture conditions in between the DoE settings. The mechanisms leading to product aggregation may be strongly product specific, explaining the differences between the results in the literature.
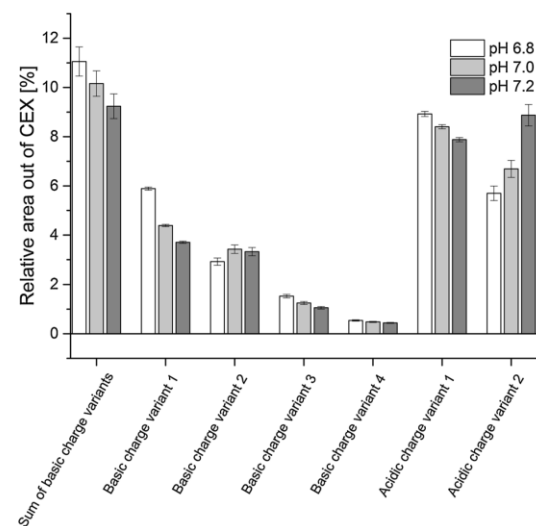
Cation exchange chromatography (CEX) for determination of antibody charge heterogeneity

Charge based antibody characterization is a frequently used tool since it is sensitive to many type of modifications as protein conformation, size, sequence species, glycosylation and posttranslational modifications [11]. Therefore, various antibody variations that occur with changing process conditions were detected.

In total, we detected 18 different charge variants, whereby significant models could be obtained for six individual variants (i)–(vi) and one sum parameter (Fig. 4; Table 4).

(i) The content of acidic charge variant 1 (deamidation of asparagine to aspartate on one light chain) was significantly influenced by culture pH (Table 4). Deamidation is an unavoidable alteration reaction that takes place in fermentation broth after secretion of the cell. Deamidation can finally contribute to heterogeneity; affect protein crystallization, stability and efficacy [38, 39]. Therefore, Liu et al. [40] considered Asn deamidation as one of the most important common modifications for mAbs. Deamidation in our batch process data differed significantly, whereas at pH 6.8 the highest protein deamidation could be observed (Fig. 4). In contradiction to the literature, our studies would suggest that lower pH values lead to higher deamidation rates [41].

(ii) Considering acidic species 2 lower pH values led to lower acidic variants (Fig. 4; Table 4). Additionally, a

Fig. 4 Relative area out of cation exchange chromatography (CEX) for various charge variants and one sum parameter at different pH set points for pCO_2 12.5 % and pO_2 25 %

Table 4 Coefficient table and summary of fit of the models obtained for the mAb charge variants and one glycan variant

	pH	pO_2	pCO_2	pH^2	pO_2^2	pCO_2^2	$pH \times pCO_2$	R^2	Q^2	MV	RP
(i) ACV 1	−0.44	–	*0.37*	*0.24*	–	*0.28*	*−0.22*	0.67	0.57	0.78	0.67
(ii) ACV 2	0.94	–	*−0.04*	–	–	–	−0.15	0.92	0.84	0.94	0.86
(iii) BCV 1	−0.65	*0.13*	0.17	–	*0.27*	*0.29*	–	0.87	0.72	0.59	0.90
(iv) BCV 2	0.74	–	–	−0.58	–	–	–	0.72	0.60	0.38	0.90
(v) BCV 3	−0.88	–	–	–	–	–	–	0.77	0.73	0.68	0.85
(vi) BCV 4	−0.73	–	0.41	–	–	–	–	0.78	0.71	0.78	0.81
sum of basic variants	−0.64	0.19	0.17	–	0.22	*0.3*	–	0.82	0.59	0.64	0.84
bG1FSA_2	*−0.03*	–	−0.26	0.67	–	–	−0.48	0.76	0.53	0.84	0.68

The coefficients according to the individual factors of the DoE are normalized. Coefficients that are shown in italic are not considered as significant regarding the applied significance. Acidic charge variants (ACV), basic charge variants (BCV) and one glycan variant are presented

significant interaction term for pH and pCO_2 affecting acidic variant 2 was identified.

(iii) Isomerization of Asp on one heavy chain, basic charge variant 1, is congeneric to the deamidation reaction leading to acidic charge variant 1. The isomerization reaction occurs spontaneously in the culture media [38]. Data shows that pH had a significant effect on isomerization whereby at lower pH values, higher amounts of isomerized variants occurred (Fig. 4; Table 4). These findings are in agreement with the literature [42]. Analogous to Asn deamidation, Asp isomerization is considered as one of the most important common modifications for mAbs [40].

(iv, v) The presence of lysine residues on one heavy chain, basic charge variant 2, was significantly affected by culture pH (Fig. 4; Table 4). Moreover, the amount of lysine residues on both heavy chains, basic charge variant 3, was also significantly affected by culture pH but with opposite outcome (Fig. 4; Table 4). For charge variant 2, lower culture pH led to lower amount of lysine residues compared to runs at higher pH values. In contrast, models obtained for charge variant 3 showed the opposite effect. C-terminal lysine residues are a very common modification observed during monoclonal antibody production. After cell lysis, the release of basic carboxypeptidase is supposed to be the reason for lysine heterogeneity, since no spontaneous reactions were found in other studies [39, 43–45]. Lower cell viabilities and prolonged process time at pH 6.8, therefore, should have led to a better cleavage of lysine residues from the antibody. Interestingly, this is only the case for lysine residue 2 whereas for charge variant 3 the opposite effect is visible. C-terminal lysine residues are considered as a rather less important mAb modification [40].

(vi) The amount of basic charge variant 4 was significantly influenced by process pH. The higher the pH value, the lower the amount of basic charge variant 4 (Fig. 4; Table 4). Moreover, a significant linear correlation with pCO_2 could be conducted out of the PLS model.

Glycosylation profile analysis for determination of N-glycosylation heterogeneity

Proper glycosylation of mAbs is of upmost importance since it can influence stability, effector functions, immunogenicity and pharmacokinetics of the desired product [17]. 21 different glycosylation patterns could be identified whereby the only significant model concerning data from glycosylation analysis could be obtained for glycosylation pattern bG1FSA_2 (di-*N*-acetylneuraminic acidylated, mono-galactosylated, biantennary, fucosylated) (Table 4). Significant single effects of process pH and an interaction term with pCO_2 on glycosylation variant bG1SA_2 were obtained. Analogous to Zanghi et al. [19], these results would suggest a lower sialylation at higher dissolved carbon dioxide and higher pH values. Around 75 % of the observed glycosylation profiles consisted of bG0F (biantennary, fucosylated) and bG1F (biantennary, mono-galactosylated, fucosylated) independent from process conditions similar to Agarabi et al. [46] and as reported by Raju et al. [47]. Furthermore, galactosylation, sialylation and afucosylation level (GI, SI, aFI) variations stayed in between narrow limits, mostly 25–30 % GI, 0.5–1.5 % SI and 4–8.0 % aFI, for all batch processes. Moreover, GI, aFI and SI variation between center point runs covered most glycosylation variations observed.

When plotting GI over SI and aFI, GI values correlate positively with aFI and SI values (Fig. 5a linear determination coefficient $R^2 = 0.66$; Fig. 5b linear determination coefficient $R^2 = 0.36$). This indicates that afucosylation, sialylation and galactosylation were all influenced likewise by process conditions. Additionally, highest SI levels could be observed mostly for pH values of 7.2. Furthermore, lowest SI levels did not occur for high pO_2 values at 40 %. Regarding sialylation and process pH similar trends could be detected from Ivarsson et al. [17]. Moreover, high sialylation correlated with high Mannose 8 (Fig. 5c linear determination coefficient $R^2 = 0.82$) variants but not with Mannose 6 variants. Finally, highest amounts of mannose 6 and 8 variants
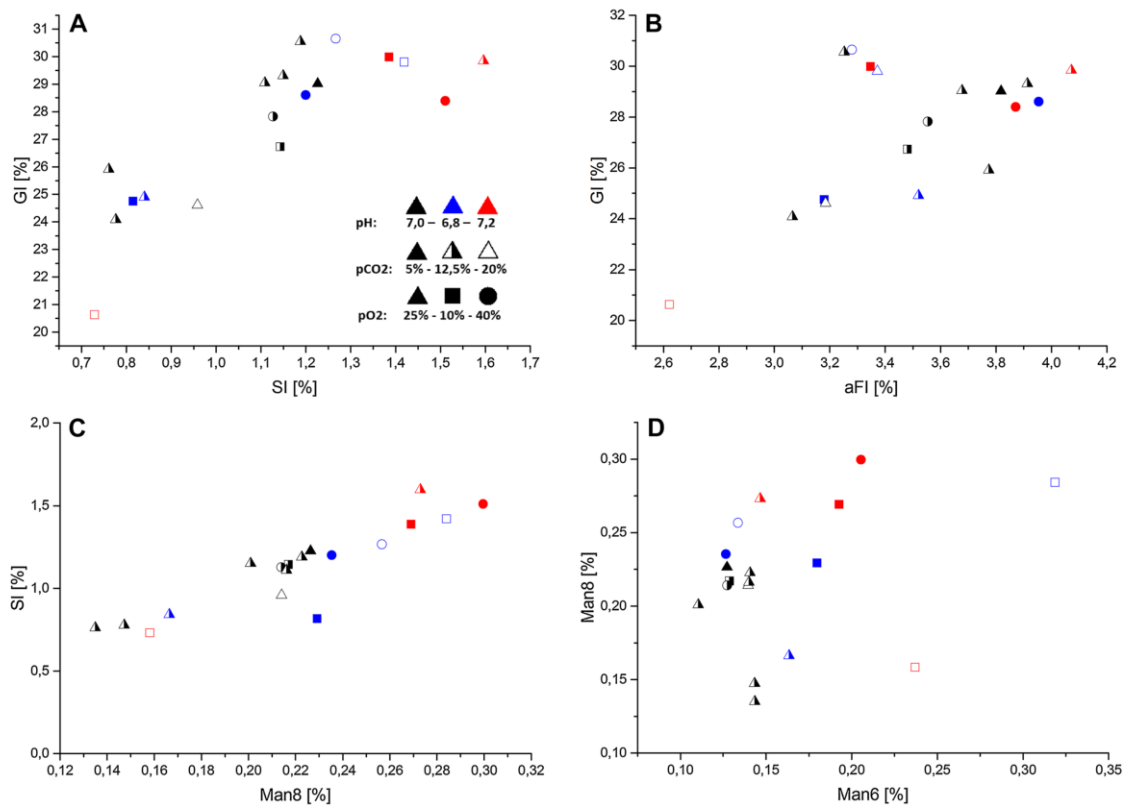
Fig. 5 Correlations and trends of glycosylation variants. (*Black symbols* represent processes at pH 7.0, *blue symbols* at pH 6.8, *red symbols* at pH 7.2; *closed symbols* represent processes at pCO_2 5 %, *half-closed* at 12.5 % and *open symbols* at 20 %; *triangles* represent processes at pO_2 25 %, *squares* at 10 %, *circles* at 40 %). Antibody galactosylation level (GI) over **a** sialylation (SI) and **b** afucosylation could only be observed for pH values at 6.8 and 7.2 (Fig. 5d).

(aFI). Antibody galactosylation seemed to correlate positively with afucosylation and sialylation. A strong correlation between sialylation and mannosylation 8 were derived from C. In D, mannose 8 levels are plotted over mannose 6, it can be derived that highest mannosylation levels only occurred for processes at pH 6.8 and 7.2

A huge amount of process variables affecting protein glycosylation in mammalian cells have been reported as substrate concentrations, media composition, by-product accumulation, temperature, cell viability and shear stress [48]. Literature about the influence of process parameters on mAb glycosylation are partly contradicting and seem to be strongly dependent on the specific cell line, product and cultivation conditions. Concerning pO_2 variations different results are reported but consistent glycosylation profiles can be expected for DO between 10 and 100 % [48]. Ivarsson et al. [17] stated a slight increased protein galactosylation and sialylation at low DO 10 % and high DO 90 % compared to 50 % DO. Studies about the influence of pCO_2 on glycosylation are less represented. Nevertheless, Zanghi et al. [19] and Kimura and Miller [49] showed decreased polysialylation and *N*-glycolylneuraminic acid (NGNA) when increasing pCO_2. Trummer et al. [13] reported no effect on EPO-FC sialylation

when varying DO between 10 and 100 % and pH between 6.8 and 7.3. In contrast, Ivarsson et al. [17] recently showed that galactosylation and sialylation levels slightly increased when pH increased between 6.8 and 7.2.

Finally, through our applied control strategy and experimental design, we could not only detect independent single process parameter effects on cell physiology and product quality but also furthermore derive several new process parameters interaction effects. A short summary of several key responses affected by process parameter interactions is given in Table 5.

Conclusions

The goal of this contribution was to assess the interactions of scale dependent process parameters and their independent effects in a multivariate manner. Only, the decoupled

Table 5 Summary table of key responses affected by process parameter interactions as well as the observed single parameter effects and literature comparison

	Observed single parameter effects	Process parameter interactions	Literature
$\mu_{average}$	Higher at increased pH, and pO_2; quadratic pCO_2 effects	pH × pCO_2	Similar single effects [13, 15, 18, 25]
q_p	Higher at increased pH, and pO_2; quadratic pCO_2 effects	pH × pCO_2	Similar single effects [15, 20]; Contrary single effects [13, 25]
q_{AA}	Higher uptake rates and lower production rates of several amino acids at increased pH and pO_2; contrary effects of pCO_2	pH × pCO_2/ pH × pO_2	Similar single effects of process pH [13]
mAb acidic charge variant (ACV 2)	Higher at increased process pH	pH × pCO_2	No literature available since variant identity is unknown
mAb sialylation (bG1FSA_2)	Quadratic pH effects	pH × pCO_2	Similar interaction effect [19]

Key responses with process parameter interaction effects: average specific cell growth ($\mu_{average}$), specific productivity (q_p), specific amino acid consumption/production rates (q_{AA}), acidic charge variant 2 and mAb sialylation variant bG1FSA_2. Effects are only valid inside of the experimental design space. Contradictions to/in literature may derive from cell line specific effects. More detailed information is presented in the corresponding paragraphs of the "Results and discussion" section

control of process pH, pO_2 and pCO_2, allowed us to execute a design of experiments to investigate the interactions and independent influences of these parameters on CHO cell physiology, process performance and critical product quality attributes.

Concerning cell specific growth, glucose consumption, lactate production, amino acid metabolism and specific productivity process pH seemed to provoke the strongest effects. Variations of pO_2 and pCO_2 exerted influence on cell growth as well as on specific productivity, whereby we found a positive correlation for dissolved oxygen and mostly quadratic interactions for pCO_2 with an optimum at around 10 % (90 mmHg). Amino acid metabolism was mainly affected by pH, but the gathered data revealed additional interactions and single effects of pO_2 and pCO_2.

Besides process performance, final product quality is of upmost importance for pharmaceutical bioprocesses. Therefore, critical quality attributes (CQAs), such as charge and size heterogeneity as well as N-glycosylation pattern were investigated. Concerning mAb aggregation and fragmentation no correlations with process pH, pO_2 or pCO_2 could be obtained. Significant correlations between process pH or pCO_2 with mAb charge modifications as asparagine deamidation and aspartate isomerization could be derived from data out of cation exchange chromatography. The effect of process parameters on N-glycosylation heterogeneity is reported contradictorily in the literature and seems to be strongly dependent from the specific cell line, product and further cultivation conditions. In our study, positive correlations between antibody galactosylation, afucosylation and sialylation were found. Furthermore, highest sialylation levels could mostly be detected at

pH 7.2 and highest mannose variants (Man8 and Man6) could only be observed at two distinct pH set points.

In the end, novel interactions that could be derived are pH and pCO_2 interaction effects on specific cell growth (μ_{max}, $\mu_{average}$) and specific productivity (q_P). Moreover, several interaction effects of pO_2 and pCO_2 with pH on amino acid metabolism, as well as pCO_2 and pH interactions on mAb charge variants and N-glycosylation variants were identified.

The presented results demonstrate the necessity to consider process parameter interactions on cell physiology, overall process performance and product quality. In large-scale processes, heterogeneities and gradients of process pH, pO_2 and pCO_2 can occur, exposing cells dynamically to changing environments. Therefore, not only the single parameter influences but also their interaction effects vary inside of large-scale processes. Especially process pH and pCO_2 are usually coupled in cell culture processes, whereby zones with high pH, as they can appear due to base addition from top, simultaneously lead to low pCO_2 values, whereas pCO_2 accumulation can lead to zones with lower pH values, respectively. Based on our results, pH variations that might occur due to CO_2 accumulation or base addition in large-scale are most probably the dominant factor concerning process parameter induced scale-up effects. CO_2 accumulation in large-scale can furthermore reduce specific cell growth, specific productivity and affect amino acid metabolism. In our experiments, pO_2 had the lowest effects on cell physiology and product quality. Therefore, temporary pO_2 gradients that might occur in large-scale most probably only exert minor effects on process performance and CQAs. Based on the results of

this study the consideration of process parameter interactions is recommended for mechanistic and hybrid modeling approaches as well as scale-up tasks.

Conflict of interest The authors declare no financial or commercial conflict of interest.

References

1. Spadiut O, Capone S, Krainer F, Glieder A, Herwig C (2014) Microbials for the production of monoclonal antibodies and antibody fragments. Trends Biotechnol 32(1):54–60. doi:10.1016/j.tibtech.2013.10.002
2. Kim JY, Kim YG, Lee GM (2012) CHO cells in biotechnology for production of recombinant proteins: current state and further potential. Appl Microbiol Biotechnol 93(3):917–930. doi:10.1007/s00253-011-3758-5
3. Hernandez R (2015) Top trends in biopharmaceutical manufacturing: 2015. Pharm Technol 39(6):24–29
4. Omasa T, Onitsuka M, Kim WD (2010) Cell engineering and cultivation of chinese hamster ovary (CHO) cells. Curr Pharm Biotechnol 11(3):233–240
5. Jayapal KP, Wlaschin KF, Hu W-S, Yap MGS (2007) Recombinant protein therapeutics from CHO cells-20 years and counting. Chem Eng Prog 103:40–47
6. International Conference of Harmonisation, ICH Harmonised Tripartite Guideline: Q8(R2) Pharmaceutical Development. (2009). http://www.ich.org/fileadmin/Public_Web_Site/ICH_Products/Guidelines/Quality/Q8_R1/Step4/Q8_R2_Guideline.pdf. Accessed 1 May 2016
7. von Stosch M, Davy S, Francois K, Galvanauskas V, Hamelink JM, Luebbert A, Mayer M, Oliveira R, O'Kennedy R, Rice P, Glassey J (2014) Hybrid modeling for quality by design and PAT-benefits and challenges of applications in biopharmaceutical industry. Biotechnol J 9(6):719–726. doi:10.1002/biot.201300385
8. Lara AR, Galindo E, Ramirez OT, Palomares LA (2006) Living with heterogeneities in bioreactors: understanding the effects of environmental gradients on cells. Mol Biotechnol 34(3):355–381. doi:10.1385/mb:34:3:355
9. Nienow AW (2006) Reactor engineering in large scale animal cell culture. Cytotechnology 50(1–3):9–33. doi:10.1007/s10616-006-9005-8
10. Xing Z, Kenty BM, Li ZJ, Lee SS (2009) Scale-up analysis for a CHO cell culture process in large-scale bioreactors. Biotechnol Bioeng 103(4):733–746. doi:10.1002/bit.22287
11. Rea JC, Wang YJ, Moreno TG, Parikh R, Lou Y, Farnan D (2012) Monoclonal antibody development and physicochemical characterization by high performance ion exchange chromatography. In: Agbo EC (ed) Innovations in biotechnology. InTech, pp 439–464. ISBN: 978-953-51-0096-6, http://www.intechopen.com/books/innovations-in-biotechnology/monoclonal-antibody-development-and-physicochemical-characterization-by-high-performance-ion-exchang
12. Cromwell ME (2006) Formulation, filling and packaging. In: Ozturk SS, Hu W-S (eds) Cell culture technology for pharmaceutical and cell-based therapies, chap 14. Taylor & Francis Group, London, pp 483–522
13. Trummer E, Fauland K, Seidinger S, Schriebl K, Lattenmayer C, Kunert R, Vorauer-Uhl K, Weik R, Borth N, Katinger H, Muller D (2006) Process parameter shifting: part I. Effect of DOT, pH, and temperature on the performance of Epo-Fc expressing CHO cells cultivated in controlled batch bioreactors. Biotechnol Bioeng 94(6):1033–1044. doi:10.1002/bit.21013
14. Kishishita S, Nishikawa T, Shinoda Y, Nagashima H, Okamoto H, Takuma S, Aoyagi H (2015) Effect of temperature shift on levels of acidic charge variants in IgG monoclonal antibodies in Chinese hamster ovary cell culture. J Biosci Bioeng 119(6):700–705. doi:10.1016/j.jbiosc.2014.10.028
15. Link T, Backstrom M, Graham R, Essers R, Zorner K, Gatgens J, Burchell J, Taylor-Papadimitriou J, Hansson GC, Noll T (2004) Bioprocess development for the production of a recombinant MUC1 fusion protein expressed by CHO-K1 cells in protein-free medium. J Biotechnol 110(1):51–62. doi:10.1016/j.jbiotec.2003.12.008
16. Li F, Vijayasankaran N, Shen AY, Kiss R, Amanullah A (2010) Cell culture processes for monoclonal antibody production. mAbs 2(5):466–479
17. Ivarsson M, Villiger TK, Morbidelli M, Soos M (2014) Evaluating the impact of cell culture process parameters on monoclonal antibody N-glycosylation. J Biotechnol 188c:88–96. doi:10.1016/j.jbiotec.2014.08.026
18. Dezengotita VM, Kimura R, Miller WM (1998) Effects of CO_2 and osmolality on hybridoma cells: growth, metabolism and monoclonal antibody production. Cytotechnology 28(1–3):213–227. doi:10.1023/a:1008010605287
19. Zanghi JA, Schmelzer AE, Mendoza TP, Knop RH, Miller WM (1999) Bicarbonate concentration and osmolality are key determinants in the inhibition of CHO cell polysialylation under elevated pCO(2) or pH. Biotechnol Bioeng 65(2):182–191
20. Gray DR, Chen S, Howarth W, Inlow D, Maiorella BL (1996) CO(2) in large-scale and high-density CHO cell perfusion culture. Cytotechnology 22(1–3):65–78. doi:10.1007/bf00353925
21. Ivarsson M, Noh H, Morbidelli M, Soos M (2015) Insights into pH-induced metabolic switch by flux balance analysis. Biotechnol Prog 31(2):347–357. doi:10.1002/btpr.2043
22. Goudar CT, Biener R, Konstantinov KB, Piret JM (2009) Error propagation from prime variables into specific rates and metabolic fluxes for mammalian cells in perfusion culture. Biotechnol Prog 25(4):986–998. doi:10.1002/btpr.155
23. Frahm B, Blank HC, Cornand P, Oelssner W, Guth U, Lane P, Munack A, Johannsen K, Portner R (2002) Determination of dissolved CO(2) concentration and CO(2) production rate of mammalian cell suspension culture based on off-gas measurement. J Biotechnol 99(2):133–148
24. Klein T, Heinzel N, Kroll P, Brunner M, Herwig C, Neutsch L (2015) Quantification of cell lysis during CHO bioprocesses: impact on cell count, growth kinetics and productivity. J Biotechnol 207:67–76. doi:10.1016/j.jbiotec.2015.04.021
25. Yoon SK, Choi SL, Song JY, Lee GM (2005) Effect of culture pH on erythropoietin production by Chinese hamster ovary cells grown in suspension at 32.5 and 37.0 °C. Biotechnol Bioeng 89(3):345–356. doi:10.1002/bit.20353

26. Gódia F, Cairó JJ (2006) Cell metabolism. In: Ozturk SS, Hu W-S (eds) Cell culture technology for pharamceutical and cell-based therapies. Taylor & Francis Group, London, pp 81–112

27. Carrillo-Cocom LM, Genel-Rey T, Araiz-Hernandez D, Lopez-Pacheco F, Lopez-Meza J, Rocha-Pizana MR, Ramirez-Medrano A, Alvarez MM (2015) Amino acid consumption in naive and recombinant CHO cell cultures: producers of a monoclonal antibody. Cytotechnology 67(5):809–820. doi:10.1007/s10616-014-9720-5

28. Li J, Wong CL, Vijayasankaran N, Hudson T, Amanullah A (2012) Feeding lactate for CHO cell culture processes: impact on culture metabolism and performance. Biotechnol Bioeng 109(5):1173–1186. doi:10.1002/bit.24389

29. Zagari F, Jordan M, Stettler M, Broly H, Wurm FM (2013) Lactate metabolism shift in CHO cell culture: the role of mitochondrial oxidative activity. New Biotechnol 30(2):238–245. doi:10.1016/j.nbt.2012.05.021

30. Wahrheit J, Nicolae A, Heinzle E (2014) Dynamics of growth and metabolism controlled by glutamine availability in Chinese hamster ovary cells. Appl Microbiol Biotechnol 98(4):1771–1783. doi:10.1007/s00253-013-5452-2

31. Kim HS, Lee GM (2007) Differences in optimal pH and temperature for cell growth and antibody production between two Chinese hamster ovary clones derived from the same parental clone. J Microbiol Biotechnol 17(5):712–720

32. Lu C, Liu D, Liu H, Motchnik P (2014) Characterization of monoclonal antibody size variants containing extra light chains. mAbs 5(1):102–113

33. Jing Y, Borys M, Nayak S, Egan S, Qian Y, Pan S-H, Li ZJ (2012) Identification of cell culture conditions to control protein aggregation of IgG fusion proteins expressed in Chinese hamster ovary cells. Process Biochem 47(1):69–75. doi:10.1016/j.procbio.2011.10.009

34. Liu H, Gaza-Bulseco G, Faldu D, Chumsae C, Sun J (2008) Heterogeneity of monoclonal antibodies. J Pharm Sci 97(7):2426–2447. doi:10.1002/jps.21180

35. Franco R, Daniela G, Fabrizio M, Ilaria G, Detlev H (1999) Influence of osmolarity and pH increase to achieve a reduction of monoclonal antibodies aggregates in a production process. Cytotechnology 29(1):11–25. doi:10.1023/a:1008075423609

36. Usami A, Ohtsu A, Takahama S, Fujii T (1996) The effect of pH, hydrogen peroxide and temperature on the stability of human monoclonal antibody. J Pharm Biomed Anal 14(8–10):1133–1140

37. Gomes JM, Hiller GW (2008) Use of low temperature and/or low ph in cell culture. US 2008/0269132 A1

38. Terashima I, Koga A, Nagai H (2007) Identification of deamidation and isomerization sites on pharmaceutical recombinant antibody using H218O. Anal Biochem 368(1):49–60. doi:10.1016/j.ab.2007.05.012

39. Zhong X, Wright JF (2013) Biological insights into therapeutic protein modifications throughout trafficking and their biopharmaceutical applications. Int J Cell Biol 2013:19. doi:10.1155/2013/273086

40. Liu H, Ponniah G, Zhang HM, Nowak C, Neill A, Gonzalez-Lopez N, Patel R, Cheng G, Kita AZ, Andrien B (2014) In vitro and in vivo modifications of recombinant and human IgG antibodies. mAbs 6(5):1145–1154. doi:10.4161/mabs.29883

41. Zheng JY, Janis LJ (2006) Influence of pH, buffer species, and storage temperature on physicochemical stability of a humanized monoclonal antibody LA298. Int J Pharm 308(1–2):46–51. doi:10.1016/j.ijpharm.2005.10.024

42. Yi L, Beckley N, Gikanga B, Zhang J, Wang YJ, Chih HW, Sharma VK (2013) Isomerization of Asp–Asp motif in model peptides and a monoclonal antibody Fab fragment. J Pharm Sci 102(3):947–959. doi:10.1002/jps.23423

43. Cai B, Pan H, Flynn GC (2011) C-terminal lysine processing of human immunoglobulin G2 heavy chain in vivo. Biotechnol Bioeng 108(2):404–412. doi:10.1002/bit.22933

44. Dick LW Jr, Qiu D, Mahon D, Adamo M, Cheng KC (2008) C-terminal lysine variants in fully human monoclonal antibodies: investigation of test methods and possible causes. Biotechnol Bioeng 100(6):1132–1143. doi:10.1002/bit.21855

45. Harris RJ (1995) Processing of C-terminal lysine and arginine residues of proteins isolated from mammalian cell culture. J Chromatogr A 705(1):129–134. doi:10.1016/0021-9673(94)01255-D

46. Agarabi CD, Schiel JE, Lute SC, Chavez BK, Boyne MT II, Brorson KA, Khan M, Read EK (2015) Bioreactor process parameter screening utilizing a Plackett–Burman design for a model monoclonal antibody. J Pharm Sci 104(6):1919–1928. doi:10.1002/jps.24420

47. Raju TS, Jordan RE (2012) Galactosylation variations in marketed therapeutic antibodies. mAbs 4(3):385–391. doi:10.4161/mabs.19868

48. Hossler P, Khattak SF, Li ZJ (2009) Optimal and consistent protein glycosylation in mammalian cell culture. Glycobiology 19(9):936–949. doi:10.1093/glycob/cwp079

49. Kimura R, Miller WM (1997) Glycosylation of CHO-derived recombinant tPA produced under elevated pCO_2. Biotechnol Prog 13(3):311–317. doi:10.1021/bp9700162

25

Manuscript 2: Elevated pCO$_2$ affects lactate metabolic shift in CHO cell culture processes

Authors: Matthias Brunner, Philipp, Doppler, Tobias Klein, Christoph Herwig and Jens Fricke

Research Article

Elevated pCO$_2$ affects lactate metabolic shift in CHO cell culture processes

Matthias Brunner[1,2]

Philipp Doppler[1,2]

Tobias Klein[1,2]

Christoph Herwig[1,2]

Jens Fricke[1,2]

[1]Research Division Biochemical Engineering, Vienna University of Technology, Vienna, Austria

[2]CD Laboratory on Mechanistic and Physiological Methods for Improved Bioprocesses, Vienna University of Technology, Gumpendorferstrasse 1a/166, 1060 Vienna, Austria

Correspondence: Dr. Jens Fricke, Research Division Biochemical Engineering, Vienna University of Technology, Gumpendorferstrasse 1a 166/4, 1060 Vienna, Austria.

E-mail: jens.fricke@tuwien.ac.at

Abbreviations: akdh, alpha-ketoglutarate dehydrogenase; **CHO,** Chinese hamster ovary; **g6pdh,** glucose-6-phosphate dehydrogenase; **GPI,** glucose-6-phosphate isomerase; **icdh,** isocitrate dehydrogenase; **mAb**, monoclonal antibody; **maldh,** malate dehydrogenase; **pdh,** pyruvate dehydrogenase; **pepck,** phosphoenolpyruvate carboxykinase; **pk,** puruvate kinase; **R,** redox variable; **VCD**, viable cell density

Abstract

The shift from lactate production to consumption in CHO cell metabolism is a key event during cell culture cultivations and is connected to increased culture longevity and final product titers. However, the mechanisms controlling this metabolic shift are not yet fully understood. Variations in lactate metabolism have been mainly reported to be induced by process pH and availability of substrates like glucose and glutamine. The aim of this study was to investigate the effects of elevated pCO_2 concentrations on the lactate metabolic shift phenomena in CHO cell culture processes. In this publication, we show that at elevated pCO_2 in batch and fed-batch cultures, the lactate metabolic shift was absent in comparison to control cultures at lower pCO_2 values. Furthermore, through metabolic flux analysis we found a link between the lactate metabolic shift and the ratio of NADH producing and regenerating intracellular pathways. This ratio was mainly affected by a reduced oxidative capacity of cultures at elevated pCO_2. The presented results are especially interesting for large-scale and perfusion processes where increased pCO_2 concentrations are likely to occur. Our results suggest, that so far unexplained metabolic changes may be connected to increased pCO_2 accumulation in larger scale fermentations. Finally, we propose several mechanisms through which increased pCO_2 might affect the cell metabolism and briefly discuss methods to enable the lactate metabolic shift during cell cultivations.

1 Introduction

Monoclonal antibody (mAb)-based products nowadays hold a strong share of overall biopharmaceutical product approvals, with Chinese hamster ovary cells (CHO) as their predominant expression system [1]. Media development, process optimization as well as the development of high and stable producer cell lines have led to optimized high-titer production processes [2]. Despite their extensive usage in the biopharmaceutical industry various challenges exist, especially during process scale-up [3-5]. One prominent example is the accumulation of CO_2 during large-scale and perfusion processes, which can result in reduced cell growth and productivity [6-9]. A common feature of mammalian cell culture processes is the metabolic shift from lactate production to lactate consumption, which has been shown to be beneficial for culture viability and final product titer [10, 11]. However, lactate production often increases in large-scale and the metabolic shift to lactate consumption can be reduced or completely absent in comparison to small-scale processes [10, 12]. Several methods have been developed to reduce lactate accumulation during processes, including the usage of alternative carbon sources, modified cell lines with e.g. lactate dehydrogenase-downregulation and specialized process control strategies [13-17]. Nevertheless, most of these methods are difficult to implement for large-scale bioproduction processes [15]. Moreover, the lactate metabolic shift has been shown to vary with media composition and cell lines [16, 18, 19].

Process pH has been shown to be capable of inducing the lactate metabolic shift [20] and the timing of pH shift is known to influence the time point of lactate consumption as well [21]. However, reliable control of the metabolic shift throughout different scales, cell lines and processes is not possible until today, due to missing understanding of the mechanisms leading to net lactate consumption [16, 22]. Process pCO_2 has been shown before to potentially influence specific lactate production [23], but has not been attributed so far to be a critical parameter with direct influence on the lactate metabolic shift phenomena.

In this study, we aimed at analyzing whether elevated pCO_2/HCO_3^- concentrations during batch and fed-batch cultures can affect the lactate metabolic shift. Through time resolved metabolic flux analysis, it was further possible to correlate the onset of lactate consumption to an intracellular

NAD$^+$/NADH ratio, supporting the hypothesis that this metabolic shift is connected to an intracellular redox equivalent balance. The presented results are of high importance for large-scale and perfusion processes, where increased pCO$_2$/HCO$_3^-$ concentrations are most likely to occur and subsequently might lead to a different process performance than expected from small-scale studies.

2 Materials and Methods

2.1 Cell line, seed train and fermentation processes

An industrial CHO cell line producing a monoclonal antibody (mAb) was cultivated in chemically defined media. Precultures for fermentation processes were cultivated in shake flasks and incubated at 10% (75 mmHg) pCO$_2$ and 36.5 °C temperature. Exponentially growing cells were transferred into 3 L glass bioreactors resulting in an inoculation density of 3 x 10^5 cells/mL. A specific control strategy was used to individually control pO$_2$, pCO$_2$ and process pH as described earlier in Brunner et al. [8]. pH was measured by an in-line probe (EasyFerm, Hamilton, United States) and regulated via addition of HCL and NaOH respectively. pO$_2$ was controlled by an in-line probe (VisiFerm, Hamilton, United States). pCO$_2$ was measured and controlled by use of an offgas sensor (BlueInOne, Bluesens, Germany). Batch cultivations were part of a previous Design of Experiments study [8] and processed at 37 °C and different set-points of pH at 7.0 or 7.2, pCO$_2$ at 12.5% or 20% (94 - 150 mmHg) and pO$_2$ at 10% or 25%. Fed-batch cultivations were performed at 36.5 °C and pH set-point was set to pH 7.0 (pH deadband 0.03), whereby temperature was shifted after 60 hours to 33.0 °C. Control cultivations were conducted at pCO$_2$ 12.5% (94 mmHg) and pO$_2$ 40 %. Fermentation runs at elevated pCO$_2$ were cultivated at pCO$_2$ 20% (150mmHg) and pO$_2$ 25% or 40%. Feed A was added continuously to processes starting on day 4 until day 10 and on day 12. Feed B was added continuously starting on day 6 until day 10 and on day 12. Glucose was added to processes as soon as its concentration dropped below 2 g/L with bolus addition to 2 g/L.

2.2 In-process analytics, mAb determination and amino acid measurement

Cultivation samples were taken every 12 h and cell counting/viability determination was performed using the automatic picture analyzer Cedex HiRes Analyzer (Roche, Germany). Osmolality of supernatant was determined via freeze point depression (Mikro-Osmometer TypOM806, Löser, Germany). Analyses of the metabolites glucose, lactate and ammonium were performed using the Cedex Bio HT Analyzer (Roche, Germany). Antibody titer determination was carried out by HPLC (Ultimate 3000, Dionex, United States) with a Protein A sensor cartridge (Applied Biosystems, The Netherlands). Amino acid concentrations were determined by HPLC measurement (Ultimate 3000, Dionex, United States; ZORBAX Eclipse Plus C18 column, Agilent Technologies, United States).

2.3 Time resolved metabolic flux analysis

Metabolic flux analysis was performed as described before in detail by Zalai et al. [21]. Briefly, intracellular metabolic rates were calculated for every point in time of the cultivation using a previously published metabolic network of the central carbon metabolism of CHO cells [24, 25]. Biomass composition of CHO cells was taken from literature [24, 26]. Specific rates of uptake and production of metabolites as well as the specific oxygen uptake rate at sampling time points were used as model inputs and detection of gross measurement errors was performed via data reconciliation as described in literature [27, 28]. Flux constraints and the stoichiometric matrix of the model are presented in the Supporting Information.

2.4 Calculation of specific rates and standard deviations

Calculation of specific cell growth rates and metabolite production or consumption rates was performed for every sampling interval and similar to Sauer et al. [29]. Chemical degradation of glutamine to ammonia was considered [30]. The specific oxygen uptake rate was calculated via the stationary liquid phase balance as described in Ruffieux et al. [31]. Standard deviations of the calculated mean specific rates were determined by Monte-Carlo parameter estimation to generate multiple time-courses for each fermentation similar to Murphy and Young [32] using MATLAB®

(The MathWorks, Inc., USA). Error in prime variables (viable cell density, metabolite and product concentrations) for Monte-Carlo simulation were derived from manufacturer specifications, repeated measurements and published studies that used the same analytical devices [33-35]. Monte Carlo simulation of standard deviations is a useful methodology to capture analytical variability, however all biological variability cannot be derived by this method. Errors of the intracellular fluxes were assumed to be similar to the closely related greater extracellular fluxes as shown by Goudar et al. [36].

3 Results

3.1 Batch cultivations – initial observations

In a previous study, batch fermentations were performed according to a Design of Experiments approach at different constant pH, pCO_2 and pO_2 set-points to investigate the effects of process parameter interactions on cell physiology and process performance [8]. Besides the reported effects, further investigation of the data set with focus on the lactate metabolic shift revealed that out of the 14 different set-point variations in pH, pCO_2 and pO_2, only two processes did not switch from lactate production to consumption after glutamine was depleted in the media. Remarkably, both processes were conducted at high pCO_2 levels (Fig. 1). The presented data-set consists of processes at pH 7.0 and pH 7.2 with variations in high (20%) and low pCO_2 (12.5%) as well as variable pO_2 set-points. Cell growth was reduced at increased pCO_2, resulting in a lower maximum VCD at these conditions (Fig. 1A). We found that processes at elevated pCO_2 did not follow a lactate metabolic shift until both glutamine and glucose depleted, whereas processes at lower pCO_2 already switched from lactate production to consumption right after glutamine depletion (Fig. 1B/C/D). However, at pH 7.2 and pCO_2 12.5% the data set is not that clear since glutamine and glucose depletion occurred close to each other. We have to state that glutamine depletion cannot be fully validated by the data-set due to the resolution of the analytical device at very low glutamine concentrations used in the DoE-study [37]. However, we will use the term depletion for the very low glutamine concentrations measured in the batch studies similar to the results presented by Zagari et al. [15]. To further investigate how elevated pCO_2 levels might affect the

lactate metabolic shift, additional fed-batch cultivations were conducted and metabolic flux analysis was used to reveal intracellular flux distributions.

3.2 Fed-batch cultivations – verification of batch findings

Fed-batch control experiments were conducted at a constant pH of 7.0, pCO_2 12.5% and pO_2 40%. In parallel to each control run one fed-batch culture was performed at the same pH but at elevated pCO_2 levels of 20% and at a pO_2 set-point of 25% or 40%, respectively. The viable cell densities were comparable within the two control runs and within fermentation processes at elevated pCO_2 concentrations (Fig. 2A). However, viable cell densities were reduced at high pCO_2 in comparison to the control cultures. Due to the applied feeding strategy, no depletion of glutamine nor glucose occurred during the processes (Fig. 2B/C). Cultures at high pCO_2 did produce lactate throughout the entire process, whereas both control cultures started to consume lactate around day 5 of the process (Fig. 2D). Before the lactate metabolic shift, all cultures stayed at the lower pH deadband of 6.97 whereas pH profiles slightly changed after the metabolic shift due to the differences in lactate production (data not shown). Hereby cultures at elevated pCO_2 stayed at the lower deadband whereas the control cultures moved to the upper pH deadband at 7.03. The average specific growth as well as metabolite production/consumption rates and average specific oxygen consumption of all fed-batch cultures before and after lactate uptake are presented in Figure 3, whereby the separation between those two phases is indicated by the dotted line in Figure 2. Rates after lactate uptake were calculated until the maximum viable cell density (VCD) of the respective process. Maximum viable cell densities were reached in between day 7.5 to day 8.5 for all processes. The average rates of the controls and the respective cultures at elevated pCO_2 were tested for significant differences with a students t-test and results are presented in the Supporting Information. Average rates of glucose consumption, lactate production as well as specific growth, oxygen uptake rates and specific IgG productivity at elevated pCO_2 were all decreased in comparison to the control cultures before lactate uptake occurred (Fig. 3A). After the occurrence of the metabolic shift in the control cultures, specific glucose consumption was higher at elevated pCO_2 than in the respective controls, whereas specific cell growth and specific oxygen

consumption became more similar (Fig. 3B). Specific productivity stayed at lower values for cultures at increased pCO_2 after the metabolic shift. Final product titers were strongly reduced at high pCO_2 conditions, 1.4 g/L and 1.1 g/L compared to 2.2 g/L and 2.0 g/L respectively, in consequence of the reduced integral viable cell density and specific productivity. During the control cultures a switch from ammonia production to consumption occurred, which was absent in the other fermentations. Moreover, although metabolic rates for glucose consumption and lactate consumption of the control cultures after the metabolic shift seemed to be similar, the specific rates of these metabolites for the cultivations at high pCO_2 and different pO_2 set-points showed several significant differences. Since glutamine has been shown before to be connected to the lactate metabolic shift (Fig. 1) and ammonia profiles of the fed-batch cultures differed strongly (Fig. 4A), the specific glutamine consumption was investigated in more detail. Shortly after cells started to consume lactate in the control cultures, ammonia concentrations started to decline in contrast to the cultures at high pCO_2 (Fig. 4A). The specific ammonia production correlates well with the specific glutamine uptake rate of the cells (Fig. 4B), regardless of the individual fed-batch conditions. As soon as glutamine consumption rates dropped below approx. 0.12 [pmol/(cell*day)], indicated by the horizontal dashed line in Figure 4C, ammonia concentrations decreased. After the metabolic shift occurred, it seemed that cultures at high pCO_2 showed a slightly higher specific glutamine uptake rate than the control cultures (Fig. 4C), however no significant differences could be derived through comparison of the average rates. Subsequently metabolic flux analysis was used to generate a more detailed understanding of the metabolic behavior of the cells under high and low pCO_2 conditions.

3.3 Metabolic flux analysis

Metabolic flux analysis was performed for the fed-batch experiments. A simplified metabolic network is presented in Figure 5. The metabolic model consists of fluxes of the central carbon metabolism of glycolysis, pentose phosphate pathway and TCA cycle. Analogous to the extracellular rates in Figure 3 average intracellular specific metabolite rates were calculated before the uptake of lactate occurred (Fig. 6A) and after the metabolic switch until the end of the

growth phase of the respective process (Fig. 6B). The average rates of the controls and the respective cultures at elevated pCO_2 were tested for significant differences with a students t-test and results are presented in the Supporting Information. In agreement with the results presented in Figure 3A reduced glycolytic influx via glucose-6-phosphate isomerase (GPI) and finally pyruvate kinase (pk) could be observed at increased pCO_2 levels in comparison to the control cultures before the lactate metabolic shift (Fig. 6A). Moreover, TCA cycle fluxes (isocitrate dehydrogenase (icdh), alpha-ketoglutarate dehydrogenase (akdh), malate dehydrogenase (maldh)) were significantly reduced at high pCO_2. Interestingly several fluxes with CO_2 as a reaction product (glucose-6-phosphate dehydrogenase (g6pdh), pyruvate dehydrogenase (pdh), icdh, akdh, maldh, phosphoenolpyruvate carboxykinase (pepck)), indicated by the highlighted arrows in Figure 5, were lower at elevated pCO_2 conditions, resulting in reduced specific carbon dioxide production rates (Fig. 6A). After the metabolic shift, average glycolytic fluxes were higher at processes with elevated pCO_2 set-points, whereas all other intracellular fluxes out of Figure 6Abecame similar to the control reactors (Fig. 6B). Besides the general reduction of the cells metabolism (glycolytic fluxes, TCA cycle fluxes and respiration) at increased pCO_2 before the metabolic shift, we wanted to further investigate if the activity of certain metabolic pathways changed in relation to others (Table 1). The activity of the TCA cycle was defined as the cisaconitase flux similar to Wahrheit et al. [38] and the glycolytic activity was defined by the pyruvate kinase flux.. Respirational activity was represented by the specific oxygen uptake rate. It became evident that not only the overall glycolytic flux decreased under elevated pCO_2, but furthermore the ratio of lactate per pyruvate kinase flux, leading to less lactate production per consumed glucose. Moreover, the ratio of flux entering the TCA cycle per glycolytic flux, represented by the yield of pdh vs pyruvate kinase flux, was increased at high pCO_2. However respirational activity in comparison to the TCA cycle activity was around 10% higher in the control reactors. Since differences in intracellular flux ratios can strongly affect intracellular metabolic equilibria and the redox variable R has been shown before to be connected to lactate production [21], intracellular NADH and NAD^+ production/regeneration were investigated in more detail. The redox variable R is defined as the ratio of the cytosolic NADH produced during

the glycolysis via glyceraldehyde-3-phosphate dehydrogenase (GAPDH) and the mitochondrial capacity for NAD^+ regeneration via the respiratory chain (Fig. 7). Due to a limited capacity of the cell to regenerate NAD^+ via the respiratory chain, possibly caused by NADH transfer limitations through the malate-aspartate shuttle [39], surplus cytosolic NAD^+ can be regenerated via lactate formation. R values above 1 imply that the cells keep producing lactate to regenerate cytosolic NAD^+, whereas an R value below 1 would lead to the complete regeneration of NAD^+ via the respiratory chain and even subsequent consumption of lactate leading to additional production of cytosolic NADH.

The cytosolic NADH producing flux via GAPDH, the mitochondrial NAD^+ regeneration and the redox variable R over process time are presented for all fed-batch fermentations in Figure 8. The cytosolic NADH producing flux before the lactate metabolic shift is higher in the control cultures, compared to the fermentation runs at increased pCO_2 which is in accordance with the previously investigated specific glucose uptake rates (Fig. 8A, Fig. 3). After the metabolic shift, the control cultures showed a reduced cytosolic NADH producing flux due to the lower specific glucose uptake rate in comparison to the processes at elevated pCO_2. The average mitochondrial NAD^+ regeneration was higher in the control cultures than in the processes at increased pCO_2 before the metabolic shift, however values became more similar after the switch from lactate production to consumption (Fig. 8B). The resulting redox variable out of the cytosolic NADH producing flux and the mitochondrial NAD^+ regeneration revealed that cells in the control cultures started to consume lactate as soon as the R value became lower than 1 (Fig. 8C). In contrast cultures at elevated pCO_2 stayed above the critical R value of 1 and did not switch from lactate production to consumption.

4 Discussion

4.1 Batch cultivations

The results of the conducted batch fermentation experiments at different pCO_2 set-points demonstrated that processes at elevated pCO_2 conditions of 20% did not switch from lactate production to consumption after glutamine depletion as long as glucose was available in the

media. Zagari et al. [16] reported similar effects when cultivating two different clones in a batch process. One clone switched from lactate production to consumption after glutamine depletion, whereas the other clone did continue to produce lactate until glucose was depleted as well. Interestingly, the general metabolic behavior regarding the lactate metabolic shift did not change by increasing glucose or glutamine concentrations in their study. In contrast to Zagari et al. [16] however the divergences in metabolic behavior in our experiments were observed with the same clone and only by variations of the pO_2 and pCO_2 concentrations. Due to these observations, additional fed-batch experiments were designed to further investigate the effect of elevated pCO_2 on the lactate metabolic shift phenomena.

4.2 Fed-batch cultivations

During the conducted fed-batch processes, control cultures at 12.5% pCO_2 did switch from lactate production to consumption, whereas cultures at elevated pCO_2 of 20% did produce lactate throughout the entire fed-batch process. Similar to Martinez et al. [40] and Mulukutla et al. [11] data evaluation was split into process phases before and after the lactate metabolic shift. The process phase before the lactate metabolic shift displayed reduced glucose uptake, lactate production and specific oxygen consumption at elevated pCO_2 concentrations. Differences in the cells metabolism occurring before or with the lactate metabolic shift have been hypothesized before to be the major causes for the observed lactate divergences with the observations occurring after the shift being the cellular response [18]. Furthermore, the reduced specific oxygen consumption rate at elevated pCO_2 before the metabolic shift indicates a minor oxidative capacity of the cells under these conditions, which has been linked before to be connected with continuous lactate production [16, 18]. Average rates of specific oxygen consumption and specific cell growth became similar after the shift, whereas control cultures showed a lower glucose consumption and consumed lactate and ammonia. Differences in the second process phase might be for some part a consequence of the variation in lactate metabolism, but slightly different pH profiles and strongly different osmolality values in the second phase (Fig. 4D) have to be considered as well. As can be seen in Figure 4D the osmolality values of the control cultures and

cultures at elevated pCO2 started to diverge after the metabolic shift and increased osmolality is known to potentially affect cell metabolism. Since glutamine metabolism has been shown before to correlate with the lactate metabolic shift in the batch cultivations and other studies [16, 41] and furthermore ammonia metabolite profiles were strongly different between cultures at low and high pCO_2, the role of glutamine was investigated in more detail. Differences in the ammonia profiles could be directly linked to variations in the specific glutamine consumption rate. The specific glutamine uptake rates (qgln) between the conditions at the time of lactate uptake however were not strongly different and qgln continued to decrease throughout processes at high pCO_2 without lactate consumption. Furthermore, complete glutamine depletion did not induce the lactate metabolic shift during the batch cultures at elevated pCO_2. Therefore, we concluded that the observed differences in the lactate profiles between the fed-batch processes at increased pCO_2 and the control processes did not only derive from variations in the glutamine metabolism.

4.3 Metabolic flux analysis

Via time resolved stoichiometric metabolic flux analysis it was possible to investigate intracellular flux distributions inside of the cells throughout the entire fed-batch processes. Average glycolytic fluxes as well as TCA cycle fluxes were reduced under elevated pCO_2 conditions before the metabolic shift and subsequently led to a lower specific carbon dioxide production under these conditions. A generally lower TCA cycle activity in cultures that do not switch from lactate production to consumption has been observed before by Luo et al. [18], using a metabolomics approach. Furthermore, the yield of lactate per pyruvate kinaseflux was increased and the flux entering the TCA cycle via pyruvate dehydrogenase in relation to the pyruvate kinase flux, decreased under control conditions before the metabolic shift. This led further to an increased ratio of TCA cycle activity to glycolytic activity in both cultures at high pCO_2. Lower fluxes from OAA to PEP via pepck at elevated pCO_2 seemed to contribute to this metabolic divergence. However, reduced yields of lactate from glycolysis most probably derive from a reduced specific glucose consumption as described previously by Konakovsky et al. [14] and Zalai et al. [21]. Moreover, respirational activity in respect to the TCA cycle flux seemed to be higher in the control

cultures, again underlining a correlation of high oxidative capacity and the capability to consume lactate [16, 18]. The equilibrium between cytosolic and mitochondrial reduction equivalents, NADH and NAD$^+$, has been hypothesized before to be connected to the lactate production/consumption state [13, 16, 21, 42]. Furthermore a generally reduced intracellular NADH/NAD$^+$ ratio over process time in a process including a lactate metabolic shift was measured in Templeton et al. [43]. NADH and NAD$^+$ producing/regenerating fluxes were higher in the control cultures before the metabolic shift occurred, whereas NAD$^+$ regeneration became more similar after the shift and NADH producing fluxes became even higher in the cultures at elevated pCO$_2$. These findings were in agreement with the observed differences in glycolytic and TCA cycle fluxes. However, the ratio of cytosolic NADH and mitochondrial NAD$^+$, expressed by the redox variable R, stayed at lower levels in the respective control cultures throughout most of the process. Furthermore, both control reactors dropped below the critical R-value of 1 at the same time they started to consume lactate, whereas cultures with constant lactate production stayed above R-values of 1. Considering the relationship of R and the glycolytic, TCA cycle and respirational fluxes, it could be derived that the increased R-values at elevated pCO$_2$ originated mainly from a strongly reduced respirational activity and subsequent decrease of the produced mitochondrial NAD$^+$ via respiration. Additionally, an increased ratio of TCA cycle activity/glycolytic activity contributed further to a reduced mitochondrial NAD$^+$ concentration.

4.4 Possible mechanistic explanations for the observed effects of pCO$_2$ on cell metabolism

Deriving a mechanistic explanation of the observed effects is not easy, since in contrast to microbial cultures, in mammalian cell culture only a few studies exist concerning pCO$_2$ effects. Moreover, CO$_2$ in cell culture media readily reacts with water to form HCO$_3^-$ (bicarbonate) which is further dependent from process pH [44, 45]. Furthermore, batch fermentations out of a previous study [8], at pH 6.8 and elevated pCO$_2$ values (20%) did switch from lactate production to consumption, pointing to the fact that not elevated pCO$_2$ alone but further increased HCO$_3^-$ at high pH and high pCO$_2$ might be the dominant factor. Additionally, several pH and pCO$_2$ interaction effects on CHO physiology have been reported before [8, 44]. CO$_2$/HCO$_3^-$ may act as a

substrate and product for enzymes and interacts with intracellular pH in mammalian cells, furthermore effects on membrane permeability in microbial cultures are reported [45, 46]. Regulation of enzymes via CO_2/HCO_3^- has been described for yeast by Jones and Greenfield [47]. Their review presents inhibitions of glucose-6-phosphate dehydrogenase (g6pdh), malate dehydrogenase (maldh) and succinate dehydrogenase at elevated HCO_3^- level and they further state that an extreme sensitivity of phosphoenolpyruvate carboxykinase (pepck) to elevated pCO_2 is expected. pCO_2 related product inhibition of enzymes might also occur in mammalians. HCO_3^- is one of the key molecules involved in intracellular pH regulation in mammalians [48]. Several studies have shown that mammalian cells have efficient mechanisms to regulate their intracellular pH [49, 50], however extreme conditions of elevated HCO_3^- concentrations might affect these regulation mechanisms. Intracellular pH is known to potentially affect phosphofructokinase, a key enzyme of the glycolysis [51]. At last, high concentrations of pCO_2/HCO_3^- could react increasingly with hydrogenperoxides to form peroxymonocarbonate ion (HCO_4^-) which is an extremely reactive oxygen species [52, 53]. Since mitochondria are extremely sensitive to oxidative damage [18], the capacity for oxidative phosphorylation could be impaired with increasing HCO_4^- species.

4.5 Methods to induce/facilitate lactate metabolic shift in mammalian cell culture based on the redox variable R

According to the previously shown results, two general approaches can be stated:

(I) Strong *reduction of the glycolytic NADH producing flux* will reduce R and consequently might lead to lactate consumption. Low glucose feeding as applied from Konakovsky et al. [14] can induce lactate consumption as shown in their study. Furthermore, pH-shifts to lower values can strongly reduce glucose consumption rates [8, 54] and have been shown before to induce lactate consumption [55].

(II) *Increasing the mitochondrial NAD^+ regeneration* would be the second approach to reduce R and initiate lactate consumption. At first the selection of a cell line with a generally high oxidative capacity seems to be beneficial [16, 18]. Furthermore, the respiratory capacity could be improved by supplying the phosphorylation enzymes with needed cofactors as proposed by Luo et al. [18].

In this context copper concentrations have been shown before to correlate with the lactate consumption state [19]. Reduction of the TCA cycle flux without the impairment of glycolytic activity would be another possibility to increase mitochondrial NAD^+. Glutamine is directly fed into the TCA cycle and significantly contributes to cell metabolism. Reduction of its specific uptake rate could induce lactate consumption and glutamine depletion has been shown to have the potential to induce the lactate metabolic shift in this and other studies [16].

Based on our results it seems further beneficial to reduce pCO_2/HCO_3^- concentrations to assure lactate consumption. This is especially interesting for large-scale and perfusion processes where high pCO_2 concentrations are most likely to occur. Usage of optimized buffering agents and base, e.g. Na_2CO_3 instead of $NaHCO_3$, can significantly reduce HCO_3^- concentrations [9]. Furthermore, optimized gassing strategies to reduce pCO_2 accumulation should be used [4, 6]. Finally, we have to confine our findings to the used CHO cell line since effects on lactate metabolism may vary with different cell lines as observed before in other studies. However, this publication is to our knowledge the first one to show that elevated pCO_2/HCO_3^- concentrations can potentially affect the lactate metabolic shift mechanism and therefore is intended to draw other researchers attention to consider these effects in their experiments.

Conflict of interest

The authors declare no financial or commercial conflict of interest.

5 References

[1] Walsh, G., Biopharmaceutical benchmarks 2014. *Nat. Biotech.* 2014, *32*, 992-1000.

[2] Kim, J. Y., Kim, Y. G., Lee, G. M., CHO cells in biotechnology for production of recombinant proteins: current state and further potential. *Appl. Microbiol. Biotechnol.* 2012, *93*, 917-930.

[3] Yang, J. D., Lu, C., Stasny, B., Henley, J.*, et al.*, Fed-batch bioreactor process scale-up from 3-L to 2,500-L scale for monoclonal antibody production from cell culture. *Biotechnol. Bioeng.* 2007, *98*, 141-154.

[4] Nienow, A. W., Reactor engineering in large scale animal cell culture. *Cytotechnology* 2006, *50*, 9-33.

[5] Xing, Z., Kenty, B. M., Li, Z. J., Lee, S. S., Scale-up analysis for a CHO cell culture process in large-scale bioreactors. *Biotechnol. Bioeng.* 2009, *103*, 733-746.

[6] Sieblist, C., Hageholz, O., Aehle, M., Jenzsch, M.*, et al.*, Insights into large-scale cell-culture reactors: II. Gas-phase mixing and CO_2 stripping. *Biotechnol. J.* 2011, *6*, 1547-1556.

[7] Lara, A. R., Galindo, E., Ramirez, O. T., Palomares, L. A., Living with heterogeneities in bioreactors: understanding the effects of environmental gradients on cells. *Mol. Biotechnol.* 2006, *34*, 355-381.

[8] Brunner, M., Fricke, J., Kroll, P., Herwig, C., Investigation of the interactions of critical scale-up parameters (pH, pO_2 and pCO_2) on CHO batch performance and critical quality attributes. *Bioprocess Biosys. Eng.* 2016, doi: 10.1007/s00449-016-1693-7.

[9] Goudar, C. T., Matanguihan, R., Long, E., Cruz, C.*, et al.*, Decreased pCO(2) accumulation by eliminating bicarbonate addition to high cell-density cultures. *Biotechnol. Bioeng.* 2007, *96*, 1107-1117.

[10] Abu-Absi, S., Xu, S., Graham, H., Dalal, N.*, et al.*, Cell culture process operations for recombinant protein production. *Adv. Biochem. Eng. Biotechnol.* 2014, *139*, 35-68.

[11] Mulukutla, B. C., Gramer, M., Hu, W. S., On metabolic shift to lactate consumption in fed-batch culture of mammalian cells. *Metab. Eng.* 2012, *14*, 138-149.

[12] Gao, Y., Ray, S., Dai, S., Ivanov, A. R., et al., Combined metabolomics and proteomics reveals hypoxia as a cause of lower productivity on scale-up to a 5000-liter CHO bioprocess. Biotechnol. J. 2016, 11, 1190-1200.

[13] Ma, N., Ellet, J., Okediadi, C., Hermes, P., *et al.*, A single nutrient feed supports both chemically defined NS0 and CHO fed-batch processes: Improved productivity and lactate metabolism. *Biotechnol. Prog.* 2009, *25*, 1353-1363.

[14] Konakovsky, V., Clemens, C., Müller, M., Bechmann, J., *et al.*, Metabolic Control in Mammalian Fed-Batch Cell Cultures for Reduced Lactic Acid Accumulation and Improved Process Robustness. *Bioengineering* 2016, *3*, 5.

[15] Gagnon, M., Hiller, G., Luan, Y. T., Kittredge, A., *et al.*, High-end pH-controlled delivery of glucose effectively suppresses lactate accumulation in CHO fed-batch cultures. *Biotechnol. Bioeng.* 2011, *108*, 1328-1337.

[16] Zagari, F., Jordan, M., Stettler, M., Broly, H., Wurm, F. M., Lactate metabolism shift in CHO cell culture: the role of mitochondrial oxidative activity. *N. Biotechnol.* 2013, *30*, 238-245.

[17] Altamirano, C., Illanes, A., Becerra, S., Cairó, J. J., Gòdia, F., Considerations on the lactate consumption by CHO cells in the presence of galactose. *J. Biotechnol.* 2006, *125*, 547-556.

[18] Luo, J., Vijayasankaran, N., Autsen, J., Santuray, R., *et al.*, Comparative metabolite analysis to understand lactate metabolism shift in Chinese hamster ovary cell culture process. *Biotechnol. Bioeng.* 2012, *109*, 146-156.

[19] Qian, Y., Khattak, S. F., Xing, Z., He, A., *et al.*, Cell culture and gene transcription effects of copper sulfate on Chinese hamster ovary cells. *Biotechnol. Prog.* 2011, *27*, 1190-1194.

[20] Osman, J. J., Birch, J., Varley, J., The Response of GS-NS0 Myeloma Cells to pH Shifts and pH Pertubations. *Biotechnol. Bioeng.* 2001, *75*, 63-73.

[21] Zalai, D., Koczka, K., Parta, L., Wechselberger, P., *et al.*, Combining mechanistic and data-driven approaches to gain process knowledge on the control of the metabolic shift to lactate uptake in a fed-batch CHO process. *Biotechnol. Prog.* 2015, *31*, 1657-1668.

[22] Sellick, C. A., Croxford, A. S., Maqsood, A. R., Stephens, G. M., et al., Metabolite profiling of CHO cells: Molecular reflections of bioprocessing effectiveness. Biotechnol. J. 2015, 10, 1434-1445.

[23] Takuma, S., Hirashima, C., Piret, J. M., Dependence on glucose limitation of the pCO2 influences on CHO cell growth, metabolism and IgG production. *Biotechnolo. Bioeng.* 2007, *97*, 1479-1488.

[24] Wahrheit, J., Nicolae, A., Heinzle, E., Dynamics of growth and metabolism controlled by glutamine availability in Chinese hamster ovary cells. *Appl. Microbiol. Biotechnol.* 2014, *98*, 1771-1783.

[25] Ahn, W. S., Antoniewicz, M. R., Towards dynamic metabolic flux analysis in CHO cell cultures. *Biotechnol. J.* 2012, *7*, 61-74.

[26] Sheikh, K., Forster, J., Nielsen, L. K., Modeling hybridoma cell metabolism using a generic genome-scale metabolic model of Mus musculus. *Biotechnol. Prog.* 2005, *21*, 112-121.

[27] Goudar, C. T., Biener, R. K., Piret, J. M., Konstantinov, K. B., Metabolic flux estimation in mammalian cell cultures. *Methods Mol. Biol.* 2014, *1104*, 193-209.

[28] van der Heijden, R. T., Romein, B., Heijnen, J. J., Hellinga, C., Luyben, K. C., Linear constraint relations in biochemical reaction systems: II. Diagnosis and estimation of gross errors. *Biotechnol. Bioeng.* 1994, *43*, 11-20.

[29] Sauer, P. W., Burky, J. E., Wesson, M. C., Sternard, H. D., Qu, L., A High-Yielding, Generic Fed-Batch Cell Culture Process for Production of Recombinant Antibodies. *Biotechnol. Bioeng.* 2000, *67*, 585-597.

[30] Ozturk, S. S., Palsson, B. O., Chemical Decomposition of Glutamine in Cell Culture Media: Effect of Media Type, pH, and Serum Concentration. *Biotechnol. Prog.* 1990, *6*, 121-128.

[31] Ruffieux, P.-A., von Stockar, U., Marison, I. W., Measurement of volumetric (OUR) and determination of specific (qO2) oxygen uptake rates in animal cell cultures. *J. Biotechnol.* 1998, *63*, 85-95.

[32] Murphy, T. A., Young, J. D., ETA: Robust software for determination of cell specific rates from extracellular time courses. *Biotechnol. Bioeng.* 2013, *110*, 1748-1758.

[33] Huang, L.-C., Lin, W., Yagami, M., Tseng, D.*, et al.*, Validation of cell density and viability assays using Cedex automated cell counter. *Biologicals* 2010, *38*, 393-400.

[34] Bawn, A., Lee, H. W., Downey, A., Xu, J., *et al.*, Metabolic-sensing characteristics of absorption-photometry for mammalian cell cultures in biopharmaceutical processes. *Pharm. Bioprocess.* 2013, *1*, 255-266.

[35] Compton, B. J., Lewis, M. A., Whigham, F., Gerald, J. S., Countryman, G. E., Analytical potential of protein A for affinity chromatography of polyclonal and monoclonal antibodies. *Anal. Chem.* 1989, *61*, 1314-1317.

[36] Goudar, C. T., Biener, R., Konstantinov, K. B., Piret, J. M., Error propagation from prime variables into specific rates and metabolic fluxes for mammalian cells in perfusion culture. *Biotechnol. Prog.* 2009, *25*, 986-998.

[37] Druhmann, D., Reinhard, S., Schwarz, F., Schaaf, C., *et al.*, Utilizing Roche Cedex Bio analyzer for in process monitoring in biotech production. *BMC Proc.* 2011, *5*, P106-P106.

[38] Wahrheit, J., Niklas, J., Heinzle, E., Metabolic control at the cytosol–mitochondria interface in different growth phases of CHO cells. *Metabol. Eng.* 2014, *23*, 9-21.

[39] Gelb, W. G., Brandts, J. F., Nordin, J. H., Changes in sulfhydryl groups of honeybee glyceraldehyde phosphate dehydrogenase associated with generation of the intermediate plateau in its saturation kinetics. *Biochemistry* 1974, *13*, 280-287.

[40] Martínez, V. S., Dietmair, S., Quek, L.-E., Hodson, M. P., *et al.*, Flux balance analysis of CHO cells before and after a metabolic switch from lactate production to consumption. *Biotechnol. Bioeng.* 2013, *110*, 660-666.

[41] Sheikholeslami, Z., Jolicoeur, M., Henry, O., Elucidating the effects of postinduction glutamine feeding on the growth and productivity of CHO cells. *Biotechnol. Prog.* 2014, *30*, 535-546.

[42] Nolan, R. P., Lee, K., Dynamic model of CHO cell metabolism. *Metabol. Eng.* 2011, *13*, 108-124.

[43] Templeton, N., Dean, J., Reddy, P., Young, J. D., Peak antibody production is associated with increased oxidative metabolism in an industrially relevant fed-batch CHO cell culture. *Biotechnol. Bioeng.* 2013, *110*, 2013-2024.

[44] Zanghi, J. A., Schmelzer, A. E., Mendoza, T. P., Knop, R. H., Miller, W. M., Bicarbonate concentration and osmolality are key determinants in the inhibition of CHO cell polysialylation under elevated pCO(2) or pH. *Biotechnol. Bioeng.* 1999, *65*, 182-191.

[45] Blombach, B., Takors, R., CO2 – Intrinsic Product, Essential Substrate, and Regulatory Trigger of Microbial and Mammalian Production Processes. *Front. Bioeng. Biotechnol.* 2015, *3*, 108.

[46] Isenschmid, A., Marison, I. W., von Stockar, U., The influence of pressure and temperature of compressed CO2 on the survival of yeast cells. *J. Biotechnol.* 1995, *39*, 229-237.

[47] Jones, R. P., Greenfield, P. F., Effect of carbon dioxide on yeast growth and fermentation. *Enzyme Microb. Technol.* 1982, *4*, 210-223.

[48] Casey, J. R., Grinstein, S., Orlowski, J., Sensors and regulators of intracellular pH. *Nat. Rev. Mol. Cell. Biol.* 2010, *11*, 50-61.

[49] Wu, P., Ray, N. G., Shuler, M. L., A computer model for intracellular pH regulation in Chinese hamster ovary cells. *Biotechnol. Prog.* 1993, *9*, 374-384.

[50] Brunner, M., Braun, P., Doppler, P., Posch, C.*, et al.*, The impact of pH inhomogeneities on CHO cell physiology and fed-batch process performance – two-compartment scale-down modelling and intracellular pH excursion. *Biotechnol. J.* 2017, doi: 10.1002/biot.201600633, 1600633-n/a.

[51] Erecinska, M., Deas, J., Silver, I. A., The effect of pH on glycolysis and phosphofructokinase activity in cultured cells and synaptosomes. *J. Neurochem.* 1995, *65*, 2765-2772.

[52] Richardson, D. E., Yao, H., Frank, K. M., Bennett, D. A., Equilibria, Kinetics, and Mechanism in the Bicarbonate Activation of Hydrogen Peroxide: Oxidation of Sulfides by Peroxymonocarbonate. *J. Am. Chem. Soc.* 2000, *122*, 1729-1739.

[53] Richardson, D. E., Regino, C. A., Yao, H., Johnson, J. V., Methionine oxidation by peroxymonocarbonate, a reactive oxygen species formed from CO2/bicarbonate and hydrogen peroxide. *Free Radical Biol. Med.* 2003, *35*, 1538-1550.

[54] Trummer, E., Fauland, K., Seidinger, S., Schriebl, K.*, et al.*, Process parameter shifting: Part I. Effect of DOT, pH, and temperature on the performance of Epo-Fc expressing CHO cells cultivated in controlled batch bioreactors. *Biotechnol. Bioeng.* 2006, *94*, 1033-1044.

[55] Ivarsson, M., Noh, H., Morbidelli, M., Soos, M., Insights into pH-induced metabolic switch by flux balance analysis. *Biotechnol. Prog.* 2015, *31*, 347-357.

[56] Goudar, C., Biener, R., Boisart, C., Heidemann, R*., et al.*, Metabolic flux analysis of CHO cells in perfusion culture by metabolite balancing and 2D [13C, 1H] COSY NMR spectroscopy. *Metabol. Eng.* 2010, *12*, 138-149.

Table 1. Average intracellular yields before the metabolic shift. Control cultures produced more lactate per consumed glucose (i) and showed reduced flux from glycolysis into the TCA cycle via pyruvate dehydrogenase (ii) (pdh). The ratio of TCA activity to glycolytic activity was higher at elevated pCO_2 (iii). Furthermore, the ratio of respiratory activity to TCA cycle flux was increased at the conditions of the control processes (iv).

	(i) Yield Lactate/pyruvate kinase flux [%]	(ii) Yield pdh/pyruvate kinase flux [%]	(iii) TCA activity/glycolytic activity [%]	(iv) Respirational activity/TCA activity [%]
Control run 1	62	34	40	338
pCO_2 20/pO_2 25 run 1	52	37	46	298
Control run 2	57	35	49	329
pCO_2 20/pO_2 40 run 2	51	39	53	298

Figure legends

Figure 1. Viable cell density (VCD) and metabolite concentrations over process time of the batch fermentation processes. Processes at elevated pCO_2 started to consume lactate only after glucose depletion, whereas processes at lower pCO_2 values consumed lactate early in the process after glutamine depletion.

Figure 2. Viable cell density (VCD) and metabolite concentrations over process time of the fed-batch fermentation processes. Cultures at pCO_2 20% did not switch from lactate production to consumption, in contrast to the control cultures at 12.5% pCO_2. No depletion of glucose or glutamine occurred during the processes. The time of the metabolic shift is indicated by the dashed line.

Figure 3. Average specific rates of several metabolites (glucose consumption (qgluc), lactate production (qlac), glutamine consumption (qgln), ammonia production (qamm)), specific productivity (qp), cell growth (μ) and oxygen consumption (qO_2) of the fed-batch cultures (A) before and (B) after the metabolic shift. The average rates of the controls and the respective cultures at elevated pCO_2 were tested for significant differences with a students t-test and results are presented in the Supporting Information. (A) qgluc, qlac as well as qp, μ and qO_2 were reduced under elevated pCO_2 conditions in comparison to the control cultures. (B) After the metabolic shift qgluc was lower in the control cultures than in processes at pCO_2 20%. In contrast to fermentation processes at elevated pCO_2, control cultures switched from lactate and ammonia production to consumption of these metabolites.

Figure 4. (A) Ammonia concentration over process time of the fed-batch processes. Shortly after the metabolic shift occurred in the control cultures, indicated by the dashed line, processes started to show a decline in ammonia concentrations. **(B) The relation between specific ammonia production (qNH4) and specific glutamine consumption (qGln).** The data-set consists of data from all fed-batch processes from inoculation until maximum viable cell densities were reached. **(C) Specific glutamine consumption (qGln) over process time of all fed-batch**

processes. Only slight differences in the glutamine consumption rates between processes at pCO_2 20% and the control cultures could be observed. It seemed that qGln decreased in the control cultures after the metabolic shift occurred, indicated by the vertical dashed line. As soon as glutamine consumption rates dropped below approx. 0.12 [pmol/(cell*day)], indicated by the horizontal dashed line, ammonia concentrations decreased, except from day 9 on in the control cultures when alanine is consumed.

Figure 5. Simplified version of the metabolic network used for the metabolic flux analysis. Main intracellular fluxes that produce pCO_2 (G6P to R5P, OAA to PEP, Pyr to AcoA, Cit/Icit to aKG and aKG to Suc) are highlighted inred, derived from Goudar et al. [56].

Figure 6. Average specific rates of several intracellular fluxes of the glycolysis (GPI, pk, pdh), pentose phosphate pathway (g6pdh) and TCA cycle (icdh, akgdh, maldh, pepck) as well as specific carbon dioxide production (qCO_2) of the fed-batch cultures before (A) and after the metabolic shift (B). The average rates of the controls and the respective cultures at elevated pCO_2 were tested for significant differences with a students t-test and results are presented in the Supporting Information. (A) Glycolytic and TCA cycle fluxes were reduced under elevated pCO_2 conditions in comparison to the control cultures, resulting in lower carbon dioxide production rates. (B) After the metabolic shift glycolytic influx via GPI was lower in the control cultures than in processes at pCO_2 20%. TCA cycle fluxes and qCO_2 became similar within all fed-batch processes after the metabolic shift.
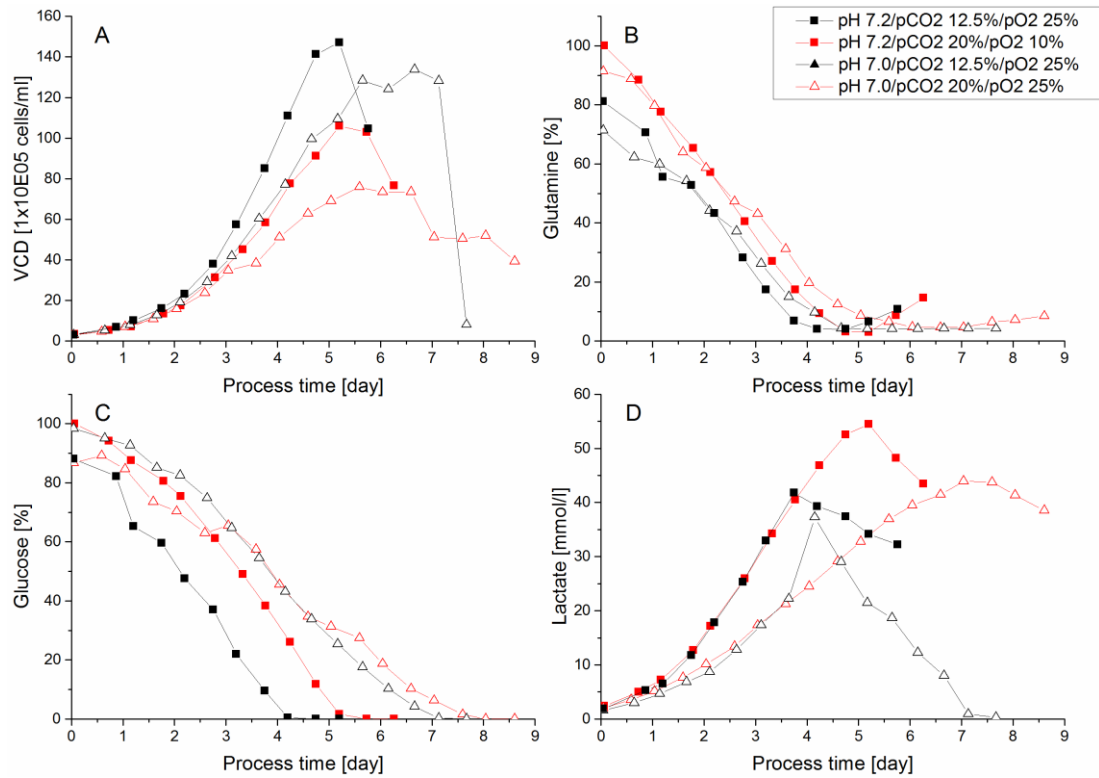
Figure 7. The redox variable R depends on the ratio of cytosolic NADH via glycolysis and the mitochondrial NAD^+ via respiration and TCA cycle. The $NADH/NAD^+$ ratio is tightly balanced, therefore R-values above 1 lead to an additional production of lactate and concurrent cytosolic NADH consumption. In contrast an R value below 1 would support cytosolic NADH production via lactate consumption.

Figure 8. Cytosolic NADH production, mitochondrial NAD^+ regeneration and the redox variable R over process time of the fed-batch cultivations. The time of metabolic shift is
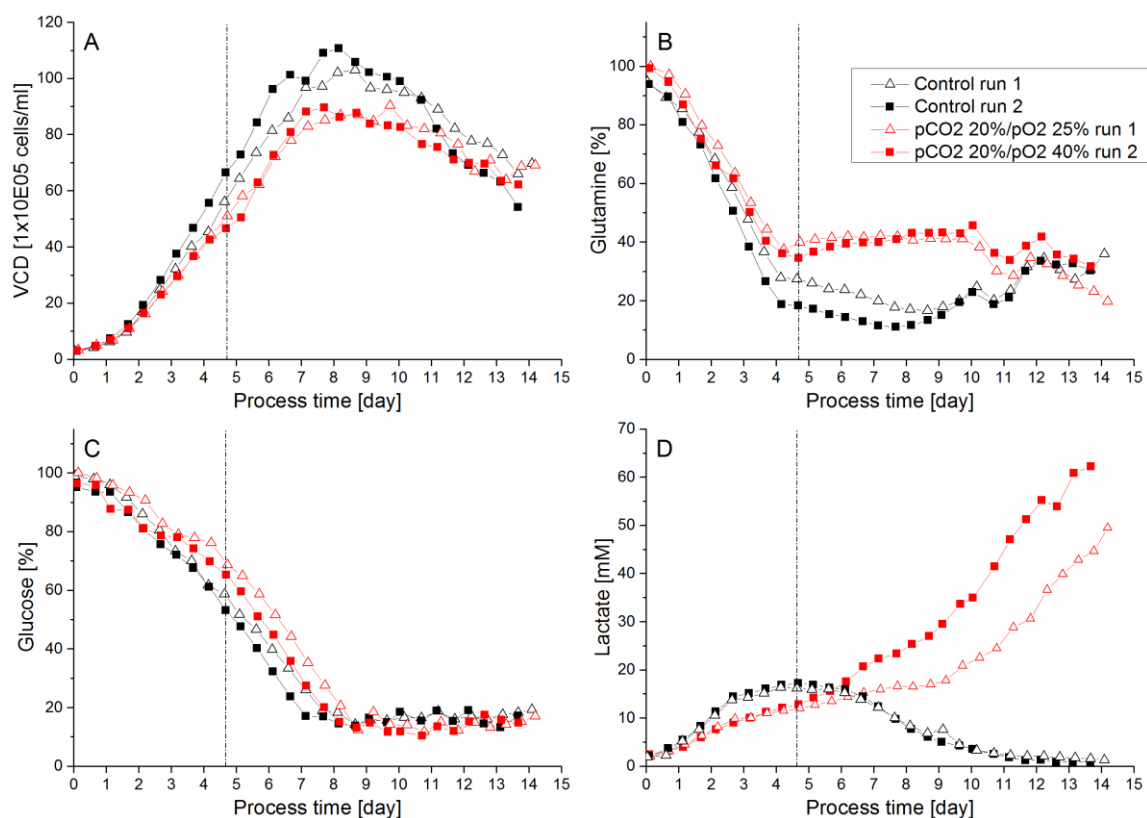
indicated by the dashed line. Presented fluxes are interpolated between the data points via B-splines. (A) The NADH producing flux via glycolysis is higher at the control cultures in comparison to the processes at elevated pCO_2 before the metabolic shift. After the shift fluxes increased at high pCO_2 when compared to the control runs. (B) Mitochondrial NAD^+ regeneration was higher in the processes at control conditions, however fluxes seemed to become more similar after the metabolic shift. (C) The value of the redox variable R stayed above the critical value of 1, indicated by the horizontal dashed line, for processes at elevated pCO_2 values. Fed-batch cultures at control conditions dropped below an R-value of 1 as soon as the metabolic shift occurred.
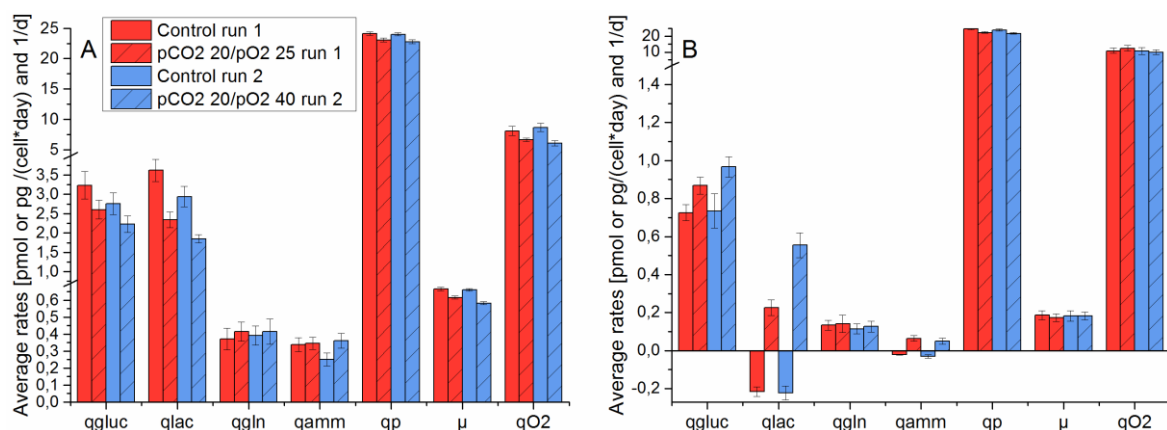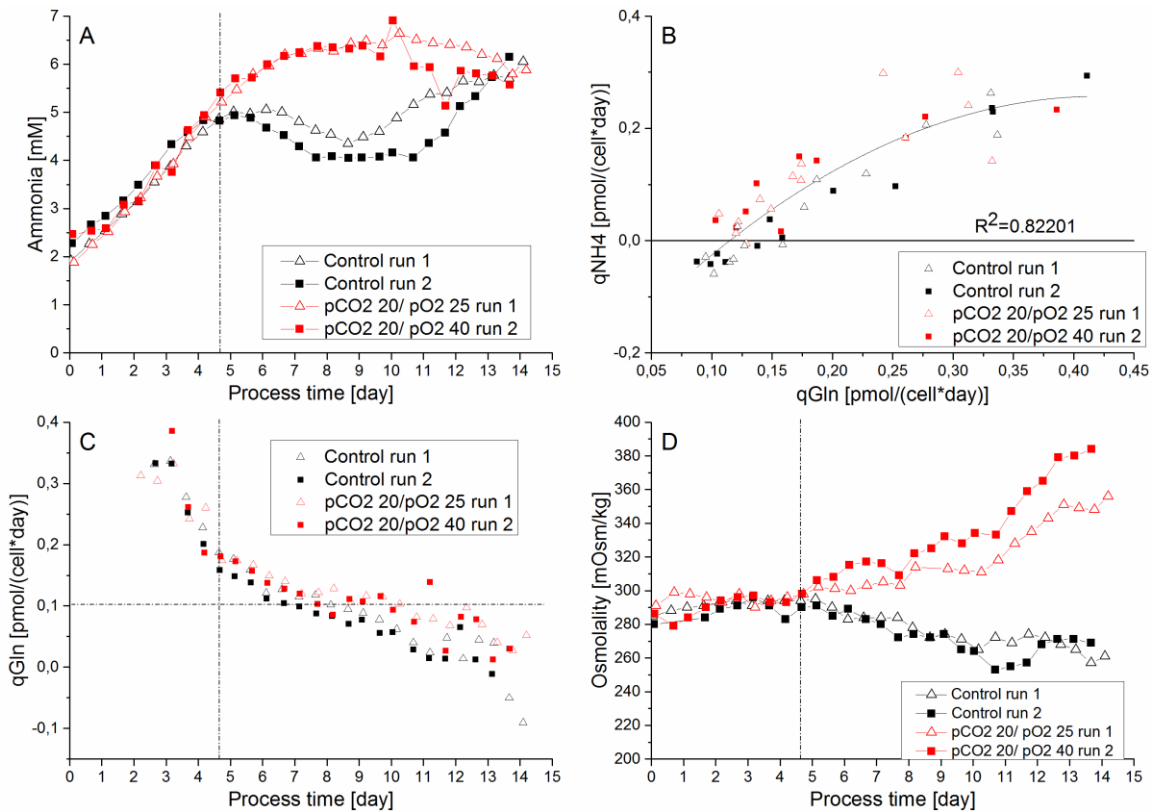
Figures

Figure 1. Viable cell density (VCD) and metabolite concentrations over process time of the batch fermentation processes. Processes at elevated pCO_2 started to consume lactate only after glucose depletion, whereas processes at lower pCO_2 values consumed lactate early in the process after glutamine depletion.
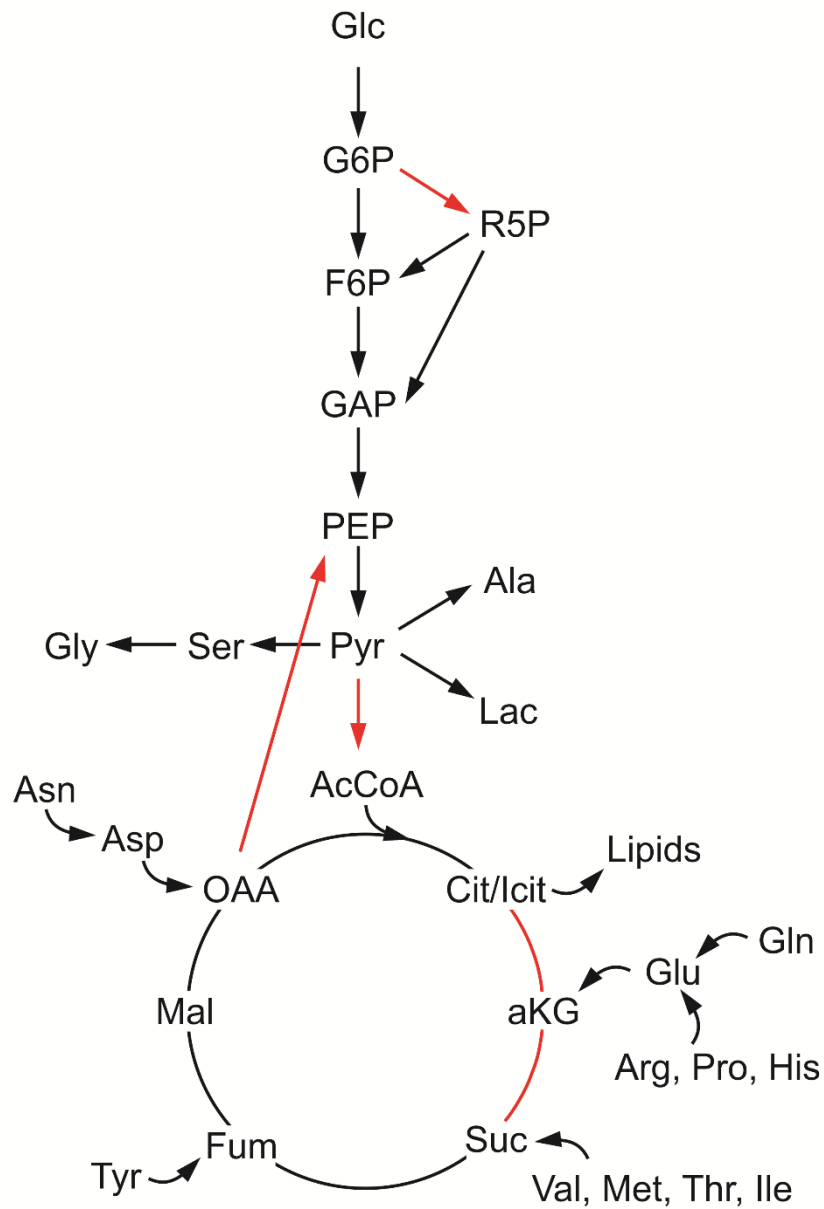
Figure 2. Viable cell density (VCD) and metabolite concentrations over process time of the fed-batch fermentation processes. Cultures at pCO_2 20% did not switch from lactate production to consumption, in contrast to the control cultures at 12.5% pCO_2. No depletion of glucose or glutamine occurred during the processes. The time of the metabolic shift is indicated by the dashed line.

Figure 3. Average specific rates of several metabolites (glucose consumption (qgluc), lactate production (qlac), glutamine consumption (qgln), ammonia production (qamm)), specific productivity (qp), cell growth (μ) and oxygen consumption (qO$_2$) of the fed-batch cultures (A) before and (B) after the metabolic shift. The average rates of the controls and the respective cultures at elevated pCO$_2$ were tested for significant differences with a students t-test and results are presented in the Supporting Information. (A) qgluc, qlac as well as qp, μ and qO$_2$ were reduced under elevated pCO$_2$ conditions in comparison to the control cultures. (B) After the metabolic shift qgluc was lower in the control cultures than in processes at pCO$_2$ 20%. In contrast to fermentation processes at elevated pCO$_2$, control cultures switched from lactate and ammonia production to consumption of these metabolites.
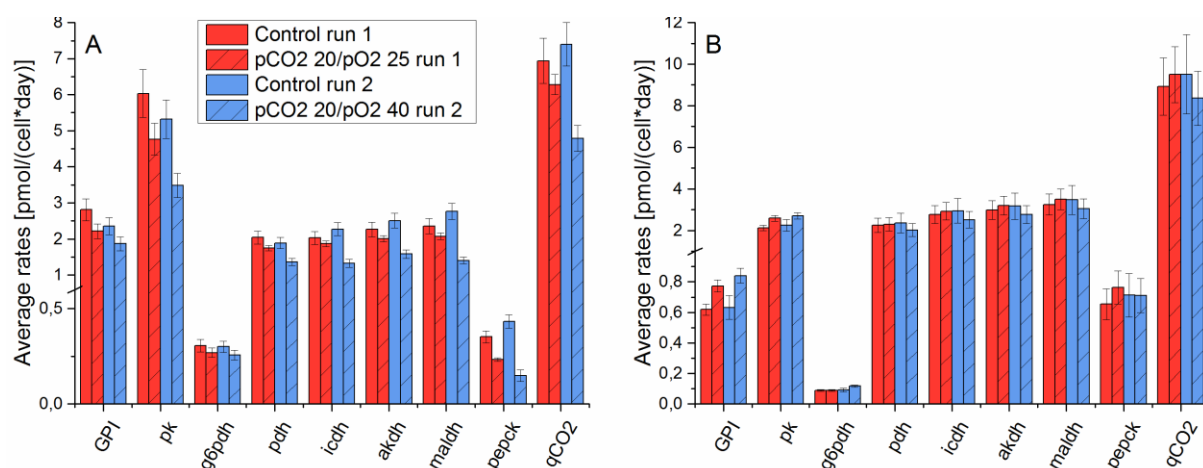
Figure 4. (A) Ammonia concentration over process time of the fed-batch processes. Shortly after the metabolic shift occurred in the control cultures, indicated by the dashed line, processes started to show a decline in ammonia concentrations. **(B) The relation between specific ammonia production (qNH4) and specific glutamine consumption (qGln).** The data-set consists of data from all fed-batch processes from inoculation until maximum viable cell densities were reached. **(C) Specific glutamine consumption (qGln) over process time of all fed-batch processes.** Only slight differences in the glutamine consumption rates between processes at pCO_2 20% and the control cultures could be observed. It seemed that qGln decreased in the control cultures after the metabolic shift occurred, indicated by the vertical dashed line. As soon as glutamine consumption rates dropped below approx. 0.12 [pmol/(cell*day)], indicated by the horizontal dashed line, ammonia concentrations decreased, except from day 9 on in the control cultures when alanine is consumed.
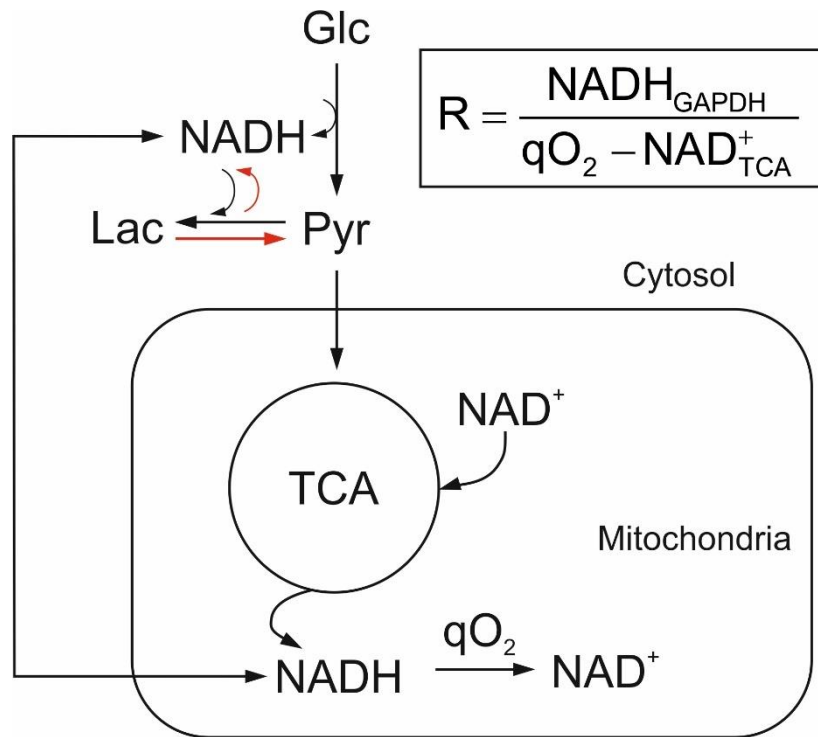
Figure 5. Simplified version of the metabolic network used for the metabolic flux analysis.

Main intracellular fluxes that produce pCO$_2$ (G6P to R5P, OAA to PEP, Pyr to AcoA, Cit/Icit to aKG and aKG to Suc) are highlighted inred, derived from Goudar et al.

Figure 6. Average specific rates of several intracellular fluxes of the glycolysis (GPI, pk, pdh), pentose phosphate pathway (g6pdh) and TCA cycle (icdh, akgdh, maldh, pepck) as well as specific carbon dioxide production (qCO₂) of the fed-batch cultures before (A) and after the metabolic shift (B). The average rates of the controls and the respective cultures at elevated pCO₂ were tested for significant differences with a students t-test and results are presented in the Supporting Information. (A) Glycolytic and TCA cycle fluxes were reduced under elevated pCO₂ conditions in comparison to the control cultures, resulting in lower carbon dioxide production rates. (B) After the metabolic shift glycolytic influx via GPI was lower in the control cultures than in processes at pCO₂ 20%. TCA cycle fluxes and qCO₂ became similar within all fed-batch processes after the metabolic shift.

Figure 7. The redox variable R depends on the ratio of cytosolic NADH via glycolysis and the mitochondrial NAD⁺ via respiration and TCA cycle. The NADH/NAD⁺ ratio is tightly balanced, therefore R-values above 1 lead to an additional production of lactate and concurrent cytosolic NADH consumption. In contrast an R value below 1 would support cytosolic NADH production via lactate consumption.

Figure 8. Cytosolic NADH production, mitochondrial NAD⁺ regeneration and the redox variable R over process time of the fed-batch cultivations. The time of metabolic shift is indicated by the dashed line. Presented fluxes are interpolated between the data points via B-splines. (A) The NADH producing flux via glycolysis is higher at the control cultures in comparison to the processes at elevated pCO_2 before the metabolic shift. After the shift fluxes increased at high pCO_2 when compared to the control runs. (B) Mitochondrial NAD⁺ regeneration was higher in the processes at control conditions, however fluxes seemed to become more similar after the metabolic shift. (C) The value of the redox variable R stayed above the critical value of 1, indicated by the horizontal dashed line, for processes at elevated pCO_2 values. Fed-batch cultures at control conditions dropped below an R-value of 1 as soon as the metabolic shift occurred.

Manuscript 3: The impact of pH inhomogeneities on CHO cell physiology and fed-batch process performance – two-compartment scale-down modelling and intracellular pH excursion

Authors: Matthias Brunner, Philipp Braun, Philipp Doppler, Christoph Posch, Dirk Behrens, Christoph Herwig and Jens Fricke

Research Article

The impact of pH inhomogeneities on CHO cell physiology and fed-batch process performance – two-compartment scale-down modelling and intracellular pH excursion

Matthias Brunner[1,2], Philipp Braun[1,2], Philipp Doppler[1,2], Christoph Posch[3], Dirk Behrens[3], Christoph Herwig[1,2] and Jens Fricke[1,2]

[1] Research Division Biochemical Engineering, Institute of Chemical Engineering, Vienna University of Technology, Vienna, Austria
[2] CD Laboratory on Mechanistic and Physiological Methods for Improved Bioprocesses, Vienna University of Technology, Vienna, Austria
[3] Sandoz GmbH, Langkampfen, Austria

Due to high mixing times and base addition from top of the vessel, pH inhomogeneities are most likely to occur during large-scale mammalian processes. The goal of this study was to set-up a scale-down model of a 10–12 m^3 stirred tank bioreactor and to investigate the effect of pH perturbations on CHO cell physiology and process performance. Short-term changes in extracellular pH are hypothesized to affect intracellular pH and thus cell physiology. Therefore, batch fermentations, including pH shifts to 9.0 and 7.8, in regular one-compartment systems are conducted. The short-term adaption of the cells intracellular pH are showed an immediate increase due to elevated extracellular pH. With this basis of fundamental knowledge, a two-compartment system is established which is capable of simulating defined pH inhomogeneities. In contrast to state-of-the-art literature, the scale-down model is included parameters (e.g. volume of the inhomogeneous zone) as they might occur during large-scale processes. pH inhomogeneity studies in the two-compartment system are performed with simulation of temporary pH zones of pH 9.0. The specific growth rate especially during the exponential growth phase is strongly affected resulting in a decreased maximum viable cell density and final product titer. The gathered results indicate that even short-term exposure of cells to elevated pH values during large-scale processes can affect cell physiology and overall process performance. In particular, it could be shown for the first time that pH perturbations, which might occur during the early process phase, have to be considered in scale-down models of mammalian processes.

1 Introduction

The number of biopharmaceutical protein therapeutics continues to increase with a strong share of mammalian derived products, especially monoclonal antibodies (mAb)

Correspondence: Dr. Jens Fricke, Vienna University of Technology, Gumpendorferstrasse 1a 166/4, 1060 Vienna, Austria
E-mail: jens.fricke@tuwien.ac.at

Abbreviations: CHO, chinese hamster ovary; **mAb,** monoclonal antibody; **PFR,** plug flow reactor; **pHi,** intracellular pH; **STR,** stirred tank reactor

[1–3]. Chinese hamster ovary cells (CHO) hereby represent the most common expression system for industrial large-scale manufacturing [1, 4]. Through the course of bioprocess development and final commercial production, the process has to be properly scaled to avoid late-stage campaign failure. However, mammalian scale-up is still challenging and deviations between the small-scale and large-scale performances nowadays have been mostly attributed to unavoidable inhomogeneities in large-scale [5–7]. One prominent example are pH gradients which can occur due to base or feed addition, resulting in a serious scale-up problem [8, 9].

1.1 Scale-down system design

To investigate the effect of large-scale inhomogeneities on cell physiology and process performance several multi-compartment scale-down models have been established in the past [10–16]. Regarding pH inhomogeneities, these systems simulated the effect of concentrated base or feed zones in large-scale, by addition of these components to a second smaller reactor, usually a plug flow reactor (PFR) or stirred tank bioreactor (STR), which is connected to a larger homogeneous stirred tank bioreactor. Whilst STR-PFR systems can be generally easier integrated with the PFR system consisting of e.g. simple neoprene tubing, STR-STR systems strongly benefit from the fact that essential process parameters as temperature, pH, pO_2 and mixing can be easily controlled [17]. More advanced PFR systems with static mixers and aeration as well as gassing and sampling systems exist, but are generally more complex than the STR solutions [18, 19].

Up to date in mammalian cell culture two studies about the effect of pH inhomogeneities in two-compartment systems exist. Osman et al. used a STR-STR bioreactor system to particularly study the effect of the frequency and amplitude of elevated pH zones on cell growth [13]. Whereas Nienow et al. used a STR-PFR system to evaluate mainly the effect of mixed feed and base addition as well as different residence times of the cells in the PFR on cell growth and product quality attributes [12]. The set-up of a two-compartment system for the investigation of pH inhomogeneities requires the consideration of several important parameters: (i) volume of the alkali zone, (ii) mixing time, (iii) residence time, (iv) pH overshoot amplitude and (v) frequency of pH overshoots. Hereby the scale-down model conditions should be similar to the large-scale reality as stated by Noorman [20].

(i) The volume of elevated pH values, due to base addition from top of the large-scale bioreactor, is defined as the volume of the alkali zone and should represent the volume of the small compartment. Literature about the extent of the alkali zone is rare and in fact only a few publications present estimated or measured ranges. Namdev et al. stated 0.5% of the total reactor volume as smallest volume of the inhomogeneous zone in their network-of-zones model of a 300 m³ stirred tank bioreactor for baker's yeast production [21]. Experiments in their study were conducted between 1.5 and 5%, which were estimated as realistic values for the modelled system. Nienow et al. stated that they observed ≈5% of total bioreactor volume being occupied by a feed plume in earlier visualization studies in a 8 m³ stirred tank bioreactor [8, 12, 22]. Wayte et al. measured 1% of total volume being occupied by an alkali plume in a 2 m³ air-lift bioreactor [13]. The alkali zone from Osman et al. in their two-compartment system occupied 14% of the total volume, however authors stated that this system represented extreme conditions [13].

(ii) The time duration to reach 90% homogeneity in a mixed reactor system after addition of a tracer component is often defined as mixing time [6]. Therefore, the time how long pH inhomogeneities exist, for example due to base addition, in the two-compartment system should equal the large-scale mixing time. For mammalian processes Lara et al. reported 120–360 s of mixing time in a 12 m³ STR [5]. Furthermore, Xing et al. measured mixing times of >100 s in a 5 m³ stirred tank bioreactor operated at cell culture conditions [23]. Additionally Nienow et al. measured mixing times up to approx. 200 s in a 8 m³ cell culture STR [22]. The two-compartment system from Osman et al. [13] used a fixed mixing time of 200 s.

(iii) The time how long a single cell is exposed to the unfavorable conditions inside of the alkali zone is defined by their mean residence time. The circulation time is described as the time between consecutive passages of a particular cell through a specified zone of a bioreactor [24], therefore the mean residence time can be estimated through knowledge of the circulation time. Circulation time itself can be approximated to be a quarter of the mixing time if no measurement or simulated values are available [5]. The residence times used in two-compartment studies from Osman et al. and Nienow et al. varied between 180 s and 60–120 s respectively [12, 13].

(iv) The amplitude of the pH in the alkali zone varies with process conditions and individual pH controller settings, thus different maximum values have been reported in literature. Langheinrich and Nienow observed pH increases of up to 0.8 units in a 8 m³ STR [8]. Wayte et al. reported values of 1.7 units above the pH setpoint in a 2 m³ air lift reactor [13]. A study in a 5 m³ STR operated at cell culture conditions from Xing et al. showed an increase of approx. two units in pH at the top of the bioreactor due to base addition from top [23]. The two-compartment system from Osman et al. [13] investigated pH increases of 0.7 and 1.7, reaching maximum values of 9.0 in pH.

(v) The frequency of base additions and therefore of possible pH overshoots is strongly dependent from the individual control strategy and process conditions. Using a narrow pH deadband around a specific pH set-point would need a more frequent base addition than process using wide pH control deadbands. Furthermore, cell metabolism and accumulation of by-products as lactate can alter the pH value dramatically, thus leading to a variable need of base addition. Therefore, it seems most suitable to not define a fixed frequency but rather to simulate pH overshoots as soon as the pH value in the homogeneous zone drops below the predefined deadband. Through this control strategy cells should be exposed to pH inhomogeneities in the two-compartment system in a frequency similar to the large-scale process. This strategy was also implemented in the two-compartment system from Nienow et al. [12]. Osman et al. used artificial fixed frequencies between 1/6 and 1/60 min⁻¹, starting on day

two as well as a defined upper limit of max. 100 or 10 pH overshoots at pH 8.0 or 9.0 respectively [13].

1.2 Intracellular pH

Variations in extracellular pH have been often hypothesized to affect intracellular pH and therefore leading to different process performances [25, 26]. Nevertheless, only few studies exist that investigated intracellular pH changes due to extracellular pH alterations [27–29]. Most of these studies were not conducted in controlled bioreactor environments and included extended incubation times of cells (between 30 and 60 min.) in specific buffers prior to intracellular pH measurement. Therefore, several authors suggest that these studies do not necessarily reflect what is happening inside of a bioreactor culture [30, 31]. To evaluate if extracellular pH inhomogeneities might affect the intracellular pH of the cells, one-compartment batch fermentations with controlled pH shifts were conducted. Hereby pH values were shifted to higher values and short-term responses of the cells intracellular pH were investigated. Through the usage of a fluorescent dye and a rapid measuring method similar to Ozkan et al. [32] changes in intracellular pH due to extracellular pH alterations could be observed highly time resolved, thus provid-

ing information about the intracellular effects of temporary large-scale pH inhomogeneities.

The overall goal of this study was to (i) set-up a two-compartment system that is capable of simulating pH inhomogeneities due to base addition as they might occur in an industrial approx. 10–12 m^3 scale stirred tank bioreactor for mammalian cell culture and to (ii) investigate the effects of elevated pH perturbations on cell physiology and process performance.

2 Materials and methods

2.1 Two-compartment system and control

In this study a STR-STR system was chosen as a scale-down model, because it was considered to be easier to implement and control than a STR-PFR system. This system was designed and set-up especially for the purpose to investigate the effect of pH inhomogeneities on cell physiology and fed-batch process performance. The system consisted of a 3 L total volume (TV) bioreactor, representing the well mixed-zone of a large-scale bioreactor and of a 0.7 L TV bioreactor representing the alkali zone (Figure 1).
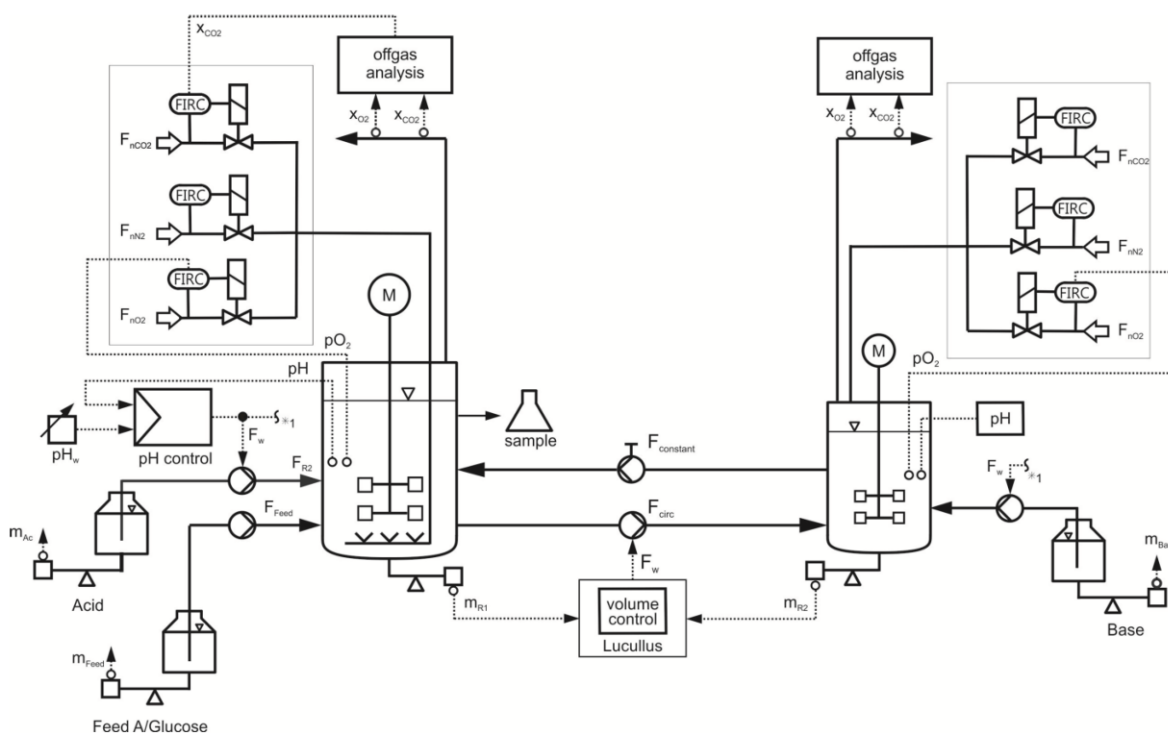
Figure 1. Design and control of the two-compartment system. The large stirred tank bioreactor (3 L TV) represents the well mixed zone out of the large-scale bioreactor, whereas the small stirred tank reactor (0.7 L TV) simulates the alkali zone with elevated pH values. Temperature and pO_2 were controlled in both bioreactors at defined set-points. pH was measured in the large-compartment, whereas base was solely added into the small-compartment.

Table 1. Summary of process conditions used in this publication and previous two-compartment studies for mammalian cell culture as well as ranges out of literature for a 10–12 m³ scale mammalian STR. Literature for estimated ranges are presented in the introduction in the corresponding text chapters. In comparison to our study, Osman et al. used a three times higher alkali zone volume, double the residence time and artificial pH overshoot frequencies. Nienow et al. conducted experiments in a STR-PFR system and did not measure or specify the pH overshoot amplitude or mixing time of the system.

	Estimated/measured ranges in a 10–12 m³ STR	Brunner et al. [this study]	Osman et al. [13]	Nienow et al. [12]
Organism	–	CHO cells	GS-NS0 myeloma cells	CHO cells
Process	Fed-batch	Fed-batch	Batch	Fed-batch
Two-compartment system	–	STR-STR	STR-STR	STR-PFR
Large-scale – scale-down model	–	10–12 m³ STR	Not specified	20 m³ STR
Volume of the alkali zone (%)	~5	5	14	5
Mixing time (s)	120–360	360	200	Not specified
Residence time (s)	30–90	90	180*	60–120
pH overshoot amplitude (–)	0.8–2	2.0	0.7 + 1.7	Not specified
Frequency	pH signal < pH deadband	pH signal < pH deadband	Starting day 2 – artificially every 6, 18 or 60 min with max. 10 to 100 overshoots and min = mixing time	pH signal < pH deadband

* The residence time was not specified from Osman et al. but calculated from the applied circulation rate and reactor volume.

Appropriate ranges for several scale-down model parameters (e.g. volume of the alkali zone, mixing time, residence time, pH amplitude and frequency of pH overshoots) had to be defined to mimic a 10–12 m³ large-scale STR. Table 1 gives an overview of the estimated and measured ranges for large-scale processes out of literature as well as the chosen conditions for this scale-down model and two reference studies for mammalian cell culture.

Control of the reactor volumes and circulation of the cell suspension between the vessels were realized with two peristaltic pumps. The mean residence time was calculated by the theoretical space time (ratio of the volume inside of the small compartment and the applied volumetric flow rate) since good correspondence with mean residence times were observed in other two-compartment systems [17]. The mixing time of the systems is dependent on the applied volumetric flow rate since it defines the exchange rate between the small and large compartment. To realize a mixing time of 360 s in the two-compartment system and a mean residence time of cells in the small compartment of 90 s the peristaltic pumps were set to a volumetric flow rate of 100 mL/min.

The volume of the alkali zone represents the culture volume inside of the small (0.7 L) bioreactor and was controlled to 5% by an automated operation including the two reactor weights and continuous small adjustments of the flow rate of one of the peristaltic pumps. pH was measured in both bioreactors. The pH probe in the large compartment, representing the well mixed zone, was used for pH control, with base addition only to the small compartment (Fig. 1). A predefined volume of base was added with each pH overshoot to the small-compartment resulting in defined pH overshoot amplitudes. Acid addition into the large-compartment led to pH control in between the predefined pH deadband inside of the large-compartment.

2.2 Cell line, seed train and fermentation processes

An industrial CHO cell line producing a monoclonal antibody (mAb) was cultivated in chemically defined media. Precultures for batch fermentation processes were cultivated in shake flasks and incubated at 10% pCO_2 and 36.5°C temperature. Exponentially growing cells were transferred into the bioreactor system resulting in an inoculation density of 3×10^5 cells/mL.

One-compartment batch cultivations, were carried out in 3 L or 0.7 L TV glass vessels at 36.5°C and 40% pO_2. pH regulation was realized by addition of 1 M NaOH and 1 M HCl respectively. pH set-points for the intracellular pH-studies were shifted from 7.0 to 7.8 or 9.0 after approx. 60 h of process time (pH deadband 0.01). pH-shifts were induced through manual control of acid/base pumps and reached their new set-point in less than 45 s.

One-compartment fed-batch cultivations were performed in 3 L bioreactors at 36.5°C and 40% pO_2. Temperature was shifted after 60 h to 33°C. pH set point was 7.0 and regulation was realized by addition of 1 M NaOH and 1 M HCl respectively (pH deadband 0.03). pCO_2 was controlled at 12.5% via offgas measurement based on calculations similar to Frahm et al. [33]. Feed A was added continuously to processes starting on day 4 until day 10 and on day 12. Feed B was added continuously starting on day 6 until day 10 and on day 12. Glucose was added to processes as soon as its concentration dropped below 2 g/L with a one-time step addition (bolus) to 2 g/L.

Two-compartment fed-batch cultivations were performed analogous to the one-compartment fed-batch runs. Feeds as well as HCl for pH regulation were added

to the large bioreactor compartment. In fermentation runs with simulation of pH inhomogeneities pH was controlled through addition of 2 M NaOH into the small STR in response to the pH signal measured in the large compartment (Figure 1).

2.3 In-process analytics, mAb determination and calculation of specific rates

Cultivation samples were taken every 12 h and cell counting/viability determination was performed using the automatic picture analyzer Cedex HiRes Analyzer (Roche, Germany). Osmolality of supernatant was determined via freeze point depression (Mikro-Osmometer TypOM806, Löser, Germany). Analysis of metabolites glucose, glutamine, glutamate, lactate and ammonium were performed using the Cedex Bio HT Analyzer (Roche, Germany). Antibody titer determination was carried out by HPLC (Ultimate 3000, Dionex, United States) with a Protein A sensor cartridge (Applied Biosystems, Netherlands).

Calculation of specific cell growth and metabolite production or consumption rates was performed similar to Sauer et al. [34]. Standard deviations of the calculated mean specific rates were determined by Monte-Carlo parameter estimation to generate multiple time-courses for each fermentation similar to Murphy et al. [35] using MATLAB® (The MathWorks, Inc., USA). Error in prime variables (viable cell density, metabolite and product concentrations) for Monte-Carlo simulation were derived from published studies that used the same analytical devices [36–38].
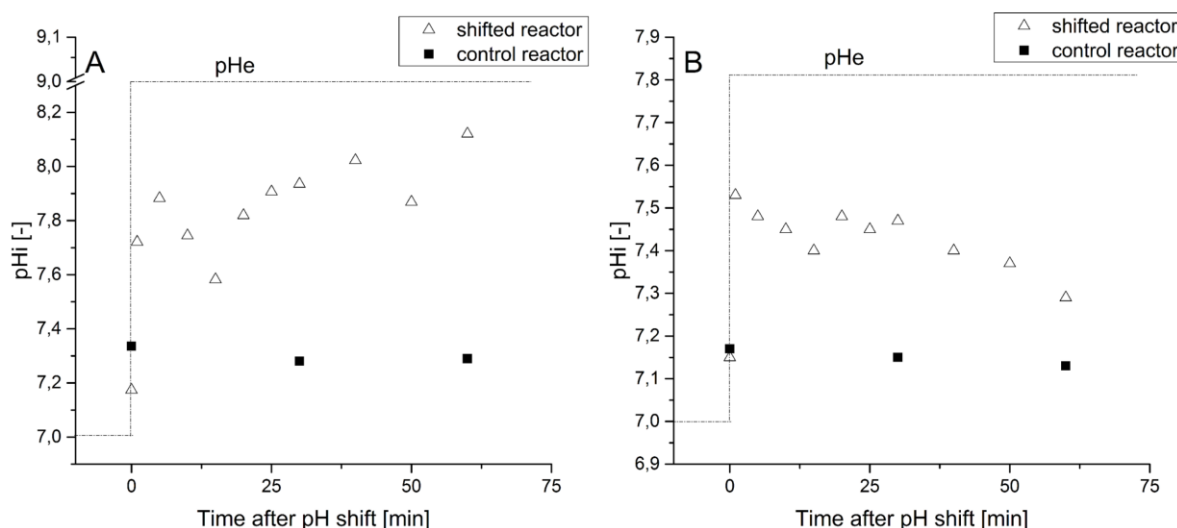
2.4 Intracellular pH

Intracellular pH measurements were performed, similar to Ozkan et al. [32], using the fluorescent dye 2',7'-bis(2-carboxyethyl)-5,6-carboxyfluorescein acetoxymethyl ester (BCECF-AM) (Life Technologies, USA) and a spectrofluorometer (TECAN Infinite M200 Pro, Switzerland). After sampling, the dye was immediately added to the suspension, exposing cells to a concentration of 0.5 µM BCECF-AM, followed by immediate measurement at the preheated spectrofluorometer (36.5°C). Background fluorescence was recorded using samples without BCECF-AM addition and subtracted from the final results. Excitation wavelengths were set to 505/439 nm at an emission wavelength of 535 nm. Calibration of intracellular pH was performed using nigericin (10 µM) (Sigma Aldrich, Germany) and potassium buffers with different pH values from 6.8 to 9.0. Samples for pHi determination were taken immediately after the pH shift occurred and then approx. every 5 min to generate a highly time resolved data set.

3 Results

3.1 Short-term intracellular pH response to extracellular pH alterations

The relatively short exposure time of the cells to elevated pH values in large-scale was hypothesized to not significantly affect averaged enzymatic reaction rates but may initiate intracellular reactions or cascades, since pHi is

Figure 2. Response of the intracellular pH (pHi) of CHO cells in controlled bioreactor environments due to extracellular pH (pHe) shifts. (**A**) As soon as pHe was shifted to 9.0, pHi increased to elevated values. Moreover, cells started to agglomerate and die after approx. 20 min. of exposure to pH 9.0. (**B**) A similar immediate increase in pHi could be observed for pHe shift to 7.8. pHi declined steadily to more physiological values with increasing incubation time.

known to be an important secondary messenger in mammalian cells [29]. In order to evaluate if short-term pH inhomogeneities as they might occur in large-scale affect intracellular pH of the cells, batch fermentations including controlled pH shifts were conducted. Hereby, process pH was shifted after approx. 60 h of cultivation time from pH values of 7.0 to 7.8 or 9.0 and kept constant during the rest of the batch process. Fig. 2 presents the intracellular pH values of two different control reactors with constant extracellular pH (pHe) and two shifted reactors with a pH shift to 9.0 (Fig. 2A) and 7.8 (Fig. 2B). Immediately after the pH shift was conducted the intracellular pH increased dramatically to values around 7.8 or 7.5 for pHe shifts to 9.0 and 7.8 respectively. Most interestingly, pHi started to decline shortly after the pH shift at pH 7.8, although extracellular pH was kept constant after the shift. At pH 9.0 an early decline in pHi may occur but cannot be fully confirmed by the data-set, since cells started to agglomerate and die after around 20 min followed by an increase in pHi. Cell agglomeration could be observed by accumulation of large cell clumps inside of the reactor, and cell death was detected by a decreased viability obtained from Cedex HiRes measurements (data not shown). In contrast, control cultures at constant extracellular pH values of 7.0 showed steady intracellular pH values during the observed time (Fig. 2). Considering pH 7.8, it seems that the cells have efficient mechanisms to steer their intracellular pH values towards physiological conditions. However, this cannot be fully validated by the data-set at pH 9.0 because cells started to agglomerate and die shortly after exposure to these conditions.

Since strong effects on intracellular pH and cell growth were observed at pH 9.0 and these values were reported to be possible in large-scale fermentations [23], first pH inhomogeneity studies using the scale-down model were performed with a pH overshoot amplitude reaching pH 9.0.

3.2 Evaluation of growth characteristics of the two-compartment system, subsequent optimization studies and final experimental procedure

### 3.2.1 Growth characteristics and optimization studies

Due to the different set-up and process design, including two different types of STR and circulation with peristaltic pumps, we assessed whether cells might perform differently during a fed-batch process in a regular one-compartment system compared to the two-compartment system, even without simulation of pH inhomogeneities. Therefore, two fed-batch processes in parallel, one in the two-compartment system and the other one in a one-compartment 3 L bioreactor were initially performed. Figure 3A presents the viable cell densities and cell viabilities obtained from these experiments. We found that cells reached lower viable cell densities in the two-compartment system, whereas cell viabilities were almost identical until 170 h of process time.

Reduced growth in the two-compartment system was speculated to be associated with the circulation system or the small-compartment vessel. Therefore, initially batch fermentations were conducted in regular one-compartment systems one of those equipped with an
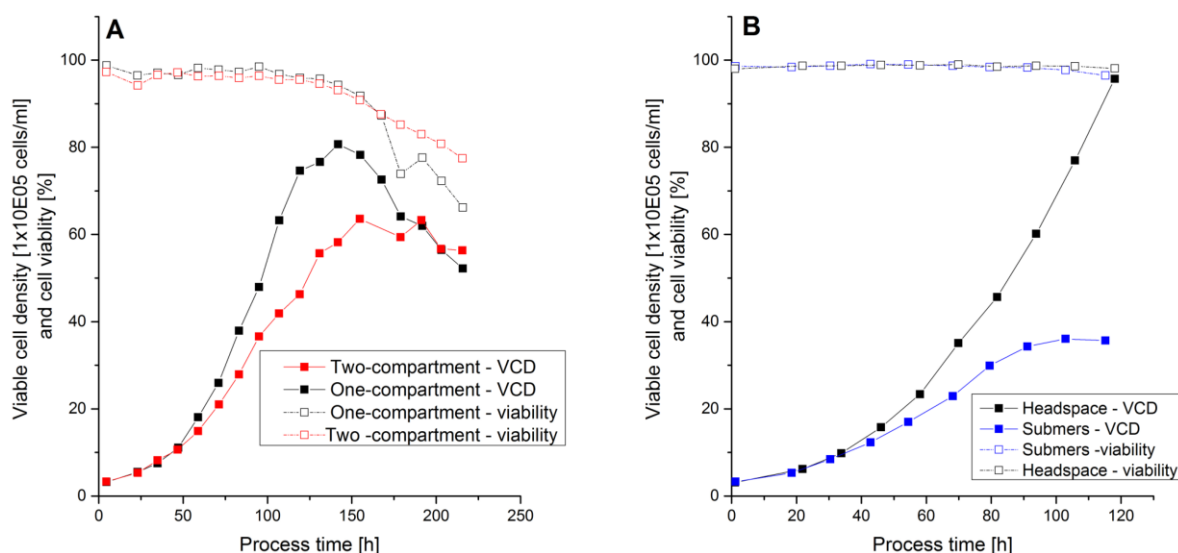
Figure 3. (**A**) Cell growth and cell viabilities of fed-batch processes conducted parallel in two-compartment and one-compartment experiments. Viable cell densities were reduced in the two-compartment system, whereas cell viabilities showed similar values. (**B**) Viable cell density and cell viability of batch fermentations in the small-compartment vessel with submerse and headspace aeration. Viable cell densities increased strongly after switch from submerse to headspace aeration.
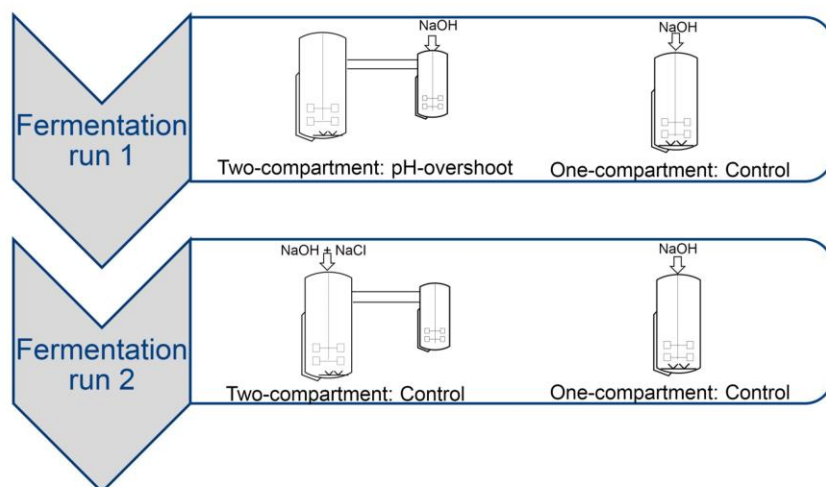
Figure 4. Experimental procedure of the two-compartment studies. At first fermentation run 1 was conducted, which consisted of a two-compartment and an one-compartment fed-batch process in parallel. Base was added to the small bioreactor of the two-compartment system. Afterwards fermentation run 2 was conducted, including a one-compartment fed-batch process and a two-compartment fermentation with base addition to the large bioreactor. Base was spiked with NaCl to achieve similar osmolality profiles between the two-compartment fermentation runs.

external recirculation loop and a peristaltic pump at a set-point of 300 mL/min. Both batch fermentations showed almost identical viable cell densities and cell viabilities (data not shown). Due to this observation, the recirculation system was not considered to influence the cell growth of the used cell line.

Subsequently, batch fermentations were performed solely in the small-compartment bioreactor to evaluate the cells' growth behavior inside of that system. The gathered data revealed that the viable cell density was strongly reduced in the small-compartment bioreactor although cell viabilities stayed at high values (Fig. 3B). Increased volumetric gas flow (vvm 0.04) as well as an increased surface-to-volume ratio and smaller bubble diameters in the small compartment, in comparison to the large-bioreactors (vvm 0.01), were then hypothesized to be the major contributors to the reduced cell growth of the two-compartment system, as observed in Fig. 3A. Due to limitations of the mass flow controller, the aeration of the small-compartment was changed from submerse to headspace aeration (10 mL/min). This resulted in a strong increase of approx. 70% in viable cell density in a second batch fermentation (Fig. 3B). Based on these results headspace aeration in the small-compartment bioreactor was used for the following two-compartment studies.

Finally, although cell growth in the small-compartment bioreactor could be significantly improved, the two-compartment and one-compartment systems were not considered to be directly comparable and therefore a special experimental procedure had to be applied for the pH inhomogeneity studies.

### 3.2.2 Experimental procedure of the two-compartment studies

As derived from previous results the two-compartment and one-compartment systems were not suitable for direct comparison. Ideally, the availability of two two-compartment scale-down models would allow for controls within experimental fermentation runs and thereby ensure an unconfounded comparison between fermentations with and without simulated pH inhomogeneities. Since this was not the case in this study, a different experimental procedure had to be established. Figure 4 shows a scheme of the applied strategy in this study. At first, a two-compartment fed-batch fermentation with simulation of pH inhomogeneities and a parallel fed-batch process in a regular one-compartment system were conducted (fermentation run 1). In a subsequent fermentation run, a two-compartment fed-batch process without pH overshoots and in parallel another one-compartment fed-batch process were performed (fermentation run 2). Through this methodology confounding effects of uncontrolled parameters like preculture age, media batch, etc. can be detected in the one-compartment system and considered in the two-compartment study. The simulation of pH overshoots led to an increase in media osmolality, as observed in similar studies [13, 39]. Since increased osmolality values can have significant effects on cell physiology [40], media osmolality between the two-compartment runs had to stay in between comparable levels. Therefore, in the two-compartment control fermentation run the alkali solution was spiked with NaCl (Fig. 4).

Through the applied strategy it was possible to investigate the effect of simulated pH inhomogeneities on cell physiology and fed-batch performance conducting two fermentation runs and without the instalment of a second two-compartment system.

3.3 Simulation of pH inhomogeneities in a fed-batch process using the two-compartment scale-down model

The two-compartment control strategy and the introduced experimental procedure were applied for the simu-
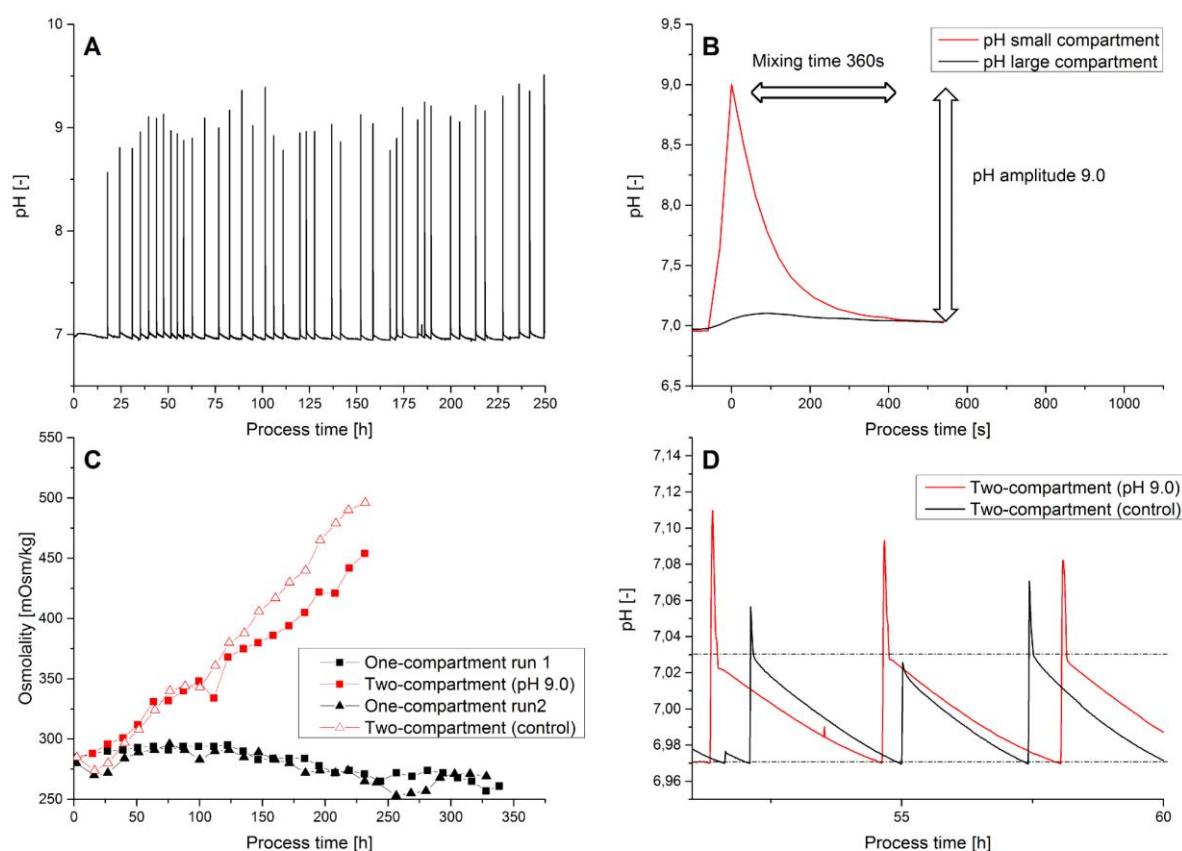
Figure 5. Two-compartment process control. (**A**) pH overshoot values in the small compartment. In total 40 pH overshoots occurred with frequencies ranging from approx. 1/3.3 h^{-1} to 1/9.5 h^{-1}. The mean overshoot value was 9.08 (standard deviation +/–0.24). (**B**) Example of a pH overshoot with a defined mixing time of 360 s and an amplitude maximum at pH 9.0. Each pH overshoot in the small-compartment led to a small pH increase in the large-compartment. (**C**) Osmolality profiles of the conducted fermentation runs. Due to the applied control strategy, osmolality strongly increased in the two-compartment systems when compared to the one-compartment runs. Osmolalities of the two-compartment fermentation runs stayed in similar ranges. (**D**) pH profiles of the large-compartment during both two-compartment fermentation runs. Each base addition in the small-compartment during the pH inhomogeneity study led to a small increase in the pH of the large-compartment. This effect was considered in the control fermentation run through application of the same pH-profile in the large-compartment as in the pH inhomogeneity study. pH deadbands are shown trough dotted lines.

lation of pH inhomogeneities with a pH amplitude up to pH 9.0. In total 40 pH overshoots occurred during the two-compartment fermentation (Fig. 5A). The mean measured overshoot pH value was 9.08 (standard deviation 0.24) and the time between pH overshoots varied in a range of 3.3 to 9.5 h. Already seven to 17 overshoots occurred in the early process phase, until 50 or 100 h of process time. Figure 5B shows in more detail one single pH overshoot out of Fig. 5A. The mixing time in this example was confirmed to be 360 s with a measured amplitude maximum at pH 9.0. Media osmolality within the two-compartment fermentation runs and within the one-compartment runs, showed comparable values (Fig. 5C). Due to the simulation of pH inhomogeneities or addition of base spiked with NaCl in the two-compartment control run (Fig. 4), osmolalities in the two-compartment fermentation runs reached higher values than those

in the one-compartment systems. The volume of the alkali zone was successfully controlled at 5% of the total liquid volume throughout the fermentation process (data not shown). Each pH perturbation in the small-compartment led to a subsequent pH increases in the large-compartment (Fig. 5B and 5D). This effect was considered during the two-compartment control fermentation runs and pH profiles in the large-compartment were similar between the two-compartment experiments (Fig. 5D). Therefore, differences between the two-compartment fermentations could only be addressed to the pH perturbations in the small-vessel.

Metabolite profiles as well as viable cell densities (VCD), cell viabilities and cell specific rates were reproducible in between the one-compartment processes (Fig. 6A–D and Table 2). Therefore, no effects of different preculture ages or media batches on process performance
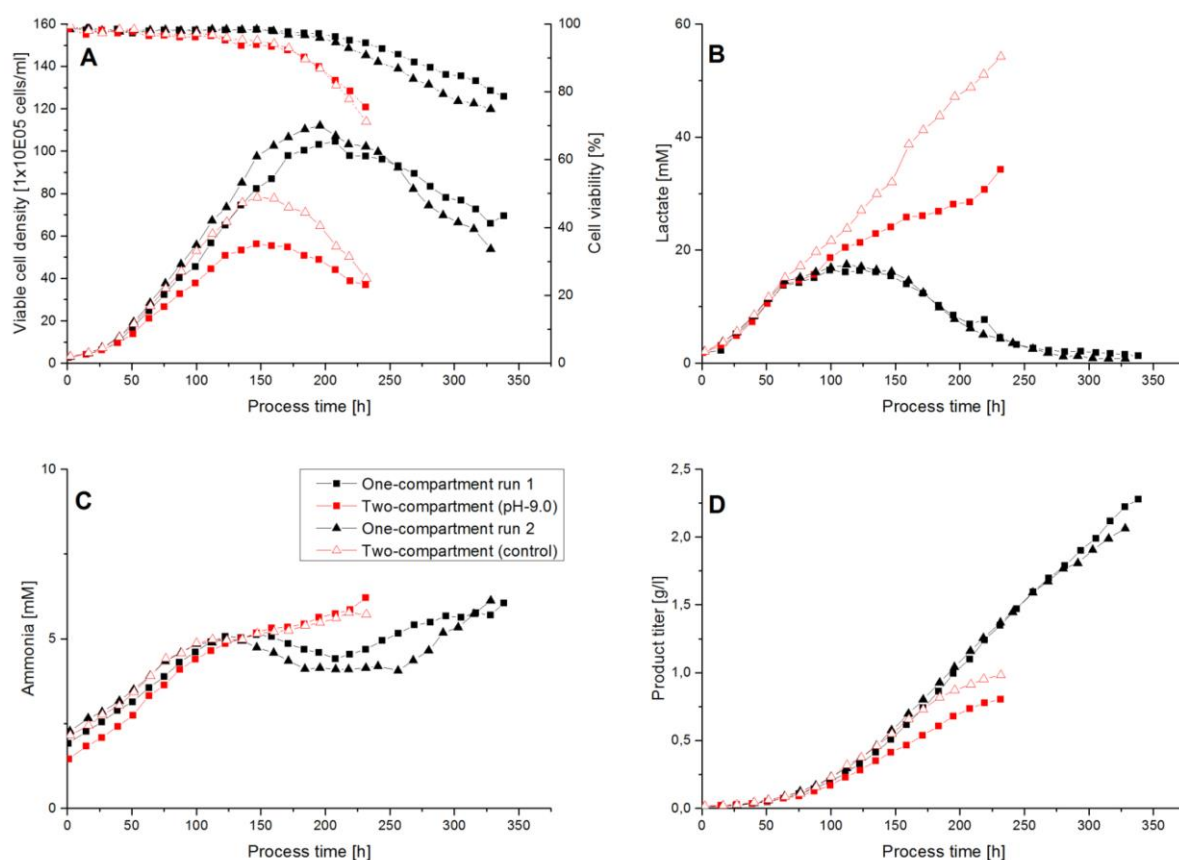
Figure 6. (**A**) Viable cell density (VCD) and cell viability, (**B**) lactate concentration and (**C**) ammonia concentration as well as (**D**) product titer over process time for fermentation run 1 and 2. One-compartment fermentation runs behaved similar in their process performance. The two-compartment runs both showed an early decrease in cell viability, lower maximum VCDs and no lactate and ammonia consumption when compared to the one-compartment runs. The two-compartment process with pH inhomogeneities showed decreased maximum VCD and product titer than the two-compartment control runs.

could be detected between the fermentation runs 1 and 2 of the experimental procedure (Fig. 4). Fermentation processes conducted in the two-compartment system showed different process performance when compared to the one-compartment runs. Both fermentation runs in the two-compartment system reached lower maximum VCDs and cell viabilities started to decrease after approx. 120 h of process time (Fig. 6A). Furthermore, no uptake of lactate or ammonia occurred during these fermentations when compared to the one-compartment runs (Fig. 6B and 6C). However, specific lactate production rates seemed to be slightly increased in the two-compartment system (Table 2).

Metabolite profiles as well as cell viabilities between the two-compartment studies showed similar trends. However, final lactate concentrations and maximum viable cell densities were higher, approximately 37 and 30% respectively, in the two-compartment control run (Fig. 6A and 6B). No significant effect of pH inhomogeneities on specific metabolite consumption or production rates were observed (Table 2). Specific rates were only evaluated until critical osmolality values were reached, since high osmolalities can strongly affect cell metabolism [40]. Additional shake-flask experiments conducted at our institute revealed increased byproduct formation and decreased cell growth above a critical osmolality value of approx. 360 mOsm/kg for the applied cell line (data not shown). Specific ammonia production q_{amm}, lactate production q_{lac}, glucose consumption q_{gluc}, glutamine consumption q_{gln} as well as specific productivity q_p were comparable between the two-compartment fermentations (Table 2). The average specific growth rate μ was reduced when pH overshoots to 9.0 occurred compared to the control. Additionally, already during the exponential growth phase, specific cell growth (μ_{max}) seemed to be affected by the simulated pH inhomogeneities, whereas μ_{max} showed similar values between the one-compartment runs and the two-compartment control run (Table 2). Lower maximum viable cell densities were observed in the pH inhomogeneity

Table 2. Specific metabolite rates and cell growth for the conducted one-compartment and two-compartment experiments out of fermentation runs 1 and 2 until critical osmolality values above 360 mOsm/kg were reached. Standard deviations were determined by Monte-Carlo simulation as described in the Materials and methods section.

	One-compartment run 1	One-compartment run 2	Two-compartment (pH 9.0) run 1	Two-compartment (control) run 2
q_{lac} [pM/(day*cell)]	3.44 (+/− 0.24)	3.28 (+/− 0.23)	3.56 (+/− 0.25)	3.76 (+/− 0.26)
q_{gln} [pM/(day*cell)]	−0.77 (+/− 0.13)	−0.75 (+/− 0.13)	−0.82 (+/− 0.14)	−0.76 (+/− 0.13)
q_{gluc} [pM/(day*cell)]	−2.93 (+/− 0.60)	−2.57 (+/− 0.53)	−2.88 (+/− 0.59)	−3.35 (+/− 0.69)
q_{amm} [pM/(day*cell)]	0.56 (+/− 0.07)	0.51 (+/− 0.06)	0.63 (+/− 0.08)	0.53 (+/− 0.06)
q_p [pg/(day*cell)]	24.17 (+/− 0.31)	24.25 (+/− 0.31)	22.75 (+/− 0.29)	21.96 (+/− 0.28)
μ (1/10^2 h)	2.67 (+/− 0.04)	2.91 (+/− 0.04)	2.46 (+/− 0.03)	2.82 (+/− 0.04)
μ_{max} (1/10^2 h)	3.59 (+/− 0.07)	3.65 (+/− 0.07)	3.35 (+/− 0.06)	3.73 (+/− 0.07)

(pH 9.0) fermentation (Fig. 6A), as a consequence of the lower maximum as well as average specific cell growth. Different product titer levels (Fig. 6D) can be mostly attributed to the differences in cell growth since specific productivities were comparable for all processes and only slightly reduced during the two-compartment runs when compared to the one-compartment fermentations (Table 2).

4 Discussion

The goal of this study was to establish a scale-down model which is capable of simulating the effect of large-scale pH inhomogeneities during an industrial fed-batch process and to investigate the effects of pH inhomogeneities on cell physiology and process performance.

4.1 Short-term intracellular pH response to extracellular pH alterations

Extracellular pH inhomogeneities to elevated values were hypothesized to affect intracellular pH and hence cell physiology. The results showed that intracellular pH immediately increased to higher values when extracellular pH was shifted to pH 9.0 or 7.8. Since extracellular pH shifts to higher values subsequently induced withdrawal of CO_2 from the cell culture media, CO_2 inside of the cells was stripped out and most probably led to a short-term intracellular alkalinisation effect, similar to those reported by Jockwer et al. [41]. The intracellular pH response of the cells was similar to those observed by Wu et al. [29], however their study was not conducted in bioreactors and cells were incubated in buffer systems prior to pHi disturbances with NH_4Cl. Intracellular pH is known to be an important secondary messenger [29, 42] and elevated values might initiate strong cell responses. The presented results show that cell physiology was immediately affected by extracellular pH changes, indicating that similar effects will arise during temporary pH gradients as they might occur in large-scale processes.

4.2 Evaluation of growth characteristics of the two-compartment system, subsequent optimization studies and final experimental procedure

The design and process parameters (e.g. volume of the alkali zone) of a two-compartment model were specified to match a large-scale 10–12 m^3 STR, using estimated or measured values from literature. Initial growth characteristic studies revealed reduced growth in the two-compartment system when compared to one-compartment fermentations. Circulation conditions between the two compartments was a factor that had to be considered during the design of the scale-down model. Commonly peristaltic pumps are used since they are available in most labs, easy to implement and have no direct contact to the cell suspension [10, 11, 13]. However, the use of peristaltic pumps can lead to significant hydrodynamic damage, affecting cell growth and cell viability, which is furthermore strongly dependent on the specific cell line and clone [12, 43]. Therefore, other circulation systems as syringe pumps or centrifugal pumps might be more suitable for the application in scale-down models [12, 44]. However, batch fermentations including a recirculation loop and peristaltic pumps revealed no effects of the circulation system on the applied cell line in this study (data not shown) and thus the circulation system was not considered to be the root cause for the decreased cell growth in the two-compartment system. Bubble-associated cell damage at increased volumetric flow rates, higher surface-to volume ratio and smaller bubble diameter have been shown before to cause reduced cell growth in bioreactors [43, 45, 46] and were speculated next to be the reason for low cell densities reached in the small-compartment bioreactor. In fact, switch from submerse to headspace aeration in the small-compartment strongly increased cell growth. Nevertheless, due to the observed differences between the one-compartment and two-compartment system a special experimental procedure had to be applied for the pH inhomogeneity studies.

The applied experimental procedure considered osmolality increase due to pH overshoot simulation simi-

lar to Osman et al. [13]. In contrast to Nienow et al. [12] and Osman et al. [13] parallel control fermentations to the two-compartment experiments, ensured that variability in the observed results due to different preculture ages [47–49] or media batches [49] were considered.

4.3 Simulation of pH inhomogeneities in a fed-batch process using the two-compartment scale-down model

Subsequently two-compartment fermentation runs were conducted, including simulation of pH overshoots to pH 9.0. Maximum viable cell densities were lower in the two-compartment runs than in the one-compartment fermentations. Furthermore, no lactate or ammonia decrease could be observed during those fermentation processes. These differences may be attributed to the high osmolality values of 370–390 mOsm/kg reached after approx. 120 h in the two compartment systems. Increased media osmolalities might affect specific cell growth as well as byproduct formation as reported from Zhu et al. [40]. Possible negative influences from the recirculation system were neglected in this study since (i), as stated above, a batch study with recirculation by peristaltic pumps showed no effects (data not shown) and (ii) the cell growth of the two-compartment control fermentation showed similar viable cell densities in comparison to the one-compartment fermentations until a critical osmolality was reached (Fig. 6A). Furthermore, both two-compartment studies were recirculated by peristaltic pumps and only differed in their pH profile, which allowed us to separate the impact of the pH inhomogeneities from a potential effect of the recirculation pumps or other effects of the bioreactor system.

pH perturbations in the small-compartment and large-compartment as well as osmolality values in the control and perturbation fermentation run were successfully controlled. In total 40 pH perturbations occurred during the two-compartment fed-batch run with simulation of pH inhomogeneities. Duration of pH perturbations was controlled to 360 s with a mean amplitude of 9.08. No effects of simulated pH inhomogeneities on most specific metabolite production or consumption rates as well as on specific productivity could be derived, however specific cell growth and specific lactate production seemed to be slightly reduced. In comparison to state of the art literature [12, 13], cells were exposed to defined pH perturbations using conditions, e.g. alkali zone volumes and perturbation starting times and frequencies, as they might occur during an industrial large-scale 10–12 m^3 fed-batch process. Due to the applied strategy, several pH overshoots occurred already in the early process phase. This observation represents what might occur during large-scale fermentations and can have a significant effect on overall process performance. Therefore, an artificial start of pH overshoot simulations after a process time of 48 h,

as applied from Osman et al. [13] might not represent the large-scale reality. In fact, especially the specific growth rate during exponential growth phase was decreased, resulting in a significantly lower maximum viable cell density as well as lower final product titer than in the two-compartment control culture. In contrast, Nienow et al. stated that they could not conclude anything concerning the effect of pH inhomogeneities from their studies [12]. However, since the pH amplitude was not defined in Nienow et al., it is not possible to directly compare our results with this study. Osman et al. observed reduced cell growth dependent on the applied frequency and number of perturbations started after 48 h of process time [13]. However as stated above important scale-down model parameter as the volume of the alkali zone, as well as the starting time point and frequency of pH perturbations were artificially set. Although the volume of alkali zone was three times smaller and the residence time of the cells in the inhomogeneous zone was halved in our study, cell growth and thus maximum viable cell densities were decreased due to the pH perturbations. These results demonstrate for the first time, that even short-term exposure of a small compartment of the total cell count to elevated pH values, as it is expected to occur in large-scale mammalian cell culture, can affect overall process performance. Thus, sub-surface base addition in large-scale could most probably reduce these negative effects as suggested by other authors and applied by Khan [6, 50, 51]. The two-compartment system could be further used to mimic the industrial large-scale process. However, to be representative of the large-scale, reliable information of important scale-down parameters (e.g. volume of the alkali zone and pH amplitude) out of the actual large-scale bioprocess would be necessary. This would require the installment of novel multiposition sensors or in flow follower which are still under development and far away from application in biopharmaceutical production processes [20, 52–54].

Finally, within this study a two-compartment scale-down model, mimicking a 10–12 m^3 STR, was successfully established. Intracellular pH measurements revealed that cell physiology is immediately affected by extracellular pH changes, as they might occur at large-scale. It could be further derived that pH inhomogeneities affected cell growth, especially in the early process phase, thus scale-down models should not include an artificial frequency and start of pH perturbations if they intend to simulate the large-scale reality. Moreover, large-scale processes do benefit from submerse addition of base as long as Cleaning-in-Place considerations can be resolved. Furthermore, usage of week bases as well as increased mixing and optimized pH controller strategies could result in reduced alkali zones and pH amplitudes in large-scale. The presented results might be further interesting for other bioreactor systems with high mixing times as e.g. single-use wave bag bioreactors [55].

5 References

[1] Walsh, G., Biopharmaceutical benchmarks 2014. *Nat. Biotechnol.* 2014, *32*, 992–1000.

[2] Abu-Absi, S., Xu, S., Graham, H., Dalal, N. et al., Cell culture process operations for recombinant protein production. *Adv. Biochem. Eng. Biotechnol.* 2014, *139*, 35–68.

[3] Blackstone, E. A., Joseph, P. F., The economics of biosimilars. *Am. Health Drug Benefits* 2013, *6*, 469–478.

[4] Kim, J. Y., Kim, Y. G., Lee, G. M., CHO cells in biotechnology for production of recombinant proteins: Current state and further potential. *Appl. Microbiol. Biotechnol.* 2012, *93*, 917–930.

[5] Lara, A. R., Galindo, E., Ramirez, O. T., Palomares, L. A., Living with heterogeneities in bioreactors: Understanding the effects of environmental gradients on cells. *Mol. Biotechnol.* 2006, *34*, 355–381.

[6] Nienow, A. W., Reactor engineering in large scale animal cell culture. *Cytotechnology* 2006, *50*, 9–33.

[7] Hu, W., Wiltberger, K., Industrial cell culture process scale-up strategies and considerations, in: Hauser, H., Wagner, R. (Eds.), *Animal Cell Biotechnology In Biologics Production*, De Gruyter, Berlin, Boston 2014, pp. 455–488.

[8] Langheinrich, C., Nienow, A. W., Control of pH in large scale, free suspension animal cell bioreactors: Alkali addition and pH excursion. *Biotechnol. Bioeng.* 1999, *66*, 171–179.

[9] Brunner, M., Fricke, J., Kroll, P., Herwig, C., Investigation of the interactions of critical scale-up parameters (pH, pO_2 and pCO_2) on CHO batch performance and critical quality attributes. *Bioprocess Biosyst. Eng.* 2016, doi: 10.1007/s00449-016-1693-7.

[10] Sandoval-Basurto, E. A., Gosset, G., Bolivar, F., Ramirez, O. T., Culture of *Escherichia coli* under dissolved oxygen gradients simulated in a two-compartment scale-down system: Metabolic response and production of recombinant protein. *Biotechnol. Bioeng.* 2005, *89*, 453–463.

[11] Cortes, J. T., Flores, N., Bolivar, F., Lara, A. R., Ramirez, O. T., Physiological effects of pH gradients on *Escherichia coli* during plasmid DNA production. *Biotechnol. Bioeng.* 2016, *113*, 598–611.

[12] Nienow, A. W., Scott, W. H., Hewitt, C. J., Thomas, C. R. et al., Scale-down studies for assessing the impact of different stress parameters on growth and product quality during animal cell culture. *Chem. Eng. Res. Des.* 2013, *91*, 2265–2274.

[13] Osman, J. J., Birch, J., Varley, J., The response of GS-NS0 myeloma cells to single and multiple pH pertubations. *Biotechnol. Bioeng.* 2002, *79*, 398–407.

[14] Buchholz, J., Graf, M., Freund, A., Busche, T. et al., CO_2/HCO_3^- perturbations of simulated large scale gradients in a scale-down device cause fast transcriptional responses in *Corynebacterium glutamicum*. *Appl. Microbiol. Biotechnol.* 2014, *98*, 8563–8572.

[15] Lemoine, A., Martínez-Iturralde, N. M., Spann, R., Neubauer, P., Junne, S., Response of *Corynebacterium glutamicum* exposed to oscillating cultivation conditions in a two- and a novel three-compartment scale-down bioreactor. *Biotechnol. Bioeng.* 2015, *112*, 1220–1231.

[16] Neubauer, P., Junne, S., Scale-down simulators for metabolic analysis of large-scale bioprocesses. *Curr. Opin. Biotechnol.* 2010, *21*, 114–121.

[17] Limberg, M. H., Pooth, V., Wiechert, W., Oldiges, M., Plug flow versus stirred tank reactor flow characteristics in two-compartment scale-down bioreactor: Setup-specific influence on the metabolic phenotype and bioprocess performance of *Corynebacterium glutamicum*. *Eng. Life Sci.* 2016, *16*, 610–619.

[18] George, S., Larsson, G., Enfors, S.-O., A scale-down two-compartment reactor with controlled substrate oscillations: Metabolic response of *Saccharomyces cerevisiae*. *Bioprocess Biosys. Eng.* 1993, *9*, 249–257.

[19] Neubauer, P., Haggstrom, L., Enfors, S. O., Influence of substrate oscillations on acetate formation and growth yield in *Escherichia coli* glucose limited fed-batch cultivations. *Biotechnol. Bioeng.* 1995, *47*, 139–146.

[20] Noorman, H., An industrial perspective on bioreactor scale-down: What we can learn from combined large-scale bioprocess and model fluid studies. *Biotechnol. J.* 2011, *6*, 934–943.

[21] Namdev, P. K., Thompson, B. G., Gray, M. R., Effect of feed zone in fed-batch fermentations of *Saccharomyces cerevisiae*. *Biotechnol. Bioeng.* 1992, *40*, 235–246.

[22] Nienow, A. W., Langheinrich, C., Stevenson, N. C., Emery, A. N. et al., Homogenisation and oxygen transfer rates in large agitated and sparges animal cell bioreactors: Some implications for growth and production. *Cytotechnology* 1996, *22*, 87–94.

[23] Xing, Z., Kenty, B. M., Li, Z. J., Lee, S. S., Scale-up analysis for a CHO cell culture process in large-scale bioreactors. *Biotechnol. Bioeng.* 2009, *103*, 733–746.

[24] Davidson, K. M., Sushil, S., Eggleton, C. D., Marten, M. R., Using computational fluid dynamics software to estimate circulation time distribution in bioreactors. *Biotechnol. Progr.* 2003, *19*, 1480–1486.

[25] Zalai, D., Koczka, K., Parta, L., Wechselberger, P. et al., Combining mechanistic and data-driven approaches to gain process knowledge on the control of the metabolic shift to lactate uptake in a fed-batch CHO process. *Biotechnol. Progr.* 2015, *31*, 1657–1668.

[26] Konakovsky, V., Clemens, C., Müller, M., Bechmann, J. et al., Metabolic control in mammalian fed-batch cell cultures for reduced lactic acid accumulation and improved process robustness. *Bioengineering* 2016, *3*, 5.

[27] Salvi, A., Quillan, J. M., Sadée, W., Monitoring intracellular pH changes in response to osmotic stress and membrane transport activity using 5-chloromethylfluorescein. *AAPS PharmSci.* 2002, *4*, E21.

[28] L'Allemain, G., Paris, S., Pouysségur, J., Growth factor action and intracellular pH regulation in fibroblasts. *J. Biol. Chem.* 1984, *259*, 5809–5815.

[29] Wu, P., Ray, N. G., Shuler, M. L., A computer model for intracellular pH regulation in Chinese hamster ovary cells. *Biotechnol. Progr.* 1993, *9*, 374–384.

[30] Sureshkumar, G. K., Mutharasan, R., Intracellular pH based controlled cultivation of yeast cells: I. Measurement methodology. *Biotechnol. Bioeng.* 1992, *41*, 118–128.

[31] Cherlet, M., Franck, P., Nabet, P., Marc, A., Develpoment and validation of a methodology for intracellular pH Measurement of hybridoma cells under bioreactor culture conditions. *Biotechnol. Progr.* 1999, *15*, 630–639.

[32] Ozkan, P., Mutharasan, R., A rapid method for measuring intracellular pH using BCECF-AM. *Biochim. Biophys. Acta* 2002, 143–148.

[33] Frahm, B., Blank, H. C., Cornand, P., Oelssner, W. et al., Determination of dissolved CO_2 concentration and CO_2 production rate of mammalian cell suspension culture based on off-gas measurement. *J. Biotechnol.* 2002, *99*, 133–148.

71

[34] Sauer, P. W., Burky, J. E., Wesson, M. C., Sternard, H. D., Qu, L., A high-yielding, generic fed-batch cell culture process for production of recombinant antibodies. *Biotechnol. Bioeng.* 2000, *67*, 585–597.

[35] Murphy, T. A., Young, J. D., ETA: Robust software for determination of cell specific rates from extracellular time courses. *Biotechnol. Bioeng.* 2013, *110*, 1748–1758.

[36] Huang, L.-C., Lin, W., Yagami, M., Tseng, D. et al., Validation of cell density and viability assays using Cedex automated cell counter. *Biologicals* 2010, *38*, 393–400.

[37] Bawn, A., Lee, H. W., Downey, A., Xu, J. et al., Metabolic-sensing characteristics of absorption-photometry for mammalian cell cultures in biopharmaceutical processes. *Pharm. Bioprocess.* 2013, *1*, 255–266.

[38] Compton, B. J., Lewis, M. A., Whigham, F., Gerald, J. S., Countryman, G. E., Analytical potential of protein A for affinity chromatography of polyclonal and monoclonal antibodies. *Anal. Chem.* 1989, *61*, 1314–1317.

[39] Osman, J. J., Birch, J., Varley, J., The response of GS-NS0 myeloma cells to pH shifts and pH pertubations. *Biotechnol. Bioeng.* 2001, *75*, 63–73.

[40] Zhu, M. M., Goyal, A., Rank, D. L., Gupta, S. K. et al., Effects of elevated pCO_2 and osmolality on growth of CHO Cells and production of antibody-fusion protein B1: A case study. *Biotechnol. Progr.* 2005, *21*, 70–77.

[41] Jockwer, A., Klinger, C., Gätgens, J., Eisenkrätzer, D., Noll, T., Towards pCO_2-optimised fermentations – Reliable sampling, pCO_2 control & cellular metabolism, in: Smith, R. (Ed.), *Cell Technology for Cell Products*, Springer Netherlands 2007, pp. 509–518.

[42] Madshus, I., Regulation of intracellular pH in eukaryotic cells. *Biochem. J.* 1988, *250*, 1–8.

[43] Hu, W., Berdugo, C., Chalmers, J. J., The potential of hydrodynamic damage to animal cells of industrial relevance: Current understanding. *Cytotechnology* 2011, *63*, 445.

[44] Blaschczok, K., Kaiser, S. C., Löffelholz, C., Imseng, N. et al., Investigations on mechanical stress caused to CHO suspension cells by standard and single-use pumps. *Chem. Ing. Tech.* 2013, *85*, 144–152.

[45] Chisti, Y., Animal-cell damage in sparged bioreactors. *Trends Biotechnol.* 2000, *18*, 420–432.

[46] Handa-Corrigan, A., Emery, A. N., Spier, R. E., Effect of gas-liquid interfaces on the growth of suspended mammalian cells: Mechanism of cell damage by bubbles. *Enzyme Microb. Technol.* 1989, *11*, 230–235.

[47] Li, F., Vijayasankaran, N., Shen, A. Y., Kiss, R., Amanullah, A., Cell culture processes for monoclonal antibody production. *MAbs* 2010, *2*, 466–479.

[48] Bailey, L. A., Hatton, D., Field, R., Dickson, A. J., Determination of Chinese hamster ovary cell line stability and recombinant antibody expression during long-term culture. *Biotechnol. Bioeng.* 2012, *109*, 2093–2103.

[49] Gilbert, A., Huang, Y.-m., Ryll, T., Identifying and eliminating cell culture process variability. *Pharm. Bioprocess.* 2014, *2*, 519–534.

[50] Larsson, G., Törnkvist, M., Wernersson, E. S., Trägårdh, C. et al., Substrate gradients in bioreactors: Origin and consequences. *Bioprocess Eng.* 1996, *14*, 281–289.

[51] Khan, M., Bioreactor for the cultivation of mammalian cells. US Patent Application 20160040110, 2016.

[52] Zimmermann, R., Fiabane, L., Gasteuil, Y., Volk, R., Pinton, J.-F., Characterizing flows with an instrumented particle measuring Lagrangian accelerations. *New J. Phys.* 2013, *15*.

[53] Bockisch, A., Biering, J., Päßler, S., Vonau, W. et al., In situ investigation of the liquid phase in industrial yeast fermentations with mobile multiparameter sensors. *Chem. Ing. Tech.* 2014, *86*, 1582–1582.

[54] Kielhorn, E., Sachse, S., Moench-Tegeder, M., Naegele, H.-J. et al., Multiposition sensor technology and lance-based sampling for improved monitoring of the liquid phase in biogas processes. *Energy Fuels* 2015, *29*, 4038–4045.

[55] Eibl, R., Werner, S., Eibl, D., Bag bioreactor based on wave-induced motion: Characteristics and applications, in: Eibl, R., Eibl, D. (Eds.), *Disposable Bioreactors*, Springer Berlin Heidelberg, Berlin, Heidelberg 2010, pp. 55–87.

Conclusions and Outlook

Conclusions

Within this thesis a scale-down approach was used to assess scale-up induced process variability due to process parameter inhomogeneities. The specific methodologies used in the manuscripts can be seen as a toolset in scale-down studies to understand variations between different fermentation scales (Figure 4).
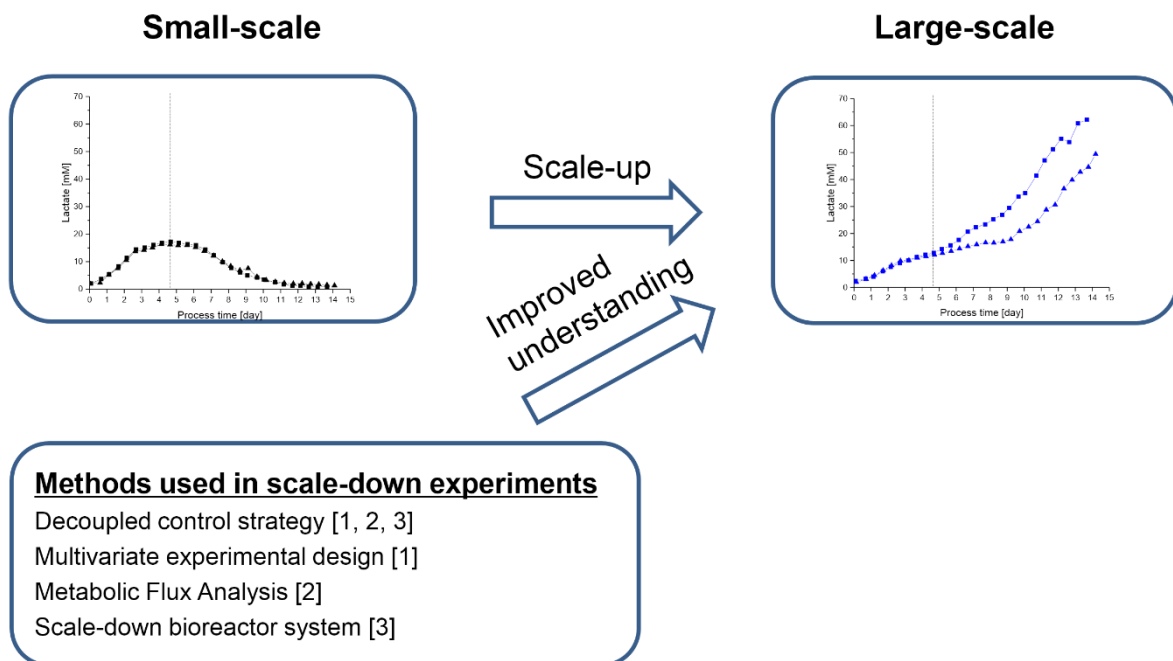
Figure 4. The scale-down approach can improve the understanding of scale-up effects. The specific methodologies used in the manuscripts are presented. Numbers in square brackets refer to the specific manuscripts included in this thesis.

The decoupled control of process pH, pO_2 and pCO_2 in combination with the multivariate experimental design in manuscript 1 allowed us to reveal significant interaction effects of process parameters, in particularly of pH and pCO_2, on cell physiology and product quality attributes. Interaction effects of process parameters are usually not considered during process scale-up but especially pH and pCO_2 are closely related in mammalian cell culture whereby pCO_2 is usually introduced as an acidic reagent to control pH (Abu-Absi et al. 2014).

Furthermore, bicarbonate concentrations are dependent from process pH and pCO_2 levels. Increased pCO_2 values in large-scale can therefore further result in differences in pH and bicarbonate concentration. The interaction effects discovered in manuscript 1 built the basis for the investigations in manuscript 2.

In manuscript 2 we could show that elevated pCO_2/bicarbonate concentrations can change metabolic key events during cell culture processes and therefore should be considered during process scale-up. Metabolic Flux Analysis was demonstrated to be a relevant tool during the scale-down studies to improve the understanding of intracellular flux distributions and overall cell metabolism. Through this methodology the onset of lactate uptake could be correlated to an intracellular ratio of reducing equivalents. Based on these results, it seems to be beneficial to reduce bicarbonate and pCO_2 levels during process scale-up by usage of optimized gassing strategies and alternative bases (e.g. NaOH instead of Na_2CO_3).

The two-compartment scale-down bioreactor used in manuscript 3 is generally an excellent tool to investigate the effect of transient perturbations in process parameters on cell physiology and overall process performance (Neubauer and Junne 2010). The results out of manuscript 3 revealed that even short-term exposure of cells to elevated pH values affects the cells intracellular pH and overall process performance. However, the applied settings in this study were based on extreme conditions out of literature and are not representing the industrial large-scale reality. Nevertheless, the results indicate that optimized mixing, the usage of weak bases and submerse base addition would be beneficial during large-scale cell culture processes to reduce the impact of pH inhomogeneities.

Finally, the goal of a scale-down approach is not only to generate knowledge of possible scale-up effects but to further transfer that gained knowledge back to the large-scale (Noorman 2011). However, due to the lack of knowledge of the exact large-scale conditions, which would require multiposition sensors or in-flow follower (Bockisch et al. 2014; Zimmermann et al. 2013), it is

only possible to derive general conclusions out of the scale-down studies. Furthermore, static process parameter conditions applied in two out of the three scale-down studies in this thesis might provoke different cell responses than the dynamic environmental conditions experienced by cells in large-scale processes. However, the applied scale-down approach and individual methodologies in this thesis allowed the identification of novel process parameter effects and intracellular metabolic regulations that occur during mammalian cell culture process scale-up. The results of this thesis finally contribute to an improved understanding of scale-up variability and can therefore be applied to improve process scale-up robustness e.g. by application of submerse base addition. Furthermore, the scale-down approach and methodologies can be used to investigate scale-up effects under the individual large-scale process conditions.

Outlook

Process parameter interactions of pH and pCO_2 as well as elevated pCO_2/bicarbonate have been shown in manuscript 1 and 2 to affect cell physiology, product quality and overall process performance. The scale-down studies should be expanded in future work with different cell lines and under variable pCO_2 conditions to gain deeper understanding of these effects. Furthermore, the application of dynamic pCO_2 profiles during fed-batch processes might provide results that are closer to the large-scale reality. Moreover, the linkage of intracellular reducing equivalents with the onset of lactate consumption should be confirmed and evaluated in more detail using different cell lines or clones. The two-compartment bioreactor system in manuscript 3 is capable of exposing the cells to transient environmental conditions and therefore can give a better approximation of the large-scale conditions. The results of the presented study suggest that short-term exposure of cells to elevated pH conditions strongly affect the cells physiology and overall process performance. Through further optimization of the two-compartment system and the knowledge of the actual large-scale conditions this

bioreactor system could become an efficient tool to investigate the effect of large-scale inhomogeneities and could be furthermore used to screen for cell lines or clones with good performance under inhomogeneous conditions (Neubauer and Junne, 2010).

References Conclusions and Outlook

Abu-Absi S, Xu S, Graham H, Dalal N, Boyer M, Dave K. 2014. Cell culture process operations for recombinant protein production. Adv. Biochem. Eng. Biotechnol. 139:35-68.

Bockisch A, Biering J, Päßler S, Vonau W, Junne S, Neubauer P. 2014. In Situ Investigation of the Liquid Phase in Industrial Yeast Fermentations with Mobile Multiparameter Sensors. Chem. Ing. Tech. 86(9):1582-1582.

Neubauer P, Junne S. 2010. Scale-down simulators for metabolic analysis of large-scale bioprocesses. Curr. Opin. Biotechnol. 21(1):114-21.

Noorman H. 2011. An industrial perspective on bioreactor scale-down: what we can learn from combined large-scale bioprocess and model fluid studies. Biotechnol. J. 6(8):934-43.

Zimmermann R, Fiabane L, Gasteuil Y, Volk R, Pinton J-F. 2013. Characterizing flows with an instrumented particle measuring Lagrangian accelerations. New J. Phys. 15(1).

Appendix

List of Tables

List of Figures

Abbreviations

A	cross-sectional area of the bioreactor
C	Oxygen concentration in the liquid
C*	Oxygen concentration at the boundary layer
CHO	Chinese Hamster Ovary Cells
CFD	Computational Fluid Dynamics
CO_2	Carbon dioxide
IEC	Ion Exchange Chromatography
Kla	Volumetric mass transfer coefficient
NaOH	Sodium hydroxide
NA2CO3	Sodium bicarbonate
O_2	Oxygen
OTR	Oxygen transfer rate
pCO_2	dissolved carbon dioxide
pO_2	Dissolved oxygen
PQ	Product quality
P/V	Specific power input
Qs	Volumetric productivity
Vl	Volume of the culture broth
Vs	Superficial gas velocity
Vvm	Volumetric flow rate

Curriculum Vitae

Matthias Brunner

Date and place of birth: 30.12.1983 in Nuremberg
Address: Auchtertweg 1-13
88400 Biberach
Mobile phone No.: +43 6803327408
Email: matthiasbrunner1@gmx.de

Education

Since 01/2014   **Ph.D. (Dr. techn.) in Biochemical Engineering**
Vienna University of Technology (Vienna, AT)
- Research topic: Investigation of scale-up effects in mammalian cell culture
- Experimental design (incl. DoE), execution and advanced data evaluation (incl. MVDA) of fermentation processes
- Establishment of a two-compartment bioreactor system
- Reporting to industrial partner (presentations and written reports)
- Peer-reviewed publications in Biotechnology Journal and Bioprocess and Biosystems Engineering
- Conferences
ESBES 2016 – Poster presentation
BioProScale 2016 – Talk: Investigation of scale-up effects on mammalian cell culture process performance and critical quality attributes
- Supervision of master and bachelor students

10/2004 – 03/2011   **Dipl.-Ing. in Chemical and Bioengineering**
University of Erlangen-Nuremberg (Nuremberg, DE)
- Study focus and graduation note: Bioengineering (1,7)
- Diploma thesis at Roche Diagnostics GmbH
Automated sampling and analysis for process monitoring in mammalian fermentation processes

09/1994 – 06/2003   **A-levels (Abitur)**
Willstätter-Gymnasium (Nuremberg, DE)

Professional experience

Since 02/2017   **Post-Doc – Late stage process development USP**
Boehringer Ingelheim (Biberach, DE)
- Principal investigator for state-of-the-art cell culture technology development projects, including supervision of technical staff and planning, execution and implementation

10/2011 – 12/2013 **Bioengineer - Division Cell Culture Research**
Roche Diagnostics GmbH (Penzberg, DE)
- Planning, execution and documentation of mammalian fermentation processes for cell line selection and material supply (2 -250 L scale)
- Evaluation and presentation of the gathered data
- USP development and process transfer into GMP facilities

06/2011 – 09/2011 **Process engineer**
VTU Engineering (Penzberg, DE)
- Conceptional design of a synthesis plant

Personal skills

Languages:

German   -   mother tongue
English   -   fluent
French   -   basic knowledge
Spanish   -   basic knowledge

Activities: Brazilian-Jiu-Jitsu, soccer, traveling

Biberach, 01.05.2017

Matthias Brunner